

2007

Targeted Disruption of Lynx2 Reveals Distinct Functions for Lynx Homologues in Learning and Behavior

Ayse Begum Tekinay

Follow this and additional works at: http://digitalcommons.rockefeller.edu/student_theses_and_dissertations

 Part of the [Life Sciences Commons](#)

Recommended Citation

Tekinay, Ayse Begum, "Targeted Disruption of Lynx2 Reveals Distinct Functions for Lynx Homologues in Learning and Behavior" (2007). *Student Theses and Dissertations*. Paper 28.



**TARGETED DISRUPTION OF LYNX2
REVEALS DISTINCT FUNCTIONS FOR
LYNX HOMOLOGUES
IN LEARNING AND BEHAVIOR**

A Thesis Presented to the Faculty of

The Rockefeller University

In Partial Fulfillment of the Requirements for

the degree of Doctor of Philosophy

by

Ayse Begum Tekinay

June 2007

TARGETED DISRUPTION OF LYNX2 REVEALS DISTINCT FUNCTIONS FOR LYNX HOMOLOGUES IN LEARNING AND BEHAVIOR

Ayse Begum Tekinay, Ph.D.

The Rockefeller University 2007

Endogenous short peptide modulators of ion channels provide a new level of regulation of nervous function. Lynx1 was identified as an endogenous mammalian homologue of snake venom peptide neurotoxins capable of binding to and functionally modulating nicotinic acetylcholine receptors (nAChR). Lynx1 is a member of the Ly6- α -neurotoxin superfamily (Ly6SF) of genes.

Through extensive database searches, I identified 85 members of this superfamily including previously unidentified vertebrate and invertebrate family members. I show that these proteins are very divergent in their sequences, and identify two conserved subfamilies, snake toxins and immune system expressed Ly6 genes through phylogenetic inference. I also discovered conserved sequences among Ly6SF proteins additional to the cysteines that characterize the three-dimensional topology of Ly6 domain. From these Ly6SF molecules, I characterize three lynx1 homologues: lynx2, lynx3 and Ly6H. These have different and specific expression patterns in the central and peripheral nervous systems. Importantly, like lynx1, lynx2 and lynx3 are able to bind specific nAChR

combinations and modulate their desensitization properties, while Ly6H does not bind nor modulate the function of nAChRs.

I have also analyzed the *in vivo* function of lynx2, through the targeted deletion of lynx2 in mice. Lynx2 null mutant (*lynx2*^{-/-}) mice exhibited increased anxiety, better associative learning and better motor coordination and learning than wild type (WT) mice.

Nicotine and nicotinic receptor antagonist, mecamylamine, show distinct effects on motor learning in *lynx2*^{-/-} mice and WT mice. The properties of this new family of lynx1-like molecules, taken together with those of lynx1 and the secreted Ly6SF member SLURP1 (secreted Ly6/UPAR related protein), suggest a general role for Ly6SF proteins in the modulation of nAChRs and other receptor proteins.

Turgay'a

Acknowledgements

I would like to thank my advisor, Nathaniel Heintz, for helping me whenever I had a tough time during my studies and giving me valuable advice whenever I needed it.

I also would like to thank MaryBeth Hatten, David Gadsby and Joseph LeDoux for providing valuable scientific advice and introducing me to their lab members, who were very helpful.

Joseph P. Doyle was extremely nice and patient with my never-ending questions in the first years of grad school and continued to be very supportive till the end. I'm grateful to Julie Miwa, Laura Kus, Tanya Stevens, Inez Ibanez-Tallon and Shiaoqing Gong for their great scientific advice and helping me with my experiments. Laura Kus was incredibly helpful on anatomical annotations and characterizing expression pattern of lynx3. I'm grateful to Mayte Farinas, who has helped me with the statistical analysis of the behavioral data. I would like to thank Wendy Lee for spending a lot of time doing transfections for my co-immunoprecipitation studies and Jie Xing for making maxi-preps. I also would like to thank members of Heintz lab and GENSAT project, who made graduate school tolerable. Aylin Aslantaş was a great help with her summer work. Ivo Lieberam was a very helpful collaborator.

I owe thanks to my college professors Mehmet Öztürk and Tayfun Özçelik for their advice and guidance, which they continued to provide long after college.

I'm indebted to my parents, my sisters Aysun and Aylin, my nephew Batuhan and my family for raising me, supporting my education and taking care of my daughter for 19 months staying in a city, where they don't even know the language. Minnettirim...

My precious daughter, Sarah Hümeyra, has beared with her mommy working late for two years with her beautiful smile. Seni seviyorum kızım. I also would like to thank my husband, Turgay, from the bottom of my heart, for being my best friend, helping me when I felt down, supporting me and believing in me. I'll always be grateful.

Table of Contents

| | |
|--|-----------|
| CHAPTER 1: | 1 |
| Introduction | 1 |
| <i>Summary</i> | 2 |
| <i>Ly6 Superfamily of genes</i> | 3 |
| Structure, Evolution and Diversity | 3 |
| Expression Patterns | 8 |
| Activity and Function | 12 |
| <i>Nicotinic Acetylcholine Receptors</i> | 16 |
| Diversity and Structure | 16 |
| Expression patterns | 19 |
| Function | 21 |
| <i>Lynx1</i> | 28 |
| Sequence and Structure..... | 28 |
| Expression..... | 28 |
| Function | 29 |
| Chapter 2: | 33 |
| Phylogenetic Inference of Ly6 Superfamily of Proteins | 33 |
| <i>Introduction</i> | 34 |
| <i>Identification of Ly6SF proteins and Alignment of Sequences</i> | 34 |
| <i>Phylogenetic Inference</i> | 42 |
| Lynx Subfamily of Proteins | 43 |

| | |
|---|-----------|
| Exon-Intron Structures of Ly6SF genes | 46 |
| CHAPTER 3: | 50 |
| Expression and Functional Analysis of Lynx1 Homologues | 50 |
| <i>Summary</i> | 51 |
| <i>Expression Analysis of Lynx1 Homologues</i> | 52 |
| Database analysis for expression of human and mouse Ly6 genes | 52 |
| RT-PCR Analysis of Ly6 Genes and Northern Blots | 56 |
| BAC Transgenic Mice Show Expression Patterns of Lynx Homologues | 61 |
| Western Blot Analysis | 78 |
| Lynx2 is a membrane protein | 82 |
| Lynx2 is a membrane protein | 83 |
| Immunohistochemistry | 83 |
| <i>Functional Analysis of Lynx1 homologues</i> | 87 |
| Co-immunoprecipitation analysis | 87 |
| Electrophysiology | 92 |
| CHAPTER 4: | 95 |
| Gene-targeted Deletion Analysis for Lynx2 and Lynx3 | 95 |
| <i>Summary</i> | 96 |
| <i>Lynx2</i> | 97 |
| Straight KO Construct Preparation | 97 |
| Conditional KO construct properties | 99 |
| Anatomical Analysis of lynx2 ^{-/-} Animals | 101 |
| Behavioral Phenotyping of lynx2 ^{-/-} Mice..... | 101 |

| | |
|---|------------|
| KO construct preparation | 120 |
| Chimeras and Breeding | 120 |
| CHAPTER 5: | 122 |
| Lynx3 Modulates A Novel <i>Xenopus</i> Oocyte Channel..... | 122 |
| <i>Summary</i> | 123 |
| <i>Characterization of Lynx3 Affected Channel</i> | 123 |
| <i>Finding the reversal potential of the channel</i> | 130 |
| <i>Pharmacological Characterization of Lynx3 Target Channel</i> | 130 |
| CHAPTER 6: | 134 |
| Discussion | 134 |
| <i>Summary</i> | 135 |
| <i>Identification and Phylogenetic Inference of Ly6 Gene</i> | 137 |
| <i>Expressional and Functional Characterization of Lynx1 Homologues</i> | 139 |
| <i>Gene-targeted Deletion Analysis of lynx2 and lynx3</i> | 143 |
| Effects of lynx2 null mutation on fear and anxiety..... | 144 |
| Effects of lynx2 null mutation on motor coordination and learning..... | 148 |
| Review of Behavioral Phenotype of Lynx2 KO mice | 151 |
| <i>Lynx3 is Modulating A Novel <i>Xenopus</i> Oocyte Channel</i> | 152 |
| <i>Future Directions</i> | 154 |
| CHAPTER 7: | 159 |
| Materials and Methods | 159 |
| <i>Identification and Phylogenetic Inference of Ly6 Genes</i> | 160 |

| | |
|--|-----|
| <i>Cloning</i> | 160 |
| <i>RT-PCR:</i> | 161 |
| <i>Northern Blot</i> | 163 |
| <i>Western Blot</i> | 163 |
| <i>In situ hybridization</i> | 164 |
| <i>Polyclonal Antibody Production:</i> | 164 |
| <i>Immunocytochemistry</i> | 165 |
| <i>Histology and Immunohistochemistry</i> | 166 |
| <i>Expression and Immunoprecipitation from HEK293T Cells</i> | 166 |
| <i>Injection of Xenopus Oocytes with mRNA:</i> | 167 |
| <i>Electrophysiology</i> | 167 |
| Functional Analysis of Lynx1 homologues in Oocytes | 167 |
| Analysis of the <i>Xenopus</i> Ion Channel opened by Lynx3 | 167 |
| <i>Antibodies</i> | 169 |
| <i>Behavioral Phenotyping Experiments</i> | 169 |
| Open-Field Exploration Test..... | 169 |
| Hanging Wire Assay and Reflex Checks..... | 170 |
| Rotarod Assay..... | 170 |
| Light-Dark Box Test..... | 171 |
| Social Interaction Test | 172 |
| Elevated Plus Maze Test..... | 173 |
| Fear Conditioning Test | 173 |
| Hot Plate Test..... | 174 |

| | |
|--------------------------------|------------|
| Finding Buried Food Test | 174 |
| Statistical Analysis..... | 174 |
| Bibliography | 176 |

List of Figures

Chapter 1

Figure 1: Basic scheme of Ly6 domain sequence

Figure 2: Domain structures of GPI anchored and secreted Ly6 proteins

Figure 3: Three-dimensional structures of several Ly6 superfamily members.

Figure 4: nAChR Phylogenetic Tree.

Chapter 2

Figure 5: Sequence Alignment of Ly6 domains of Ly6SF proteins.

Figure 6: Phylogeny of Ly6SF proteins and sequence alignment of lynx1 homologues.

Figure 7: Scheme of ly6 domain structure after our analysis.

Figure 8: Species distribution of Ly6SF genes.

Figure 9: The alignment of Lynx1, Lynx3 and Lynx4 on murine chromosome 15.

Figure 10: Exon-intron structures of Lynx homologues.

Figure 11: Sequence alignment of Ly6 domains of avian Ly6SF proteins.

Figure 12: Ch6Ly is a homologue of mPscA.

Chapter 3

Figure 13: RT-PCR analysis of Ly6 proteins in seven different tissues

Figure 14: Northern blot analysis of lynx2.

Figure 15: Dot blot analysis of lynx2 expression.

Figure 16: Differential expression of lynx1, lynx2, lynx3 and Ly6H in the mouse cerebral cortex and hippocampus.

Figure 17: Expression analysis of Lynx1 homologues in brains sections from E15.5 mouse embryos with colorimetric in situ hybridization.

Figure 18: Expression analysis of lynx3 in heads of BAC-transgenic animals at age E15.5.

Figure 19: Expression of lynx3 in BAC-transgenic embryos at age E15.5.

Figure 20: Expression of lynx3 in BAC-transgenic mice at age P7.

Figure 21: Expression of lynx3 in brain sections from the adult BAC-transgenic mice.

Figure 22: lynx3 is expressed in olfactory epithelia and respiratory epithelia.

Figure 23: lynx3 expression in trachea and lungs.

Figure 24: lynx3 expression esophageal epithelium.

Figure 25: lynx3 expression in thymus of BAC-transgenic mice.

Figure 26: Expression of lynx3 in vaginal mucosa.

Figure 27: Expression of lynx3 in neurons surrounding blood vessels in spleen.

Figure 28: lynx4 expression analyzed in BAC-transgenic mice at age E15.5.

Figure 29: Expression of Ly6H at age E15.5 in BAC-transgenic mice.

Figure 30: lynx4 expression analyzed in BAC-transgenic mice brain sections.

Figure 31: Expression of Ly6H in BAC-transgenic mice at age P7.

Figure 32: Ly6H expression analyzed in the adult brain and spinal cord.

Figure 33: lynx2 expression analyzed in multiple tissue Western blot.

Figure 34: Analysis of developmental expression of lynx1 and lynx2.

Figure 35: lynx2 is a membrane protein.

Figure 36: lynx2 expression in brain analyzed with immunohistochemistry.

Figure 37: Distinct interactions of lynx1, lynx2, lynx3 and Ly6H with nAChRs.

Figure 38: lynx1, lynx2 and lynx3 enhance desensitization of ACh-evoked currents mediated through $\alpha 4\beta 2$ nAChRs in oocytes.

Chapter 4

Figure 39: Lynx2 KO construct.

Figure 40: Lynx2 Conditional KO construct.

Figure 41: RT-PCR analysis shows lynx2 mRNA is absent in *lynx2^{-/-}* mice.

Figure 42: Representative pictures of hippocampus and retrosplenial cortex in *lynx2^{-/-}* and WT mice.

Figure 43: Open Field Exploration Test.

Figure 44: Hanging wire test.

Figure 45: Rotarod test.

Figure 46: Effects of nAChR agonists and antagonists on rotarod performance of WT and *lynx2^{-/-}* mice.

Figure 47: Effects of nicotine and nAChR antagonists on the motor skills of *lynx2^{-/-}* mice and WT mice.

Figure 48: Elevated Plus Maze test.

Figure 49: Fear Conditioning test.

Figure 50: Light-Dark Box Test.

Figure 51: Effect of nicotine on anxiety related behavior.

Figure 52: *lynx2^{-/-}* mice were tested for anxiety related behavior with the Social Interaction test.

Figure 53: *lynx2^{-/-}* mice and wild type mice behave differently in Part 1 of Social Interaction Test.

Figure 54: KO and WT mice behaved similarly in the Social Interaction test Part 2.

Figure 55: Hot Plate test.

Figure 56: Finding Buried Food Test.

Figure 57: Olfactory learning tested with buried food finding test.

Figure 58: Lynx3 KO construct.

Chapter 5

Figure 59: A representative recording demonstrating the effect of NMG.

Figure 60: Ba²⁺ partially blocks lynx3-effected channel.

Figure 61: Na⁺ vs K⁺.

Figure 62: Replacing Ca²⁺ ions with Mg²⁺ ions increase the current passed through the lynx3-effected channels.

Figure 63: La³⁺ ions inhibit the currents elicited by lynx3 expression in *Xenopus* oocytes.

Figure 64: Current-Voltage Relationships (I-V curves) of control oocytes and lynx3 mRNA injected oocytes and a representative recording of lynx3 injected oocytes for evaluating the I-V curves.

List of Tables

Table 1: Summary of expression patterns of Ly6SF proteins.

Table 2: Summary of expression information of human Ly6SF genes derived from TIGR, SAGE and UNIGENE databases.

Table 3: Summary of expression information of mouse Ly6SF genes derived from TIGR, SAGE and UNIGENE databases.

Table 4: Summary of co-immunoprecipitation analysis with nAChRs and lynx homologues.

Table 5: Summary of behavioral phenotyping of *lynx2*^{-/-} mice.

Table 6: Currents elicited by lynx3 expression were further augmented by presence of Mg²⁺ and absence of Ca²⁺.

Table 7: Currents in lynx3 expressing oocytes were blocked by the chemicals below.

List of Abbreviations

aa: amino acid

ACh: Acetylcholine

BP: Bisphosphonates

CNS: Central Nervous System

DH β E: dihydro-beta-erythroidine

DIDS: 4-4'-diisothiocyanosylbene-2,2'-disulphonic acid

EGFP: Enhanced Green Fluorescent Protein

ENaC: Epithelial Sodium Channel

EST: Expressed Sequence Tag

FFA: Flufenamic acid

GML: GPI-anchored molecule like protein

GPI: Glycosyl phosphatidylinositol

Ly6SF: Ly6 Super family

***lynx2*^{-/-}:** lynx2 null mutant

KO: Knock-out

MLA: methylcaconitine

MTX: Maitotoxin

nAChR: Nicotinic Acetylcholine Receptor

NMG: N-methyl-D-glucamine

pAb: polyclonal antibody

PSCA: Prostate stem cell antigen

RT-PCR: Reverse Transcription-Polymerase Chain Reaction

SAGE: Serial Analysis of Gene Expression

Sgp-2: Squid glycoprotein-2

SITS: 4-acetamido-4-isothiocyanostilbene-2,2-disulfonic acid

SLURP: Secreted Ly6/UPAR related protein

SSRI: Selective serotonin re-uptake inhibitor

SVS-VII: Seminal vesicle secreted protein VII

TCR: T-cell Receptor

TEA: Tetra ethyl ammonium

ThB: Thymocyte Antigen B

TIGR: The Institute for Genomic Research

UPAR: Urokinase Plasminogen Activator Receptor

WT: wild type

CHAPTER 1:

Introduction

Summary

Tobacco use is the leading preventable cause of death in the world. Nicotine, which is the addictive ingredient of tobacco, exerts its effect through nAChRs in the central nervous system (CNS). Besides mediating nicotine addiction, nAChRs have been implicated in Alzheimer's disease, Parkinson's disease, learning and memory, autism, anxiety disorders and depression.

Lynx1 has recently been identified as a modulator of nAChRs and it functions in nicotinic receptor mediated learning and neurodegeneration. Lynx1 is a member of Ly6SF, which is a large protein family that consists of proteins with a characteristic three-finger topology.

In this chapter, I will briefly review the structure, expression patterns and functions of Ly6SF proteins and nicotinic receptors. I will then go over expression and function of Lynx1 *in vitro* and *in vivo*.

Ly6 Superfamily of genes

Structure, Evolution and Diversity

Ly6 proteins were first identified in the cells of the immune system in the 1970s [1]. The immune system is a complex of organs and specialized cells that is responsible for defense of the body against foreign objects. Blood cells are a major part of the immune system. All blood cells are made by stem cells, which live mainly in the bone marrow, through a process called hematopoiesis. The stem cells produce hemocytoblasts, which mature into three types of blood cells: erythrocytes (red blood cells), leukocytes (white blood cells), and thrombocytes (platelets).

The leukocytes consist of granulocytes, which contain large granules in their cytoplasm, and agranulocytes, which don't have granules. The granulocytes are subdivided into neutrophils, eosinophils, and basophils and the agranulocytes are subdivided into lymphocytes, or lymphoid cells (B cells and T cells), and monocytes. Monocytes, granulocytes and erythrocytes are also called myeloid cells. Monocytes mature into macrophages, which attract, engulf and digest foreign bodies.

Ly6 proteins are named after their founder member that was identified as a **Lymphocyte antigen** in mouse T-cells [1]. Antibodies generated against these proteins showed that they are expressed in subpopulations of myeloid and lymphoid cells [2-4]. Thus they have been used as differentiation markers for hematopoietic stem cells and T-cells [5-7]. Most Ly6 genes that are expressed in hematopoietic cells are localized to murine chromosome 15 and human syntenic chromosome 8q24 [8-12]. Ly6 proteins are also expressed in non-hematopoietic cells. CD59, Ly6D, SLURP1 and Lynx1 are

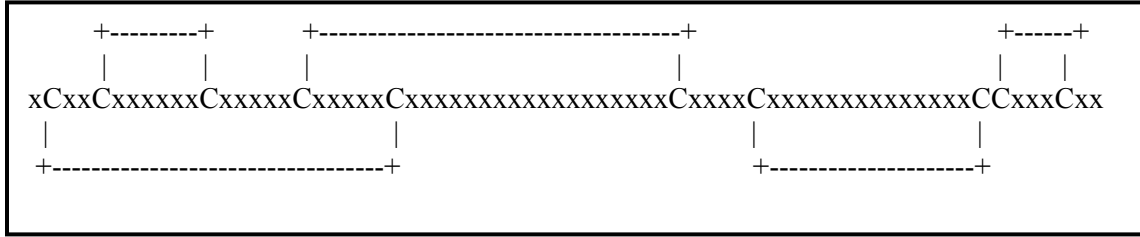


Figure 1: Basic Scheme of Ly6 Domain Sequence. Ly6 domain is a three finger structure that is made up by 8-10 cysteine residues dispersed with conserved spacings.

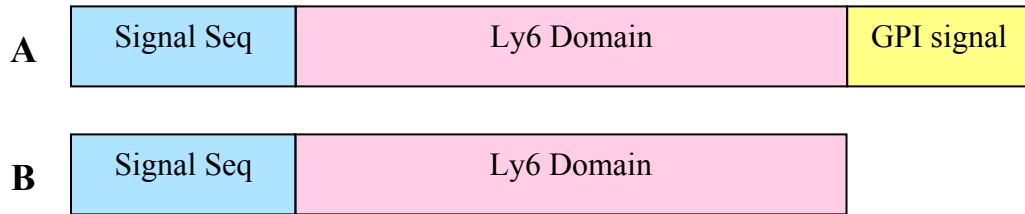


Figure 2: Domain structures of GPI anchored and secreted Ly6 proteins.
A. GPI anchored Ly6 proteins are comprised of an N-terminal signal sequence, a Ly6 domain and a C-terminal GPI-anchorage signal sequence.
B. Secreted Ly6 proteins consist of an N-terminal signal sequence and a Ly6 domain, but lack GPI-anchorage signal.

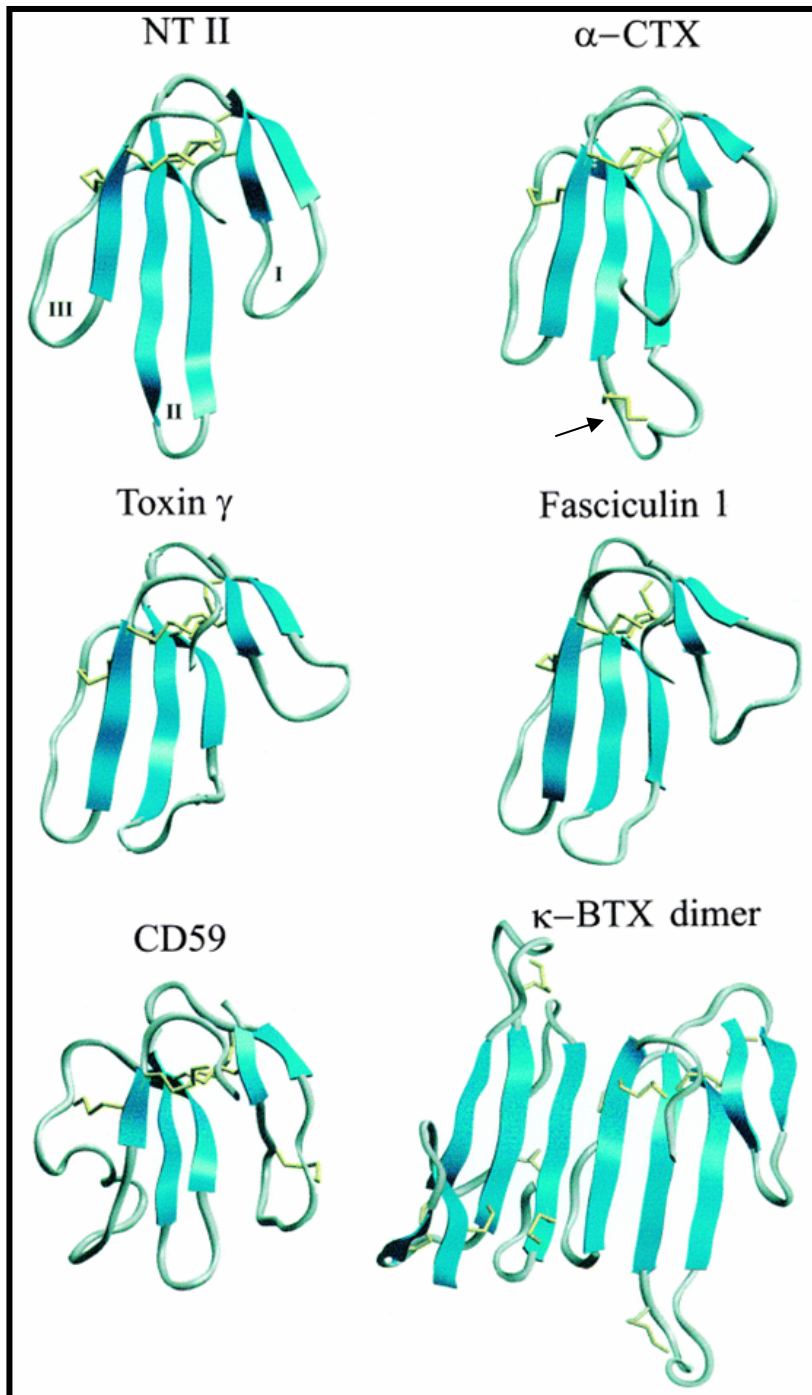


Figure 3: Three-dimensional structures of several Ly6 superfamily members. Ly6 domain is characterized by its three-looped structure that looks like three fingers. (Tsetlin V., Snake Venom α -neurotoxins and other three-finger proteins, Eur. J. Biochem, 1999)

examples of such Ly6 genes and they are localized to human chromosome 8q24 as well as other chromosomal regions including human chromosome 19q13.3 and 6p21.3 [11, 13-16].

Ly6 proteins have a three-finger structure

Ly6SF is composed of relatively short (~100 amino acid (aa) long) proteins that have characteristic three-finger Ly6/UPAR (urokinase-type plasminogen activator receptor) domain. This domain is characterized by 8-10 cysteine residues, between which there are disulfide bonds that make up the backbone of the three dimensional structure of this domain [14, 17] (Figure 1 and 3).

α -neurotoxins and other snake toxins, which are secreted Ly6SF proteins, have the same three-finger structure (60-80 aa long), but they are relatively shorter than mammalian Ly6 proteins that have been described so far. These toxins are divided into two groups in terms of the number of cysteines: the first group of toxins have 8 cysteine residues, which form 4 disulphide bridges, in their backbone, and the second group have 10 cysteines [17]. The second group is further divided into two subgroups depending on the location of the extra disulphide bridge. The first subgroup, so-called weak toxins, have the extra disulphide bridge in their first loop, whereas members of the second subgroup have the extra bridge in the second, central loop (Figure 3). The integrity of the additional disulfide bridge in the second finger of neurotoxins has been shown to be necessary for high-affinity binding to $\alpha 7$ nAChRs [18]. The removal of the additional disulfide bond in the second finger of κ -bungarotoxin also decreases the affinity of this toxin to $\alpha 3\beta 2$ nAChRs [19].

Although most three-finger toxins exert their effect by binding to a target channel and receptor, cardiotoxins (or cytotoxins) do not bind to a receptor or a channel, but form channels in the membrane [20]. Toxins have various oligomerization properties. Cardiotoxins are found in trimers [20] whereas α -neurotoxins are found as monomers and κ -bungarotoxins always form dimers [21, 22].

Almost all mammalian Ly6 proteins identified so far also have all 10 cysteines and an additional disulphide bridge in their first finger, like toxins with weaker affinity, [23] and N-terminal signal sequences. Except for SLURP1, SLURP2 and SVS-VII (seminal vesicle secretion protein VII), which are secreted like three-finger snake toxins, all the known mammalian Ly6SF members have GPI (glycosyl-phosphatidylinositol) anchorage site and signal at their C-terminal [15, 24, 25] (Figure 2).

Evolution of Ly6 Proteins

When Ly6 proteins were first described, they were put into the same protein family with the UPAR like proteins. UPAR, which is a 335 aa long protein, is one of the founding members of a superfamily of membrane-bound glycoproteins. It has an N-terminal signal and a GPI anchorage site, like Ly6SF of proteins; however, this protein has 3 three-finger domains. Since Ly6SF members have only one three-finger domain, investigators have started to classify Ly6 proteins in a superfamily distinct from the UPAR protein family, which also includes phospholipase inhibitors [26-28].

The first invertebrate Ly6SF member described was Sgp-2 (squid glycoprotein-2), which was isolated in squid in 1988 [29]. However, no functional data was published on this protein. The other invertebrate Ly6SF member, which was identified more recently, is *odr-2* and its homologues (HOT proteins) described in *C. elegans*. ODR-2 also

contains an N-terminal signal sequence followed by a Ly6 domain and a GPI-anchorage site and signal. The difference between the Ly6 domains in ODR-2 and mammalian Ly6 proteins is the spacings between the cysteines that make up the backbone of the Ly6 domain. Although the number of amino acids between the cysteines is well conserved among the *C. elegans* Ly6 proteins, their numbers are relatively higher than those of mammalian Ly6 genes. There are three isoforms of ODR-2, which differ in their N-terminal sequences. They are produced through alternative splicing, and one isoform, ODR-2b was shown to be important for olfactory behaviors and might be regulating signaling within a specific group of olfactory neurons. ODR-2b is highly expressed in sensory and motor neurons as well as interneurons. *Odr-2* mutant worms are deficient in chemotaxis [30].

Expression Patterns

Immune System Expression

Mammalian Ly6SF members are expressed in various tissues; however, a subgroup within the superfamily is expressed mainly in cells of hematopoietic origin. Since hematopoietic cells are highly differentiated, ly6 proteins have been very useful markers for different stages of differentiation. One of these genes is Ly6A/E, whose two alleles Ly6A.2 and Ly6E are mainly expressed in the bone marrow stem cells and the developing T-cells in the thymus [31]. The expression patterns and stages of these two alleles are different from each other in different T-cells [32]. Another Ly6 protein RIG-E, which is also known as TSA-1/Sca-2 and Ly6e, is expressed in various tissues as well as

| Ly6 Protein | Also known as | Expression Sites |
|--------------------|----------------------|--|
| Ly6A/E | Ly6A.2, Ly6E | Bone marrow stem cells, developing T-cells, astrocytes |
| Ly6e | RIG-E, TSA-1/Sca2 | Widespread expression, thymocytes and myeloid cell lines |
| Ly6C | | CD8 ⁺ T-cells, splenic macrophage progenitors, |
| Ly6G | | Mature granulocytes |
| Ly6I | | Bone marrow cells, granulocytes, macrophages, immature B-cells |
| CD59 | | Erythrocytes, lymphocytes, retina |
| PSCA | | Prostate epithelium, prostate cancer, pancreas cancer, retina |
| Ly6D | E48, ThB | Keratinocytes, lymphocytes |
| SLURP-1 | | Epithelium, keratinocytes, cornea, endothelium |
| SVS-VII | | Seminal vesicle secretion |
| Ly6H | | Brain, acute leukemia cell lines |
| Lynx1 | | Brain, lung |

Table 1: Summary of expression patterns of Ly6SF proteins.

thymocytes and myeloid cell lines [33, 34]. Ly6C is a useful marker for memory CD8 T cells [34], and splenic macrophage progenitors [12]. Its expression pattern allows differentiation between macrophage progenitors from mouse bone marrow and spleen [12]. Ly6G is used as Gr-1 marker for granulocytes and is only expressed in mature granulocytes during their differentiation [35]. Ly6I has a distinct pattern of expression like the other members of Ly6SF. Its expression *in vivo* is most abundant on bone marrow cells and it is co-expressed with Ly6C on granulocytes and macrophages. However, Ly6I is also expressed on immature B cell populations that do not express Ly6C, to which it is 80% similar in sequence. Expression on mature B cells in spleen is uniformly low [6]. Ly6I was isolated by homology to Ly6C and it is 70% similar at the protein level to a subset of the Ly6SF that also includes Ly6A/E, Ly6C, Ly6F and Ly6G [6].

CD59, another member of the Ly6SF that is expressed in cells of hematopoietic origin, is not located on the same chromosomal location as the other members of this subfamily [13]. CD59 is located on chromosome 2 in mice, and on 11p13 in humans. It is expressed in erythrocytes and lymphocytes in mice and humans (Table 1).

Expression in Epithelial Cells

While many Ly6SF members are expressed primarily in the cells of the immune system, others are strongly expressed in other tissues. Ly6D, which is also known as thymocyte antigen-B (ThB) in mice and E48 in humans, is expressed in keratinocytes in humans, but not in lymphocytes [9, 36, 37]. In mice, Ly6D has two alleles, one of which is expressed in both keratinocytes and lymphocytes. The second allele is only expressed

in keratinocytes. The expression of the first allele in keratinocytes is much higher than its expression in lymphocytes. There is 67% sequence homology between mouse and human Ly6D proteins [2, 11, 38]. Both Ly6D and Ly6K are over-expressed in head-and-neck squamous carcinoma [39].

SLURP-1 expression is very strong in epithelium, keratinocytes, cornea and endothelium. Together with prostate stem cell antigen (PSCA) and CD59, they constitute 0.5% of total mRNA in retina [40]. PSCA was first identified as a candidate antigen for identifying people with prostate cancer. It is expressed in basal cell epithelium in normal prostate and its expression is highly elevated in patients with prostate and pancreas cancer [41, 42]. SVS VII, another secreted Ly6SF member, is one of the seven major proteins in mouse seminal vesicle secretion [25].

Expression in Nervous System

Among the mammalian Ly6SF genes that are expressed in nervous system, Ly6A/E expression was also shown in astrocytes surrounding blood vessels in the brain [43]. Expression of lynx1 is primarily in neurons in the brain, and its expression pattern will be explained in detail later this chapter.

Ly6H is another Ly6SF member that is expressed mainly in non-hematopoietic cells. hLy6H was shown to be expressed predominantly in the brain in Northern blot analysis. Its expression is high in several regions in the brain including cerebral cortex, amygdala, hippocampus and subthalamic nucleus, whereas it's low in thalamus, corpus callosum and cerebellum in humans. Ly6H is also expressed in acute leukemia cell lines [44]. The mouse Ly6H was also isolated and shown to be highly expressed in brain, whereas its expression was undetectable in various tissues including thymus, spleen,

liver, lung, kidney, heart, skeletal and smooth muscle and prostate [45]. In embryos at age E10.5, Ly6 is expressed in ventral neural tube, and at age E12.5, scattered cells in spinal cord and rhombocephalon were positive for Ly6H expression [46].

Activity and Function

Ly6 proteins were first identified as markers for cellular differentiation, and they have also been implicated in cell-to-cell adhesion, signaling and receptor modulation. Some Ly6 proteins are over-expressed in certain types of cancers, and have been used as markers for cancer cell differentiation. Some of these functions are summarized below.

Cell Adhesion

Several Ly6SF members have been shown to be important for cell-to-cell interactions *in vivo* and *in vitro*. Transfection of mammalian cultured cells with Ly6D increases desmosomal cell-cell adhesion of keratinocytes [9], whereas anti-Ly6C monoclonal antibodies prevent cell adhesion of endothelial cells [47]. One of the secreted members of this family, SVS-VII, has binding sites that cover the entire surface of the sperm. Upon ejaculation, binding of SVS-VII to sperm surface enhances the sperm motility [25]. *In vivo* support for the role of Ly6 in cell adhesion came from Ly6A/E transgenic mice. Overexpression of Ly6A/E on lymphocytes in transgenic mice results in increased cell adhesion [32, 48]. Ly6A/E was also shown to have a role in cell adhesion in lymphocytes and bone marrow stroma *in vitro* [31, 48].

Signaling

Ly6SF members that are expressed in hematopoietic cells have been shown to be involved in various signaling processes in cell differentiation, activation and apoptosis [49-51]. Expressed in lymphocytes, Ly6e inhibits T-cell receptor (TCR) mediated T-cell activation and apoptosis. Ly6e was shown to be physically associated with CD3 ζ chains in T-cell cells with IP and confocal microscopy. When stimulated by anti-Ly6e antibodies, CD3 ζ chains were tyrosine phosphorylated [52]. *In vivo*, anti-TCR/ CD3-mediated apoptosis of thymocytes is blocked by injection of anti-Ly6e antibodies [53, 54].

Another example of Ly6 role in signaling is the role of Ly6A/E in lymphocytes. Overexpression of Ly6A/E on lymphocytes in transgenic mice causes aberrant lymphocyte maturation [55]. Studies in Ly6A/E null-mutant mice suggest that it may have an inhibitory role in regulating T-cell activation and T-cell Ag-specific immune responses [51].

CD59 is one of the best-described members of the mammalian Ly6SF of proteins [14]. CD59 inhibits formation of membrane attack complex, thus protects cells from complement mediated lysis [13]. CD59 is also implicated as a signal transducing molecule for human T-cell activation [56].

Some Ly6SF genes have been associated with cell death and malignancy of tumor cells. In cells that have gone through malignant transformation, levels of some Ly6 proteins are upregulated. PSCA expression is highly elevated in prostate cancer [42] and increased expression of Ly6A/E has been associated with malignancy of tumor cells [57]. Expression of another Ly6SF member, GPI-anchored-molecule-like protein (GML),

whose expression is regulated by p53, suppresses the growth of esophageal cancer cells [58]. Ly6e expression in promyelotic leukemia is strongly regulated by retinoic acid, which is a differentiation inducer that causes clinical remission in about 90% of the patients with acute promyelotic leukemia [10].

Ligands

Although several ligands have been identified for various Ly6SF members, physiological importance and results of Ly6-ligand binding have not been clearly established yet. Ly6A/E was shown to bind to a 66 kDa protein that is expressed in spleen, thymus, macrophages and B-cells [48]. Ly6D binds to an unknown polypeptide that is 9 kDa and has a widespread expression. This ligand was described in more detail than the first ligand and was shown to share homology with notch proteins [59]. Ly6A/E, Ly6I and Ly6C all bind to CD22 in B-cells [3]. On the other hand, SVS VII, which is a secreted Ly6SF member, is thought to bind to lipids, specifically phosphatidylethanolamine and phosphatidylserine, on the surface of sperm cells [25].

Ion Channel Modulation

In addition to α -neurotoxins that inhibit nAChRs, three-finger-toxins include several toxins that bind to muscarinic receptors [60], cardiotoxins that form channels in cell membranes [20], calciseptins and other toxins that block the L-type calcium channels [61, 62], and fasciculins that inhibit acetylcholinesterase (Cervenansky et al, In *Snake Toxins* (Harvey, A.L., ed), pp. 131-164. Pergamon Press, New York.).

The ARS-B gene encodes SLURP-1, which is one of the three known secreted mammalian Ly6SF members. ARS-B is mutated in patients with a rare autosomal

recessive skin disorder called Mal de Meleda [63]. This disease is characterized by progressive keratotic lesions, which can result in reduced mobility of hands and feet and possibly spontaneous amputation of digits. SLURP-1 was shown to increase acetylcholine elicited macroscopic currents in $\alpha 7$ nicotinic receptor expressing oocytes [64]. The modulatory effect of SLURP-1 on $\alpha 7$ receptors might explain the clinical phenotype of Mal de Meleda. SLURP-1 increases activities of caspases 3 and 8, and expressions of p21, caspase 3, cytokeratin 10 and transglutaminase type I. Carbachol, an agonist for nicotinic receptors, increases the effect of SLURP-1 on gene expression which shows this effect might be through modulation of nicotinic receptor activity [65].

SLURP-2 was first identified as a protein that is over expressed in patients with psoriasis vulgaris. Psoriasis vulgaris is a fairly common (affects ~2% of the population) genetic disorder that is characterized by hyperproliferation of epidermal keratinocytes and inflammation in the affected regions through T-cells, neutrophils, mast cells and macrophages. It has been suggested that SLURP-2 might be involved in pathophysiology of psoriasis vulgaris [24]. When cultured keratinocytes were treated with SLURP-2, their numbers increased significantly and this effect was blocked by mecamylamine treatment. Mecamylamine is a potent antagonist of nicotinic receptors. SLURP-2 also delays differentiation of keratinocytes and demonstrates anti-apoptotic effects [66].

Binding of α -neurotoxins and lynx1 to nAChRs, and modulatory effects of snake toxins, lynx1, SLURP-1 and SLURP-2 makes nicotinic receptors interesting targets for other members of the Ly6SF family as well [64-67].

Nicotinic Acetylcholine Receptors

Diversity and Structure

nAChRs are ion gated receptors and belong to a gene superfamily that also includes GABA, glycine and 5-HT₃ receptors [68]. There are ten different alpha subunits (α 1-10), four different beta subunits (β 1-4), and gamma (γ), delta (δ) and epsilon (ϵ) subunits that combine to form functional receptors. The muscle nAChR are composed of α 1, β 1, γ and ϵ subunits in adults and α 1, β 1, γ and δ subunits in embryo. The stoichiometry of the muscle subunit is 2 alpha subunits, 1 β , 1 γ and 1 ϵ or δ subunit (reviewed in [69-71]. The other subunits in nAChR family were considered neuronal nAChR until recently. However, these subunits are expressed in epithelial tissue as well (reviewed in [72, 73]).

According to the phylogenetic analysis done by Tsuyonoma and Le Novere, α 9, α 7 and α 8 are the closest subunits to the ancestral subunit (Figure 4). These subunits can form functional receptors without oligomerizing with beta subunits [74, 75]. Insect and nematode receptor subunits form the second group in the phylogenetic tree. The second group is divided into two major subfamilies. The first major subfamily is composed of non-alpha-muscle receptor subfamily (γ , ϵ , δ , β 1) and β 2– β 4 subfamily. The second major subfamily is divided into two main branches: α 1 subfamily and another group that is composed of α 5– β 3, α 2– α 4 and α 3– α 6 subfamilies. The M2

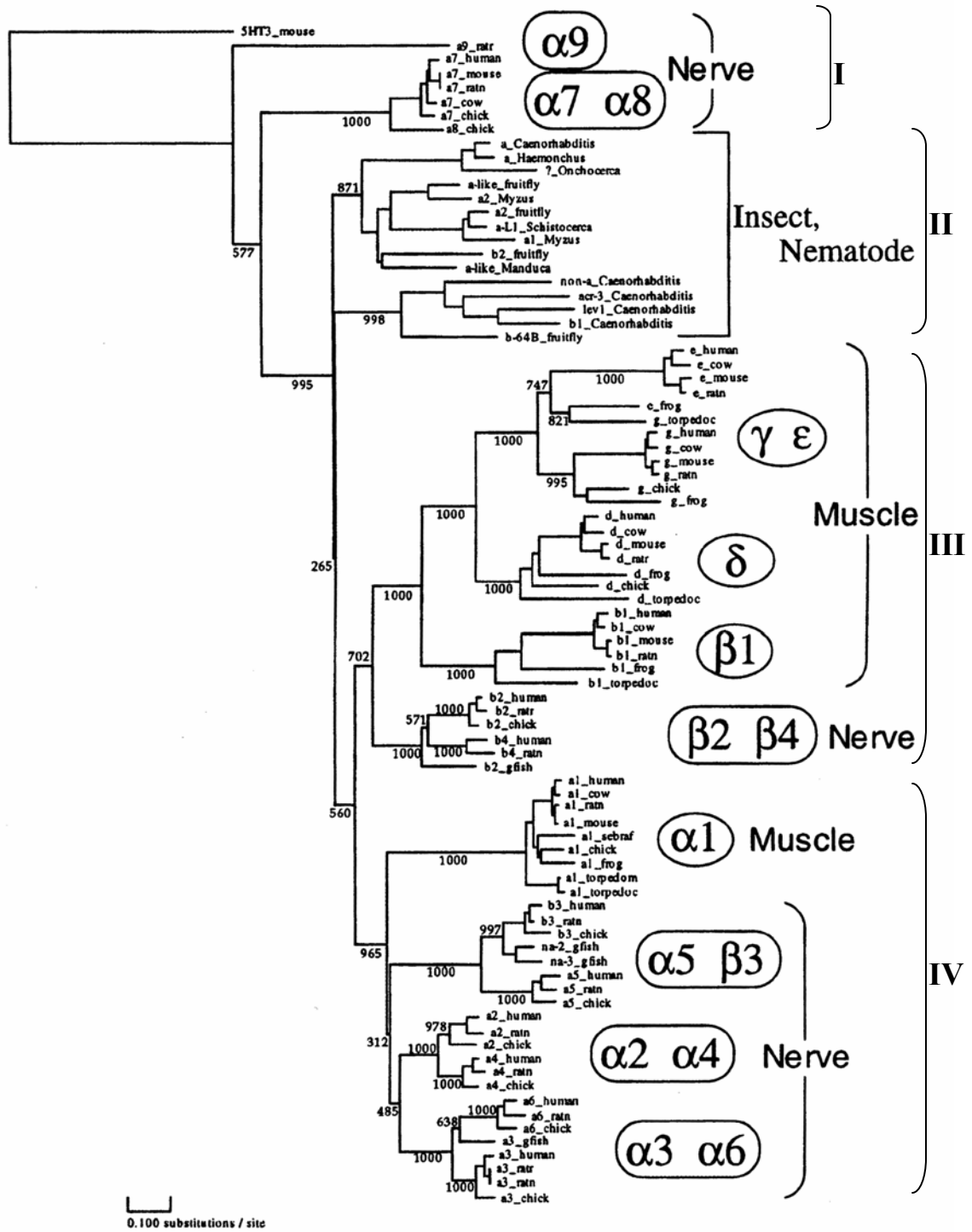


Figure 4: nAChR Phylogenetic Tree. nAChR subunits form 4 distinct groups. First group consists of homomer forming subunits $\alpha 7$, $\alpha 8$ and $\alpha 9$. Second group is composed of invertebrate nicotinic receptors. Muscle subunits $\beta 1$, γ , δ , ϵ and $\beta 2$ and $\beta 4$ subunits comprise the third group. Fourth group consists of $\alpha 1$ -muscle, $\alpha 5$, $\beta 3$, $\alpha 2$, $\alpha 4$, $\alpha 3$ and $\alpha 6$ subunits. (Tsunoyoma et. al, Evolution of Nicotinic Acetylcholine Receptor Subunits, Mol. Biol. Evol, 1998)

regions of all the subunits are the most conserved parts of the receptor amino acid sequences [74, 75].

The pharmacological properties of different homopentamers and heteropentamers of nicotinic subunits are variable *in vitro* [76, 77]. However, in nicotinic-receptor knock-out (KO) animals, it has been observed that function of one subunit can be replaced by another in several cases [78-80]. Although it is generally assumed that different pharmacological properties *in vitro* may account for the physiological diversity *in vivo*, this doesn't look like the reason for the diversity of the nicotinic receptors. Instead, the conservation of the diversity of the subunits might be due to the variety of their cellular and subcellular distribution patterns *in vivo* (reviewed in [69-71]).

Nicotinic receptors are pentameric in structure. Each subunit contains an extracellular ~200 aa long N-terminal domain, four transmembrane domains (M1-M4), and an intracellular connection between M3 and M4 that forms a large cytoplasmic domain [81, 82]. The structure of acetylcholine binding protein (AChBP) was used as a template for computational modeling of the nicotinic receptors [83-85]. These models were used to improve the electron microscopy data for the nicotinic receptor structure [86-88]. M2 transmembrane domain lines the channel pore [89]. The subunit interfaces between the N-terminal extracellular domains of the alpha subunit and the adjoining subunit forms the agonist binding site [90, 91].

Expression patterns

Neuronal

Expression patterns of nicotinic receptor subunits vary among different species and among different strains of mice [92, 93]. The most widely expressed nicotinic receptor subunits in the CNS are $\alpha 7$, $\alpha 4$ and $\beta 2$ subunits. $\alpha 7$ expression has been observed in CA2/3, subiculum, amygdala, cortex, cochlear nucleus, Purkinje cells of the cerebellum, thalamus, hypothalamus and several brainstem nuclei in rat brain [94-97]. $\alpha 7$ nicotinic receptors are also expressed in CA1 region of rat and mouse hippocampus [98-100]. $\alpha 4\beta 2$ is the most prevalent heteromeric receptor combination found in rat brain. $\alpha 4$ subunit expression is detected in olfactory bulb, purkinje and granular cells of cerebellum, cerebral cortex, amygdala, thalamus, hippocampus, midbrain, and medulla in rat brain [100-103].

In the peripheral nervous system, the most widely expressed heteromeric nicotinic receptors are $\alpha 3\beta 2$ and $\alpha 3\beta 4$ receptors. $\alpha 3$ subunit is expressed at high levels in peripheral nervous system and in low amounts in the cerebral cortex, hippocampus and cerebellum in rat [100, 104, 105]. $\alpha 3\beta 2$ expression was detected in the optic chiasm, habenula, and colliculus, and $\alpha 3\beta 4$ expression was observed in the habenula-peduncular system, cerebellum, developing brain and brainstem motor nuclei, including motor trigeminal nucleus, nucleus ambiguus, and dorsal motor nucleus of vagus [103, 106]. $\beta 4$ subunit also has a widespread expression throughout the rodent brain. In mice, $\beta 4$ subunit expression has been observed in the midbrain, dispersed cells in the hippocampus, olfactory regions, subthalamic nucleus, trigeminal system and granule cells of the

cerebellum [107]. In rat brain, $\beta 4$ expression was detected mainly in medial habenula, but also in the hippocampal formation, entorhinal cortex, trigeminal motor nucleus, interpeduncular nucleus and olfactory regions [108]. In rat cerebellum, expression of $\alpha 3\alpha 4\beta 4$ and $\alpha 3\alpha 4\beta 2$ receptors have also been detected [109].

Other nAChR subunits less widely expressed. For example, $\alpha 2$ is expressed in olfactory bulb, interpeduncular nucleus, ventral and dorsal tegmental nucleus, median raphe nucleus, and reticular nucleus, hippocampus, and amygdala in both mice and rats. $\alpha 2$ subunit is also expressed in gigantocellular reticular nucleus and raphe magnus of mice but not in rat brains [110]. $\alpha 5$, which is usually expressed together with another α subunit, is highly expressed in subiculum, parasubiculum and presubiculum of hippocampus, substantia nigra, interpeduncular nucleus, dorsal motor nucleus of vagus and ventral tegmental area [111]. $\alpha 6$ subunit has a very specific expression pattern, and it is expressed in substantia nigra, ventral tegmental area and locus coeruleus [112]. $\alpha 9$ and $\alpha 10$ subunits are expressed together in adult mechanosensory hair cells [113].

$\alpha 2$, $\alpha 3$, $\alpha 4$, $\alpha 5$, $\beta 2$ and $\beta 4$ are also expressed in rat spinal cord [110, 114].

Expression of almost all subunits are developmentally regulated, and some of them have transient expression in certain regions of CNS [115].

Non-neuronal

Acetylcholine is found not only in neurons, but also in bacteria, protozoa and algae, which shows that it has emerged very early during evolution. Acetylcholine synthesizing enzymes, as well as acetylcholine receptors are expressed in various non-neuronal tissues. $\alpha 3$, $\alpha 5$, $\alpha 7$, $\beta 2$ and $\beta 4$ AChR subunits are expressed in bronchial

epithelial cells, and $\alpha 3$, $\alpha 4$, $\alpha 5$, $\alpha 6$ and $\alpha 7$ are expressed in alveolar epithelial cells in rodent, monkey and human airways [116-119].

In human keratinocytes, expression of $\alpha 3$, $\alpha 4$, $\alpha 5$, $\alpha 7$, $\alpha 9$, $\alpha 10$, $\beta 2$ and $\beta 4$ subunits have been detected with RT-PCR (reverse transcription-polymerase chain reaction) and immunohistochemistry [120-122]. In rat urinary bladder epithelial cells, $\alpha 3$, $\alpha 5$, $\alpha 7$, $\beta 3$ and $\beta 4$ receptor subunit expression were detected with RT-PCR and western blots [123]. In mammalian sperm, expression of $\alpha 7$ subunit was observed in acrosome [124, 125]. Presence of $\alpha 3$, $\alpha 5$, $\alpha 7$ and $\beta 2$ nicotinic receptor subunits were also revealed in esophageal epithelia [126].

In lymphocytes, $\alpha 4$, $\beta 4$, $\alpha 3$, $\alpha 7$ and $\beta 2$ nicotinic receptor expression has been detected in mice, rats and humans [127-129]. Expression of $\alpha 2$, $\alpha 5$ and $\alpha 7$ has also been detected in human mononuclear leukocytes [128].

Function

Pharmacology and Physiology of nAChRs

nAChRs are allosteric ligand-gated channels. Physiological and pharmacological properties of different heteromeric and homomeric combinations of various subunits differ from each other. Mecamylamine blocks all nicotinic receptors, but the blocking mechanism differs among various subunit combinations [130]. For some combinations, it is a competitive antagonist, for others, it is non-competitive antagonist for open channels [130-133]. Mecamylamine can pass through the blood brain barrier, however, another potent antagonist for almost all nicotinic receptors, hexamethonium, cannot. Since

hexamethonium does not block muscle nAChRs, hexamethonium is used to block neuronal nicotinic receptors outside the CNS [131, 134].

The most widely expressed nicotinic receptors in the CNS, $\alpha 7$ and $\alpha 4\beta 2$ also show distinct pharmacological properties. $\alpha 7$ nAChRs are desensitized faster than $\alpha 4\beta 2$ nAChRs and are more permeable to Ca^{2+} than $\alpha 4\beta 2$ nAChRs [135-137]. In addition, $\alpha 7$ nAChRs can be activated by choline and are blocked by α -bungarotoxin and methylcaconitine (MLA), whereas $\alpha 4\beta 2$ nAChRs are not activated by choline, and are not affected by α -bungarotoxin or MLA [138, 139]. Instead, another toxin, dihydro-beta-erythroidine (DH β E) is a potent antagonist for $\alpha 4\beta 2$ receptors [140]. Pharmacological differences like these allow researchers to determine what types of receptors are present in a cell by comparing responses to such drugs.

$\alpha 3\beta 2$ and $\alpha 3\beta 4$ are the two most widely expressed nicotinic receptor combinations outside the CNS. $\alpha 4\beta 2$, $\alpha 3\beta 2$ and $\alpha 3\beta 4$ have similar channel conductances; however, their desensitization kinetics are different [82]. $\alpha 3\beta 4$ receptors desensitize faster than $\alpha 4\beta 2$ receptors, however, slower than $\alpha 3\beta 2$ or $\alpha 7$ nAChRs [76, 135, 141]. $\alpha 3$ containing nicotinic receptors are blocked by α -conotoxin-MII and κ -bungarotoxin but not by α -bungarotoxin or DH β E [142, 143].

Physiological Function

Neuronal

Nicotine was shown to enhance spatial and associative learning performances, as well as attention and memory [144]. On the other hand, nicotinic receptor antagonist, mecamylamine, deteriorates memory [145]. Nicotinic receptors also play vital roles in the

control of synaptic transmission in the peripheral nervous system as well as the CNS [146, 147]. Unlike most of the other subunits, $\alpha 3$ subunit is essential for survival of mice. $\alpha 3$ KO mice show major autonomic defects which results in 50% lethality at birth. The remaining animals die in the first three months. The phenotype of $\alpha 3$ KO mice has been proposed as a model for megacystis microcolon intestinal hypoperistalsis [148].

Although $\beta 2$ - $\beta 4$ double KO animals show a similar phenotype to $\alpha 3$ KO mice, neither $\beta 2$ KO nor $\beta 4$ KO mice show any early lethality [78]. $\beta 2$ KO animals exhibit reduced antinociception, impaired spatial learning, increased neurodegeneration with aging and loss of nicotine self-administration [149-151]. $\beta 4$ KO mice on the other hand have altered anxiety related phenotype and the excitatory postsynaptic potentials (EPSP) in these mice were strongly decreased, with a peak current of only 2% of the wild-type (WT) mice [152]. $\beta 3$ cannot form functional receptors without another β subunit, and $\beta 3$ KO mice exhibit increased locomotion [153].

Deficiency of $\alpha 4$ subunit results in reduced antinociception as well as anxiety related phenotypes [154-156]. Although $\alpha 7$ KO mice do not show any behavioral or physiological abnormalities, $\alpha 7$ -L250T mice, which have slowly desensitizing $\alpha 7$ currents, were not viable 24 hours after birth [138]. Mice that are heterozygous for this mutation are viable, but they are more vulnerable to nicotine induced seizures [157, 158]. $\alpha 6$ KO mice show normal behavior and no major physiological problems [159]. $\alpha 9$ null mutant mice have suppressed cochlear response and abnormal efferent connections between olivary complex and cochlea, however, they exhibited no major abnormalities in audition, motor coordination or balance [160] (Table 2).

Implication in Disease

Alterations in nicotinic receptor activity have been shown to be involved in the pathophysiology of various diseases including Alzheimer's disease, Parkinson's disease, autism, anxiety disorders and autoimmune diseases. Alzheimer's disease, which affects 2-6% of the population over the age of 65, is characterized by a deficit in the cholinergic activity in the brain. The activity of the two enzymes that are involved in the synthesis and degradation of acetylcholine are decreased by 90% in patients with Alzheimer's disease. Although cholinergic transmission is important in Alzheimer's pathophysiology, abnormalities in other transmission systems including glutamatergic and serotonergic transmission are also involved (reviewed in [161]). Studies have shown that expression of several nicotinic receptor subunits are down regulated in Alzheimer's patients including $\alpha 7$, $\alpha 4$, $\alpha 3$ and $\beta 2$ subunits [162-164]. It has also been demonstrated that β -amyloid activates nicotinic receptors under certain conditions, and neurons that express $\alpha 7$ nicotinic receptors are preferentially killed by beta amyloid [165, 166]. Therefore it has been hypothesized that the apoptosis induced by beta-amyloid might be through disruption of intracellular calcium levels by nicotinic receptor activation [167]. Currently, acetylcholinesterase inhibitors are used for treating symptoms of Alzheimer's disease, and cholinergic system continues to be a drug target for future therapies [168].

Parkinson's disease is a neurodegenerative disease that affects 1% of the population over the age of 65 [169], There's a significant loss of nicotinic receptors in Parkinson's disease patients [170]; therefore, nicotinic receptors have been suggested to be used as drug targets for Parkinson's disease. Nicotine has been shown to have a neuroprotective effect in Parkinson's disease patients [171, 172]. Effect of nicotine on

cognition in PD patients has also been studied, but there have been some contradictory results. Some studies have shown that nicotine improves cognition in Parkinson's disease patients while others have demonstrated nicotine has no positive effect [173-176]

Autism is a relatively common developmental disorder that affects 1 child in 166 and is considered to be primarily genetic [177-179]. Several neurotransmitter systems, including cholinergic transmission, have been implicated in the neuropathology of this disease [180-183]. A significant loss of cholinergic binding sites was observed in the cerebral cortex and cerebellum of autistic patients [182, 183]. Specifically $\alpha 4$ and $\beta 2$ subunits are down-regulated in the cortex of autistic brains whereas $\alpha 7$ subunit expression was the same as healthy subjects [184].

Although smokers generally accept nicotine as an anxiolytic [185, 186], it has been shown to have an anxiogenic effect in anxiety disorders in several studies. One study showed that young adults who smoke are more likely to have anxiety disorders than non-smoking ones [187]. Increased daily nicotine consumption was shown to be associated with a higher risk of the first time occurrence of panic attacks [188]. In animal models, the effect of nicotine depends on the administration of nicotine, the emotional and physical state of the subject and the type of test that is used to measure the levels of anxiety (reviewed in [189]). This might be due to the fact that nicotinic receptor activation regulates not only stimulatory, but also inhibitory and modulatory transmission in various brain regions. So, depending on which nicotinic receptors on which region of the brain are affected first, the outcome of the nicotinic administration might be different [189].

Non-neuronal

Tobacco smoking causes cancers in lung, oral cavity, esophagus, pancreas, stomach and bladder. In non-neuronal tissues, nicotinic receptor activation has been implicated in many functions including regulation of gene expression, adjusting intracellular Ca^{2+} , cell-adhesion, cell-differentiation. In bronchial epithelial cells, smoking increases nicotinic receptor expression, and exposure to nicotine elevates intracellular Ca^{2+} levels. Exposure to mecamylamine altered cell adhesion and motility, and these effects were reversed by nicotine. However, long-term exposure to nicotine caused a similar effect to mecamylamine, suggesting that the induction of desensitization through nicotine has a similar effect to receptor blocking [116]. $\alpha 3\beta 2\alpha 5$ nAChRs were found to modulate wound repair process in human bronchial epithelial cells. The cells that were exposed to nicotine were faster in wound healing, and the speed of cell migration to the wound site was inhibited by mecamylamine, κ -bungarotoxin and α -conotoxin-MII [190].

In cultured keratinocytes, cholinergic drugs can change cell proliferation, adhesion, migration and differentiation through adjusting levels of intracellular calcium. Changes in calcium levels then modify the expression and function of nicotinic receptors [122, 191-193]. Keratinocytes exposed to nicotinic receptor antagonists kappa-bungarotoxin and mecamylamine had cell detachment and stopped migrating [120]. Exposure to nicotine elevates expression levels of $\alpha 7$, $\beta 2$ and $\beta 4$ subunits as well as cell cycle and cell differentiation markers in oral keratinocytes. This elevation is blocked by mecamylamine, which suggests that some pathophysiological results of nicotine in oral

tissue is due to nicotinic receptor activation [194]. More specifically, blockers of $\alpha 3\beta 2$ receptor, $\alpha 3$ -antisense mRNA and α -conotoxin-MII were able to reverse the effects of nicotine on oral keratinocytes, suggesting that $\alpha 3\beta 2$ receptor combination is the main culprit in nicotine pathophysiology in the oral cavity [195].

In rat urinary bladder, exposure to nicotine, choline and a nicotinic receptor antagonist, hexamethonium, increased the interval between contractions, and an $\alpha 7$ subunit antagonist prevented this effect. These results demonstrate the importance of nicotinic receptor activation in urinary bladder control through the receptors expressed in the epithelial cells [123]. Activation of $\alpha 7$ containing nicotinic receptors was also shown to effect acrosome reaction in mammalian sperm which is crucial for fertilization [196]. Nicotinic receptors found in esophageal epithelia were demonstrated to be important for regulation of cell adhesion and motility and nicotine was shown to stimulate proliferation of gastric cancer cells [126, 197, 198]. The effect of nicotinic receptor activation on the gastric system was further demonstrated in $\alpha 5$ -subunit-KO mice. $\alpha 5$ KO mice have significantly more colitis in their colonic epithelium than WT mice [199].

In lymphocytes, nicotinic receptors regulate Ca^{2+} signaling [128, 129]. Nicotinic receptor expression is downregulated by nicotine in lymphocytes, suggesting that pathobiology of smoking in the immune system might be through this mechanism [129, 200]. $\alpha 7$ nicotinic receptors were established to be crucial for inhibition of cytokine synthesis in human macrophages [201]. $\alpha 1$, $\alpha 3$ and $\alpha 9$ subunits were also implicated in various autoimmune diseases including myasthenia gravis and pemphigus [202].

Lynx1

Sequence and Structure

Lynx1 was initially identified as a developmentally regulated gene expressed in mouse cerebellum. Lynx1 encodes a 116 aa long protein that has an N-terminal signal sequence, a Ly6 domain and a C-terminal GPI anchorage site and signal sequence (Figure 2). The sequence alignment shows that the Ly6 domain of lynx1 has all the mammalian-conserved cysteine residues as well as the N-terminal leucine/isoleucine and the C-terminal asparagines [203].

Expression

Lynx1 has very strong expression in specific regions in adult mouse brain and lungs. In brain, lynx1 is highly expressed in the CA2 and CA3 regions of hippocampus, layer 5 in cortex, Purkinje cells in the cerebellum and large pyramidal cells in deep nuclei [203]. It is also expressed in high levels in basolateral amygdala, medial habenula and mitral cells in olfactory bulb (unpublished data). In lungs, lynx1 was shown to be expressed in bronchial epithelial cells, where they colocalize with $\alpha 4$, $\beta 2$ and $\beta 4$ containing nicotinic receptors [204, 205].

Lynx1 colocalizes with $\alpha 4$ containing nicotinic receptors in neurons in several regions in adult mouse brain, including cortex, amygdala, habenula and substantia nigra. $\alpha 7$ containing nicotinic receptors colocalize with lynx1 on the membranes of neurons in cortex, hippocampus, amygdala and thalamic reticular nucleus [67].

Function

Since the expression pattern of lynx1 was similar to those of the nAChRs and it has the same three-finger structure as α -neurotoxins that block nicotinic receptors, Miwa et. al. and Ibanez-Tallon et. al. have analyzed the functional interaction between the nicotinic receptors and lynx1. lynx1 co-immunoprecipitated with $\alpha 4\beta 2$ nicotinic receptors and $\alpha 7$ nicotinic receptors when expressed in HEK293 cells and pulled down with nicotinic receptor subunit specific antibodies. This demonstrated that lynx1 forms stable complexes with nicotinic receptors [67]. In order to analyze the effect of lynx1 on nicotinic receptors, electrophysiology and lynx1 KO animal model was used.

Electrophysiology

Lynx1 was shown to modulate desensitization kinetics of $\alpha 4\beta 2$ nAChRs *in vitro*. It also alters the sensitivity of the nicotinic receptors to their agonists *in vitro* and *in vivo* [67, 203, 206] (Miwa et. al., Neuron, 2006, manuscript accepted). Detailed analysis of these modulations is described below.

Oocyte experiments

In the first paper published by Miwa, et al., secreted lynx1 was shown to increase the acetylcholine (ACh) elicited macroscopic currents when measured by voltage clamp recordings. When exposed to secreted Lynx1, *Xenopus* oocytes expressing $\alpha 4\beta 2$ nicotinic receptors did not elicit any currents, which showed that secreted lynx1 is not acting as an agonist. However, in the presence of secreted lynx1, amplitude of the ACh elicited currents increased by 30-40% [203].

When expressed together with $\alpha 4\beta 2$ nicotinic receptor subunits, GPI-anchored lynx1 was shown to significantly increase their desensitization rate in *Xenopus* oocytes. The fast time-constant for the desensitization of $\alpha 4\beta 2$ receptor without the presence of lynx1 was measured to be 2.73s, whereas the fast-time-constant was measured to be 1.09s for oocytes expressing $\alpha 4\beta 2$ receptors and lynx1 [67].

Lynx1 also decreases the sensitivity of $\alpha 4\beta 2$ receptors to their agonist, ACh. Voltage-clamp recordings on *Xenopus* oocytes expressing $\alpha 4\beta 2$ receptors which were exposed to different concentrations of ACh revealed that lynx1 shifts EC50 of $\alpha 4\beta 2$ receptors from 1.8uM to 35uM ACh [67].

According to the three-dimensional model of Lynx1 which was generated by using structures of CD59, α -bungarotoxin and cardiotoxins as independent templates, cysteines 1-5, 2-3, 4-6, 7-8 and 9-10 form disulphide bridges that determine their tertiary structure [203]. When single cysteines were mutated to alanine to test the importance of each disulfide bond, bridges between cysteines 2-3 and 4-6 were found to be the critical determinants of the effect of lynx1 on desensitization kinetics of nicotinic receptors through mutational analysis of the cysteine residues. These cysteines are located on finger 1 of the three-finger structure [67].

Cultured Mammalian Cells

Patch clamp recordings on $\alpha 4\beta 2$ transfected and $\alpha 4\beta 2$ -lynx1 transfected cultured mammalian cells revealed modulatory effect of lynx1 on single channel recordings. When perfused with ACh, $\alpha 4\beta 2$ transfected cells fired for several tens of seconds, however, when transfected with $\alpha 4\beta 2$ and lynx1, the channel events only lasted less than

10 seconds. This result provided further evidence that lynx1 enhances the rate and extent of desensitization of $\alpha 4\beta 2$ nicotinic receptors.

Slice Physiology

Patch clamp recordings in medial habenula region of WT and lynx1 KO mouse brain sections revealed that lynx1 decreases the agonist sensitivity of nAChRs. The amplitudes of currents elicited in WT brain sections were larger than the currents in KO animals. To measure the difference in the EC50 of nicotinic receptors due to lynx1, the WT and KO brain sections were exposed to different concentrations of acetylcholine, and EC50 was observed to be $\sim 89\mu\text{M}$ in WT sections whereas it was $\sim 9\mu\text{M}$ in lynx1 KO animals (Miwa et. al., Neuron, 2006, in press).

Anatomical Phenotype

Until ~ 9 months of age, there were no major anatomical differences between the KO and WT mice. After 9 months, increased vacuolation was observed in cerebellum and striatum of lynx1 KO mice with respect to WT littermates. Although the mechanism through which the vacuoles are caused is not clear, it was observed that the nicotinic receptor and lynx1 double KO mice have less vacuoles in their brains than the lynx1 KO animals (Miwa et. al., Neuron, 2006, in press).

Behavior

Lynx1 KO mice exhibited increased performance in associative learning, but no difference from WT mice in contextual learning, or anxiety tests. In fear conditioning experiments, lynx1 mice were trained to associate a tone to a mild electric shock, and next day their response to the training environment was measured. This response, which

is a measure of contextual associative learning, was the same as the WT mice. When the mice were placed in a novel environment and exposed to the training tone, the KO mice froze to tone more than WT mice, which demonstrates that lynx1 KO mice perform better in auditory-cue-associative learning tasks. Lynx1 KO mice performed similar to WT mice in two other contextual learning tests, passive avoidance conditioning test and Morris water maze learning. In anxiety related tests, elevated plus maze and light-dark box, lynx1 KO mice showed no difference from WT mice (Miwa et. al., Neuron, 2006, in press).

In rotarod test, which measures motor learning, lynx1 KO mice that drank saccharin water for 6 weeks performed similar to WT mice that were fed with saccharin water. However, lynx1 KO mice that drank nicotine for six weeks and had elevated nicotinic receptor activation due to it demonstrated better motor learning than WT mice that drank nicotine water (Miwa et. al., Neuron, 2006, in press).

Chapter 2:

Phylogenetic Inference of Ly6 Superfamily of Proteins

Introduction

Lynx1 is the founder member of a subfamily of Ly6SF proteins that modulates nicotinic receptors. Identification of SLURP-1 and SLURP-2 as modulators of nAChRs in keratinocytes further strengthened our theory that other Ly6SF members might be performing a similar function in CNS or other tissues. Nicotinic receptors have been implicated in many disease phenotypes and they have been drug targets for treating these diseases, however, the extensive diversity of its subunits and their overlapping widespread expression patterns has made it hard to find drugs that target the correct subunit or the expression area. Since one subunit might be regulating multiple functions in various regions of the brain, targeting one subunit also brings complications associated with side effects. Lynx1 has a very specific expression pattern and lynx1 KO animals have a specific phenotype related to associative learning. I have hypothesized that other members of lynx1 subfamily might target different functions related to nicotinic receptors, and therefore, will be valuable tools for understanding the mechanism of nicotinic receptor function and will be important drug targets.

Identification of Ly6SF proteins and Alignment of Sequences

In order to find other members of lynx1 subfamily, I have decided to identify and analyze phylogenetic relationships between novel and known Ly6SF members. I searched the vertebrate and invertebrate genomic DNA, cDNA and protein collections of both Celera and NCBI databases through homology searches for lynx1 and several ly6 genes. Among the genes that I have found, I selected the ones that shared gross exon-

intron structure similarity to lynx1 and the ones that had necessary cysteine residues to make up the Ly6 domain. I found 85 genes that have the same genomic structure as other characterized Ly6SF members and encode proteins containing only one Ly6 domain.

Sequence comparison of these putative proteins indicated that these Ly6 molecules are very divergent (*Figure 5*). It appears that except for the cysteines that form the backbone for the three-finger structure, primary sequences are not well conserved in Ly6SF genes. However, there were multiple amino acids that were more conserved than others. Some of these most conserved residues might be to provide structural integrity of the domain. Moreover, the aa's that are conserved exclusively in the Ly6SF proteins that modulate nicotinic receptors may be important for receptor selectivity. For example, the first residues of the Ly6 domains of most Ly6SF proteins were aliphatic amino acids, either leucine or isoleucine. The amino acids that were next to the first cysteine residue in most Ly6SF proteins were aromatic followed by a polar amino acid. Another amino acid that was conserved in most Ly6 domains was a positively charged amino acid at the end of the second loop, close to the disulphide bridge forming 6th cysteine, either a lysine or an arginine. In addition, the 5-6 amino acids at the end of the Ly6 domains of the majority of the Ly6SF proteins shared a strong sequence similarity. All the Ly6 domains ended with a cysteine-asparagine peptide, preceded by an amino acid that has a big side group. There were polar amino acids followed by amino acids with small side groups in the last 5-6 amino acids (aa) as well. The scheme is shown in figure 7.

| | | | | | | | | | | | | | | | | | | | | | | | |
|----------------|----|---------|-----|------|-------|---|---|-------|--------|----|-------|-----|------|-------|---------|------------------|----------------|------------|-------|----------|----|---|--|
| CD59-RABBIT | LM | YH | L | L | P | S | P | N | C | ST | V | TN | C | T | PN | HDA | LTAVSG | PRVYR | Q | CWRY | | | |
| CD59-PIG | LQ | YNC | I | N | P | A | G | S | C | TT | A | MN | C | S | HN | QDA | CIFVEAVPPKTTY | | Q | CWRF | | | |
| CD59-MARMOSET | LQ | YSCP | Y | S | T | A | R | C | TT | T | TN | C | T | SN | LDS | | LIAKAG | LRVYY | R | CWKF | | | |
| CD59-MONKEY | LQ | YSCP | L | P | TMESM | | E | C | TA | S | TN | C | T | SN | LDS | | LIAKAG | SGVYY | R | CWKF | | | |
| CD59-OWLMONKEY | LQ | YSCP | Y | P | T | T | Q | C | TM | T | TN | C | T | SN | LDS | | LIAKAG | SRVYY | R | CWKF | | | |
| CD59-GREENMONK | LQ | YNC | P | N | P | T | T | D | C | KT | A | IN | C | S | SG | FDT | LIARAG | LQVYN | Q | CWKF | | | |
| CD59-BABOON | LQ | YNC | P | N | P | T | T | N | C | KT | A | IN | C | S | SG | FDT | LIARAG | LQVYN | Q | CWKF | | | |
| hCD59 | LQ | YNC | P | N | P | T | A | D | C | KT | A | VN | C | S | SD | FDA | LITKAG | LQVYN | K | CWKF | | | |
| mCD59 | LT | YHCF | Q | PV | V | S | S | C | NM | N | ST | C | S | PD | QDS | | LYAVAG | MQVYQR | | CWKQ | | | |
| rLY6A | LN | YNC | T | M | IPFG | N | T | C | SST | A | T | CPY | | PDGV | | CAIQVAE | VMSSVRQKVKDHI | | C | | | | |
| mLY6A | LE | YQCY | G | VPFE | T | S | C | PS | I | T | CPY | | PDGV | | VTQEAA | IVDSQTRKVKNNL | | C | | | | | |
| PUT-LY6B | LN | YNC | T | M | IPFG | N | T | C | SST | A | T | CPY | | PDGV | | CTIQVAE | VVSVRLKVKSNL | | C | | | | |
| rLY6C | LK | YSCI | E | VPLN | A | N | C | ST | A | T | CPY | | SDGV | | CVSQVLE | AVEGSRRTAKSNL | | C | | | | | |
| mLY6F | LE | YNC | L | G | VSLG | I | A | C | KS | I | T | CPY | | PDGV | | CISQQV | ELIVDSQKNN | L | C | | | | |
| BC010764 | LQ | YECY | G | VPIE | T | S | C | PA | V | T | C | R | AS | DGF | | IAQNI | ELIEDSQRRLKTRQ | | C | | | | |
| hCP1610069 | LH | YCC | G | HE | | H | C | ES | L | VE | CAP | | TDKY | | CVITRAT | SPGGILV | MKS | C | | | | | |
| hCP49117 | IW | HQCT | G | FGG | | | C | SH | G | SR | C | L | RD | STH | | CVTTATR | VLSNTE | DLPLVTKM | | C | | | |
| mLY6I | LE | YQCY | G | VPFE | T | S | C | PS | F | T | CPY | | PDGF | | CVAQE | EEFIANSQRKVKRSRS | | C | | | | | |
| mLY6G | LE | YNC | I | G | VPPE | T | S | C | NT | T | T | CPY | | SDGF | | VALEI | IEIVDSHR | SKVKSNL | | C | | | |
| mCP17885 | LE | YNC | L | G | VSLG | I | A | C | KS | I | T | CPY | | PDGV | | CISQQV | ELIVDSQR | RKVKNNL | | C | | | |
| AK009303 | LR | YTS | | FAKP | | | C | DPV | P | RE | C | | RE | DEV | | GVS | VTSEQKEE | VIER | KQ | C | | | |
| mLY6C | LQ | YECY | G | VPIE | T | S | C | PA | V | T | CRA | | SDGF | | IAQNI | ELIEDSQR | RKLTTRQ | | C | | | | |
| hLY6E | LM | FSL | N | QKSN | L | Y | C | LK | P | TI | C | S | DQ | DNY | | VTVS | SAGIGN | LVTFGH | SLSKT | C | | | |
| mLY6E | LM | FST | D | QKNN | I | N | C | LW | P | VS | C | Q | EK | DHY | | ITLS | AAGFGN | VNLGYTLNKG | | C | | | |
| SCA-2-CHICKEN | LI | FSS | D | ASSN | W | A | C | LT | P | VK | C | A | EN | EEH | | VTTY | VGVGIG | KGQSISKG | | C | | | |
| hPSCA | LL | YSK | A | QVSN | E | D | C | LQ | V | EN | C | T | QL | GEQ | | WTAR | IRAVGL | LTV | ISKG | C | | | |
| mPSCA | LQ | YST | A | QMNN | R | D | C | LN | V | QN | C | S | LD | QHS | | FTSR | IRAI | GLVTV | ISKG | C | | | |
| mHEMT-1 | LT | HKYISN | TFS | | | | C | PKLSE | | | CS | SNL | RR | | | MTVS | FRVNI | RLLYV | LKD | C | | | |
| mHEMT-3 | MR | HSEQEHN | TFY | | | | C | PHIHY | | | CDMDI | RR | | | | LTVA | IRVNI | RLLYV | LKD | C | | | |
| mSlurp1 | FR | YTE | Q | PTAI | N | S | C | KN | I | AQ | C | K | ME | DTA | | KTVLE | TVEAA | FPFNHSP | MVTRS | C | | | |
| hSlurp1 | LK | YTK | E | PMTS | A | S | C | RT | I | TR | C | K | PE | DTA | | MTTL | VTEAE | YFPNQSP | VVTRS | C | | | |
| hGML | LR | HDAVIN | DFN | | | | C | PNIRV | | | CPYHI | RR | | | | MTIS | SIRINS | RELLVY | KN | C | | | |
| hNG24 | LR | HSCY | K | VP | V | L | G | C | VD | R | QS | C | R | LEPGQ | | LTTH | AYLGK | MWFSN | LR | C | | | |
| hLy6D | LR | HVCT | S | SSN | | | C | KHSVQ | | | CPASS | RF | | | | KTNT | TVEPL | RGNL | VK | KD | C | | |
| mLy6D | LR | HVCT | N | SAN | | | C | KNPQV | | | CPSNF | YF | | | | KTVT | SVEPL | NGNL | VLR | KE | C | | |
| AK010485 | LT | HVE | A | QNSY | A | | C | SNPSQ | | | CPGEK | KF | | | | LLAV | TRIF | ERFF | YVS | KQ | C | | |
| AK009282 | FK | FT | E | N | AGDN | Y | N | C | NR | W | AE | DKW | C | | PQDTQY | | LTV | HHFT | SHGR | STSIT | KK | C | |
| AK005760 | KD | VFE | L | T | DS | A | R | C | PGTHMR | | | C | G | D | DED | | FTGH | GVAQ | GVPI | IN | RG | C | |
| hLynx3 | LR | YVCP | E | PTGV | S | D | C | VT | I | AT | C | T | TN | ETM | | KTIL | YSRE | IVY | PFQGD | STVTKS | C | | |
| mLynx3 | LQ | YTC | A | N | PVSA | S | N | C | VT | T | TH | C | H | IN | ETM | | KTTL | YSLE | IVPFL | GDSTVTKS | C | | |
| hLynx1 | LD | HVCAY | N | GDN | | | C | FNP | MR | | CPAMV | AY | | | | MTTR | TYTP | TMKVS | KS | C | | | |
| mLynx1 | LE | HVCAY | N | GDN | | | C | FKP | MR | | CPAMA | TY | | | | MTTR | TYTP | PYRM | KVR | KS | C | | |

| | | | | | | | | | | |
|----------------|---------------------|-----------------------|-------------------|-------------------------|-------------------|-------------------------|-------------------|-------------------|----------------|-------------|
| CD59-RABBIT | -----EDC----- | -----NFEFIS----- | -----NRL----- | -----E----- | -----ENSLKYN----- | -----CRKDL----- | -----N----- | | | |
| CD59-PIG | -----DEC----- | -----NFDFIS----- | -----RNL----- | -----A----- | -----EKKLKYN----- | -----CRKDL----- | -----N----- | | | |
| CD59-MARMOSET | -----EDC----- | -----TFRQLS----- | -----NQL----- | -----S----- | -----ENELKYH----- | -----RENL----- | -----N----- | | | |
| CD59-MONKEY | -----DDC----- | -----SFKRIS----- | -----NQL----- | -----S----- | -----ETQLKYH----- | -----CKKNL----- | -----N----- | | | |
| CD59-OWLMONKEY | -----EDC----- | -----TFSRVS----- | -----NQL----- | -----S----- | -----ENELKYY----- | -----CKKNL----- | -----N----- | | | |
| CD59-GREENMONK | -----ANC----- | -----NFNDIS----- | -----TLL----- | -----K----- | -----ESELQYF----- | -----CKKDL----- | -----N----- | | | |
| CD59-BABOON | -----ANC----- | -----NFNDIS----- | -----TLL----- | -----K----- | -----ESELQYF----- | -----CKEDL----- | -----N----- | | | |
| hCD59 | -----EHC----- | -----NFNDVT----- | -----TRL----- | -----R----- | -----ENELTYF----- | -----CKKDL----- | -----N----- | | | |
| mCD59 | -----SDC----- | -----HGEIIM----- | -----DQL----- | -----E----- | -----ETKLFKR----- | -----CQFNL----- | -----N----- | | | |
| rLY6A | -----LPV----- | -----PTSP----- | -----QT----- | -----TEILG----- | -----T----- | -----VVDMKIS----- | -----NTDL----- | -----N----- | | |
| mLY6A | -----LPI----- | -----PPNI----- | -----ES----- | -----MEILG----- | -----T----- | -----KVNKTS----- | -----QEDL----- | -----N----- | | |
| PUT-LY6B | -----LPG----- | -----PKSP----- | -----QT----- | -----PEVLG----- | -----T----- | -----VVHVNTD----- | -----NTDL----- | -----N----- | | |
| rLY6C | -----LPI----- | -----PKFP----- | -----QR----- | -----TEILG----- | -----T----- | -----VVYTKVS----- | -----NTDL----- | -----N----- | | |
| mLY6F | -----FPF----- | -----PANL----- | -----EN----- | -----MEILG----- | -----T----- | -----TVNVNTS----- | -----KEDL----- | -----N----- | | |
| BC010764 | -----LSF----- | -----P----- | -----AG----- | -----VPIRD----- | -----P----- | -----NIRERTS----- | -----SEDL----- | -----N----- | | |
| hCP1610069 | -----SPT----- | -----P----- | -----NSTVSS----- | -----P----- | -----SRALSVS----- | -----CQGSQ----- | -----N----- | -----N----- | | |
| hCP49117 | -----HIG----- | -----P----- | -----DIPS----- | -----LGL----- | -----GPVVSIA----- | -----QITSL----- | -----N----- | -----N----- | | |
| mLY6I | -----HPF----- | -----PDEI----- | -----EK----- | -----KFILD----- | -----P----- | -----NTKMNIS----- | -----QEDL----- | -----N----- | | |
| mLy6G | -----LPI----- | -----PTTL----- | -----DN----- | -----TEITG----- | -----N----- | -----AVNVKTY----- | -----KEDL----- | -----N----- | | |
| mCP17885 | -----FPF----- | -----PANL----- | -----EN----- | -----MEILG----- | -----T----- | -----TVNVNTS----- | -----KEDL----- | -----N----- | | |
| AK009303 | -----LPR----- | -----AQ----- | -----P----- | -----LLGH-ATYWS----- | -----R----- | -----SYSLRHQ----- | -----EQDL----- | -----N----- | | |
| mLY6C | -----LSF----- | -----PAGV----- | -----PIKD----- | -----P----- | -----NIRERTS----- | -----SEDL----- | -----N----- | -----N----- | | |
| hLY6E | -----SPA----- | -----P----- | -----IPEGVNV----- | -----G----- | -----VASMGIS----- | -----QSFL----- | -----N----- | -----N----- | | |
| mLY6E | -----VNLG-YT-L----- | -----NKG----- | -----SPIC----- | -----PSENVN----- | -----LNL----- | -----G----- | -----VASVNSY----- | -----QSSF----- | -----N----- | |
| SCA-2-CHICKEN | -----SPV----- | -----PS----- | -----AGINL----- | -----G----- | -----IAAASVY----- | -----DSFL----- | -----N----- | -----N----- | | |
| hPSCA | -----SLN----- | -----VD----- | -----DSQDY----- | -----Y----- | -----VGKKNIT----- | -----DTDL----- | -----N----- | -----N----- | | |
| mPSCA | -----SSQ----- | -----ED----- | -----DSENY----- | -----Y----- | -----LGKKNIT----- | -----YSDL----- | -----N----- | -----N----- | | |
| mHEMT-1 | -----TKD----- | -----TF----- | -----IYR----- | -----EHVPELPRVLKD----- | -----V----- | -----KNFYFVM----- | -----SSIT----- | -----N----- | | |
| mHEMT-3 | -----TKD----- | -----TF----- | -----IYR----- | -----EHVPELPRVLKD----- | -----V----- | -----KNFYFVM----- | -----SSIT----- | -----N----- | | |
| mSlurp1 | -----SSS----- | -----LA----- | -----TDPDG----- | -----I----- | -----GVAHPVF----- | -----FRDL----- | -----N----- | -----N----- | | |
| hSlurp1 | -----SSS----- | -----VA----- | -----TDPDS----- | -----I----- | -----GAHLIF----- | -----FRDL----- | -----N----- | -----N----- | | |
| hGML | -----TNN----- | -----TF----- | -----VYA----- | -----AEQPPEAPGKIFK----- | -----T----- | -----NSFYWVC----- | -----NSMV----- | -----N----- | | |
| hNG24 | -----GTP----- | -----E-EP----- | -----QE----- | -----AFN----- | -----QT----- | -----NRK----- | -----L----- | -----GLTYNTT----- | -----NKDN----- | -----N----- |
| hLy6D | -----AES----- | -----TP----- | -----SYT----- | -----LQ----- | -----GQV----- | -----S----- | -----SGTSSTQ----- | -----QEDL----- | -----N----- | |
| mLy6D | -----ANS----- | -----TS----- | -----DYS----- | -----QQ----- | -----GHV----- | -----S----- | -----SGSEVTQ----- | -----QTDL----- | -----N----- | |
| AK010485 | -----TRR----- | -----PTPVVSPSTNP----- | -----PS----- | -----EPKEFLIEK----- | -----P----- | -----MPFLFYK----- | -----QWDS----- | -----N----- | -----N----- | |
| AK009282 | -----ASK-NE----- | -----HF----- | -----VGC----- | -----RH----- | -----SRD----- | -----S----- | -----EHTECRS----- | -----EGMI----- | -----N----- | |
| AK005760 | -----VHST----- | -----SC----- | -----GRE----- | -----EP----- | -----ISYMG----- | -----L----- | -----TYSLTTT----- | -----SGHL----- | -----N----- | |
| hLynx3 | -----ASK----- | -----C----- | -----DVDG----- | -----I----- | -----GQTLPVS----- | -----NTEL----- | -----N----- | -----N----- | | |
| mLynx3 | -----ASK----- | -----C----- | -----SDVDG----- | -----I----- | -----GQTRPVS----- | -----NSDL----- | -----N----- | -----N----- | | |
| hLynx1 | -----VPR----- | -----C----- | -----FETVY----- | -----DGY----- | -----S----- | -----KHASTTS----- | -----CQYDL----- | -----N----- | -----N----- | |
| mLynx1 | -----VPS----- | -----C----- | -----FETVY----- | -----DGY----- | -----S----- | -----KHASATS----- | -----CQYYL----- | -----N----- | -----N----- | |
| hLynx2 | -----ASS----- | -----AA----- | -----LIA----- | -----SA----- | -----GYQ----- | -----SFCSPGKLSVCIS----- | -----NTPL----- | -----N----- | -----N----- | |

| | | | | | |
|---------------|--|--|---|-----------------|----------------|
| mLynx2 | -----ASS-----AAC | -----LIA-----SA-----GYQ-----SFCSPGKLN | SVCSIS | ---NTPL--N | |
| hLy6H | -----ASS-----CDF | -----VKR-----HFFSDYLMGFINS | -----G-----ILKVDVD | ---EKDL--N | |
| mLy6H | -----ASS-----CDF | -----VKR-----HFFSDYLMGFINS | -----G-----ILKVDVD | ---EKDL--N | |
| MCP9191 | -----A-----YT | -----PD-----INH-----V-----TANSKSS | -----CNTDL--N | | |
| MCP9209 | -----SG | -----PDV-----SSLG-----L-----GPHVSI | ---A-----CQSNL--N | | |
| MCP3824 | -----S-----PQ | -----KEK-----Q-----LNT-----G-----KKLIYIM | ---CEKNL--N | | |
| a-bungarotx | -----AAT-----C | -----P-----SK-----KPYEEVT | ---CSTDK--N | | |
| a-cobratx | -----G | -----P-----SV-----KNGIEIN | ---CTDR--N | | |
| m3tx | -----AAT-----C | -----P-----IP-----ENYDSIH | ---CKTDK--N | | |
| Erb | -----G | -----P-----TV-----KPGIKLS | ---ESEV--N | | |
| k-bungarotx | -----VAT-----C | -----P-----QF-----R-----SNYRSL | ---CTDN--N | | |
| CT | -----IDV-----C | -----P-----KS-----SLLVKYV | ---CNTDK--N | | |
| FAS | -----G | -----P-----PG-----DDYLEVK | ---CTSPDK--N | | |
| HagFishLeukme | -----ATT-----EM | -----KKE-----KNVT-----ILD-----VTGTIK | ---CKDL--N | | |
| DCP34786 | ---AYMGE---PGIEGDERF | -----LM-----RTGSY---N-----IFMEF--T--NSKDG--N | | | |
| DCP5238 | ---YFGDI---NNIQAG | -----QS-----DPSMP---F-----VKQLG--DV--TKDE--N | | | |
| DCP5240 | ---YFGNI---ADTKVG | -----QT-----DPSLT---I-----NKLLS--EV--TEDE--N | | | |
| DCP19784 | ---GYIPD---ENTDNK | -----V-----RRSGT---H-----DVAAIY--S--TKDL--N | | | |
| DCP20347 | ---HFESI---GQKDNE | -----TV-----THSRQ---VES--YT--KGD--N | | | |
| DCP3405 | ---YFGDA---SPIGVS | -----D-----DGPDPVVP---F-----MNFLG--TL--DTDL--N | | | |
| DCP23672 | ---AYQNQ---TSTNY | -----YQ-----RAG---F-----GGRQVV--S--DTDN--N | | | |
| DCP20494 | ---ASVSD---TGVVGV | -----N-----WG---VYE---N-----GVWEE--Y--SSDS--N | | | |
| DCP34289 | ---ALDSGTLTDTTEIIRMSH--C | -----GKPHY--DDK---Y-----VHG---LQS--SDADA--N | | | |
| DCP5234 | ---YYTNK---SDPVEL | -----NI-----TSPEK---N-----VRRIF--ED--LTDR--N | | | |
| DCP18941 | -----LSALSFRKDI PADKYEG--RPAAHDEKLANYVNHTIKE-- | -----HDVRR---DY---Y-----TDTTF--F--FLDHR--N | | | |
| DCP33900 | ---GFIFE---KIQNA | -----FT-----ADN---E-----GYKQII--T--PDEG--N | | | |
| DCP34091 | ---SSK---DMGNY | -----DYVR---NKGDR---M-----DYRS--IYT--DTDG--N | | | |
| DCP3238 | ---VQRGPD---DNMDR | -----AD-----TIY---N-----YKKVYM--F--QGDL--N | | | |
| C15H9.9 | ---AYSGE---PVD | -----G-----L-----KKTGN---H-----AIRIHYYQ | ENE--KAGTP--N | | |
| K11H12.6 | ---AYTGE---DIE | -----R-----K-----SNKGS---L-----GVSRYVYQ | SEN---L--N | | |
| K11H12.7 | ---GYLGE---ERE | -----R-----K-----FNNTTYLNGVKE | ---PAT--VFSQ--SENL--N | | |
| TO7D1.3 | IDDPTYTGWQQK | -----KTGEY | -----RK-----SRD---Y-----GKKGEIC | ---CADDM--N | |
| PRED. PROT. | ---MQ | -----NAAAN | -----QN-----SSA---F-----GVNGATC | ---CYGDG--N | |
| CO9B9 | --VSGT-G--AK-GY-IRG | --WGSVFLFGFNRT | -----V | ---S--RGPL--N | |
| HOT-1 | MSDVLISGFNQITVTWYRWMHRDS | -----RPYRKKELFKL | -----GGESA---D-----DSTIDV | ---T--CYADH--N | |
| HOT-2 | LDRVLRHGFNQSALRTHRFHQNNHC | -----RTLRSALFNP | -----ARQTDPP---A-----LGDVQL | ---S--CYGDR--N | |
| HOT-3 | A---LTIARANNHTLSMFDRYDI | SRDM | -----S-----ASDLF---SHEHA---D-----SQRIRV | ---S--LGDR--N | |
| HOT-4 | MDRLLLFGLDDVVRNLLSAYENQRV | -----R-----HTDRKLLRFLPLS | -----G-----QTDVTF | ---S--CNGDF--N | |
| HOT-5 | A-DHIFSSMKDRPIEVEFLHRSPIC | -----VKLQLS---QI | -----YPQVQ---A-----NEIVQV | ---S--CDKDG--N | |
| ODR-2-2B | L---SDLHGYNHSLIRTLAERQGC | -----LDTTARELFLP | -----TAQRQEL | ---E-----PSRSLA | ---A--CHNNL--N |
| ODR-2-16 | L---SDLHGYNHSLIRTLAERQGC | -----LDTTARELFLP | -----TAQRQEL | ---E-----PSRSLA | ---A--CHNNL--N |
| ODR-2-18 | L---SDLHGYNHSLIRTLAERQGC | -----LDTTARELFLP | -----TAQRQEL | ---E-----PSRSLA | ---A--CHNNL--N |

Figure 5: Sequence Alignment of Ly6 domains of Ly6SF proteins. Ly6 domain sequences of 85 Ly6SF proteins were aligned with Dialign2 program and adjusted manually. Cysteines that are used for disulphide bridges and the final aa's of the ly6 domains are highly conserved. Color coding was designed as follows: **X**. aliphatic residues; **C**. conserved cysteines; **X**. aromatic residues; **X**. polar residues; **D**. small residues; **L**. aa's with large side-groups; **N**. conserved asparagines.

Since the conserved aa's above were alike in most Ly6SF proteins, they might be conserved for structural purposes. When the sequences of Lynx1, Lynx2, Lynx3 and Ly6H were analyzed separately from this group, there are certain residues that are conserved in Lynx1, 2 and 3 but not in Ly6H, which suggested that these might be involved in target receptor specificity. For instance, the serine residues that precede the 6th and 8th cysteines are conserved in Lynx1, Lynx2 and Lynx3, while in Ly6H, there is either a methionine or an aspartate instead. Serines are not only smaller than methionines, and are targets for phosphorylation, but also not charged like aspartate or hydrophobic like methionines. Since lynx1, lynx2 and lynx3 can bind to and modulate nicotinic receptors and Ly6H cannot (please see chapter 3 for further information), conserved amino acids like these serines might be important for receptor specificity (Figure 7).

In vertebrates, Ly6 proteins are mostly GPI anchored, with the exceptions of snake venom toxins, SLURP1, SLURP2 and SVSVII. Some Ly6SF proteins in *C. elegans* lack the GPI anchor signal sequence, although they still have the N-terminal signal sequence, suggesting that they may be secreted. In *D. melanogaster*, most of the Ly6 proteins have a short trans-membrane sequence instead of a GPI anchor. One of the *C. elegans* Ly6SF members has only 7 cysteine residues, but was still included since some of the three finger toxins have less cysteine residues than the α -neurotoxins.

Phylogenetic Inference

I have collaborated with Dr. Marcelo Briones for modeling the phylogenetic tree of these proteins. Phylogenetic inference was performed using the Vanilla 1.2 frontEnd to PAL 1.2 (Phylogenetic Analysis Library) [207]. An unrooted tree was inferred from maximum likelihood distance matrices. In the phylogenetic tree, there are very few branches for specific subfamilies, which also correlates with the divergence of the sequences. Some of these subfamilies, including CD59 subfamily, snake venom toxin subfamily and mammalian Ly6 genes that are expressed mainly in hematopoietic cells are highlighted in figure 6.

There were four large branches that originated from the unrooted tree. The first large branch included most of the invertebrate Ly6SF genes and the snake toxins as well as a couple of mammalian genes. The snake toxins formed a single small branch suggesting that they share a stronger homology. Some of the mammalian genes formed very small branches with invertebrate genes, which might suggest they might be orthologues. For instance, Lynx5, which was shown as AK009282, shared a small branch with one *C. elegans* and two *Drosophila* genes. In the second large branch, CD59 proteins from various vertebrate organisms formed a smaller close branch. The *C. elegans* proteins CO9B9 and the *Drosophila* protein DCP20347 might be orthologues of CD59 in invertebrates. Since complement mediated immune system is present in both these organisms, these proteins might have a similar function to their mammalian orthologues.

The third large branch in the unrooted tree included the Ly6 proteins expressed in cells of the immune system and some *Drosophila* and *C. elegans* proteins. Neither *Drosophila* nor *C. elegans* have cells of adaptive immunity. However, *Drosophila* homologues of several T-cell differentiation proteins have been shown to function in innate immunity and development. Therefore, these proteins may function as a part of innate immunity or might be involved in development.

The fourth large branch included a very divergent group of vertebrate Ly6SF proteins and *C. elegans* and *Drosophila* homologues of lynx2. In this branch, lynx3, SLURP-1, PSCA and Ly6E form a smaller branch. Lynx3 and SLURP-1 both modulate nAChRs and are expressed in keratinocytes and epithelial cells. PSCA and Ly6E are also expressed in epithelial cells, and might be involved in nicotinic receptor modulation as well. mLynx2, hLynx2 and *C. elegans* and *Drosophila* homologues of Lynx2 form another smaller branch, which is due to high level of sequence conservation of lynx2 among different organisms (Figure 6).

Among the 85 proteins that were analyzed with phylogenetic inference, 56 are expressed in vertebrates and 29 are expressed in invertebrates. There are 23 murine and 14 human Ly6SF genes. Among the human and mouse Ly6 proteins, only 23 have been previously described, 14 are encoded by novel genes (Figure 8).

Lynx Subfamily of Proteins

Lynx1 is a Ly6 protein that is expressed in the CNS and modulates nAChRs. Since sequence similarities do not point out to a subfamily of lynx1 homologues, in a search for CNS specific homologues for lynx1, lynx protein subfamily was initially

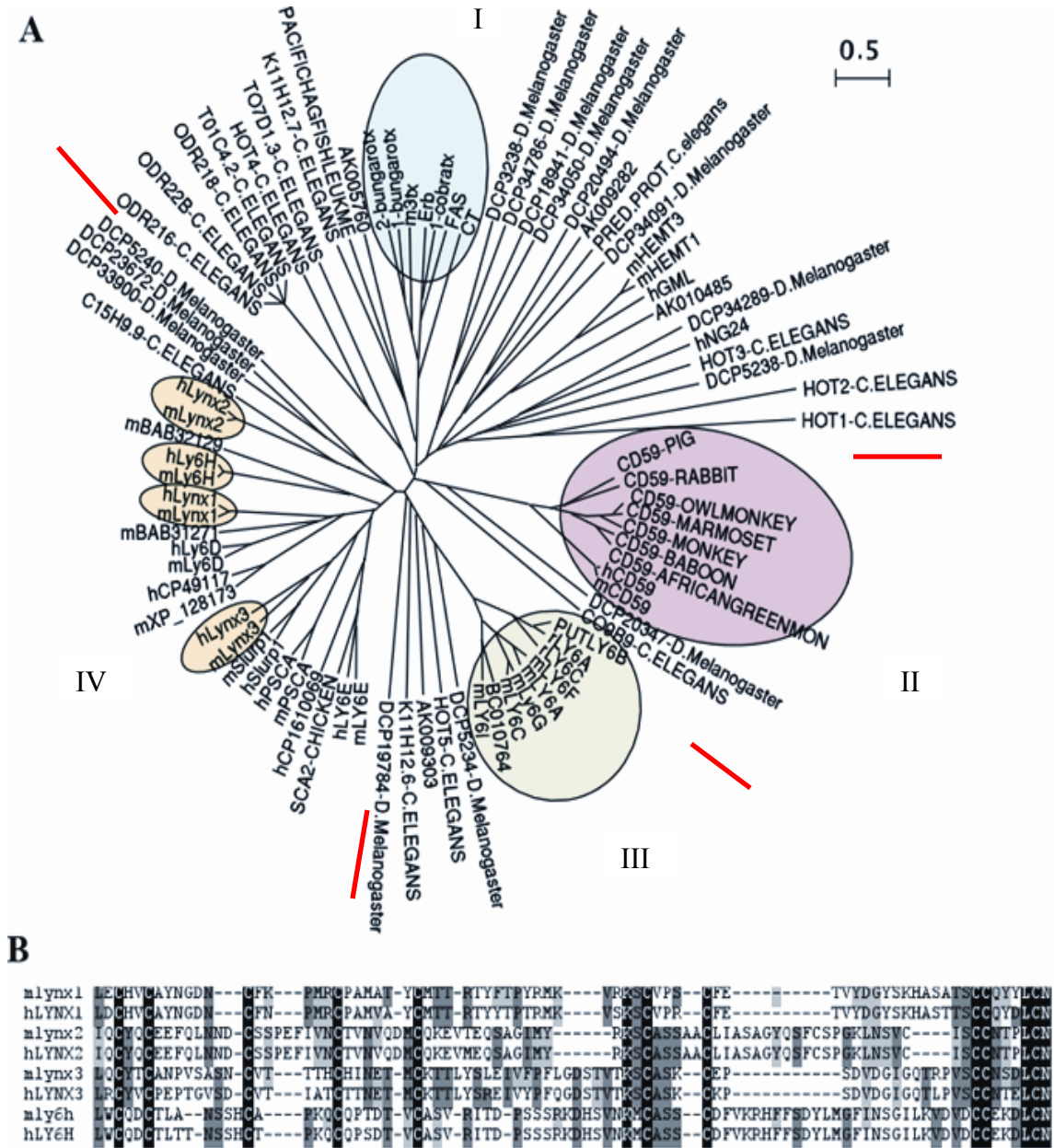


Figure 6: Phylogeny of Ly6SF proteins and sequence alignment of lynx1 homologues. Ly6 domain sequences of 85 members of Ly6SF from invertebrates and vertebrates were phylogenetically analyzed and an unrooted phylogeny was inferred. The sequences are very divergent except for the Ly6SF members expressed in hemopoietic cells (green circle), CD59 homologues in different organisms (pink circle) and toxins (blue circle). Lynx homologues are shown in yellow circles. B. Ly6 domain sequences of lynx1 homologues were aligned by Dialign2 (Morgenstern, 1999) and Boxshade programs.

identified as brain enriched Ly6 proteins. While lynx2 and lynx5 are heavily expressed in the brain, lynx3 and lynx4 were later shown to be expressed primarily in other tissues. Lynx2 was first identified as a part of Sugano brain cDNA library.

Many of the Ly6SF genes are clustered in a small region (~ 600CM) on chromosome 15 in mice and human chromosome 8. Lynx-2 and Lynx5 have been mapped to chromosome 1 in mice and chromosome 2 in humans, which are not Ly6 cluster regions. However, we already know that CD59, which is another Ly6SF member, is also on another chromosome. Lynx-1, Lynx-3, Lynx4 and Ly6H are located on the same chromosome, next to other Ly6 genes. Their alignment on mouse chromosome 15 is shown in figure 9.

Exon-Intron Structures of Ly6SF genes

All vertebrate Ly6SF genes share similar exon-intron structures including lynx1, lynx2, lynx3, lynx4 and lynx5. Thorough analysis of genomic structures of lynx1, lynx2, lynx3, lynx4 and lynx5 are shown in figure 10. There are three exons that make up the coding region. In some Ly6SF genes, there is an extra exon, which encodes the 5'UTR sequence. An example for this is the human Ly6D gene. For most Ly6SF genes, the three coding exons have the scheme shown in Figure 10. The 5'UTR region and part of the signal sequence that is required for secretion or for directing the proteins to the membrane are encoded by the first exon. The second exon encodes the rest of the signal sequence, which is approximately 30 aas long in total, and the first half of the Ly6 domain, which is shown as “mature protein” in the figure. The third coding exon has the second half of the Ly6

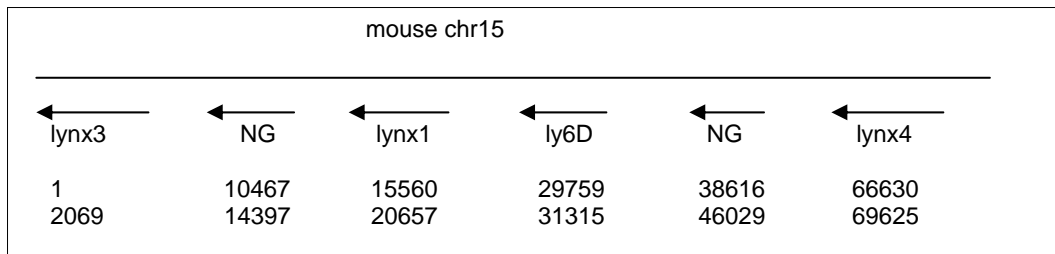


Figure 9: The alignment of Lynx1, Lynx3 and Lynx4 on murine chromosome 15. NG represents novel gene. The numbers under the gene names represent the relative distances of the coding sequences of these genes from each other in base pairs. 1 was assigned as the first base pair of the coding sequence for lynx3.

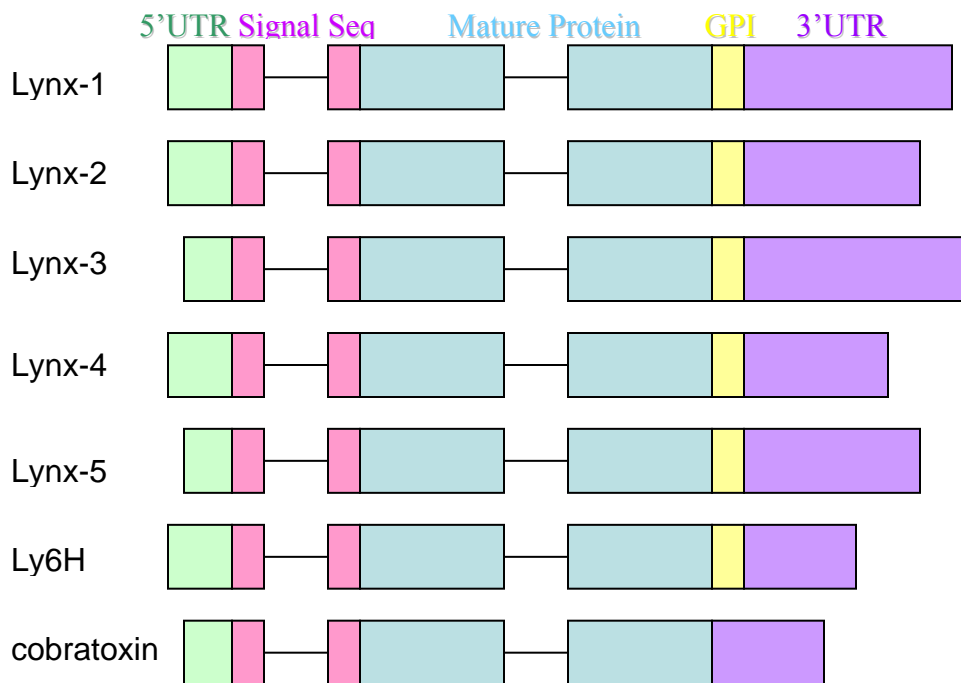


Figure 10: Exon-intron structures of Lynx homologues. Organizations of exon-intron boundaries of lynx homologues are similar to each other and other ly6 superfamily members. Exons are represented in boxes. The green boxes symbolize 5'UTR regions, the pink boxes symbolize the signal sequence, the blue boxes symbolize the mature protein, the yellow boxes symbolize the GPI anchorage sequence, and the purple boxes symbolize the 3'UTR sequence.

domain, the GPI anchorage signal in case of the GPI-anchored Ly6 proteins or the short hydrophobic – potentially transmembrane- domain in some *D. melanogaster* Ly6 genes, or no such domain in secreted Ly6SF proteins, and a 3'UTR sequence (Figure 10).

After phylogenetic inference of Ly6SF proteins was completed, the Nishi lab initiated collaboration with our lab that aims to identify lynx proteins in avian genome. Nicotinic signaling results in programmed cell death in avian ciliary ganglion. After lynx1 has been shown to modulate nAChRs, they wanted to analyze effects of lynx proteins in nicotinic induced cell death in avian ciliary ganglion. I have identified six novel avian ly6SF proteins by searching avian genome for lynx1 and lynx2 homology using the same criteria from my previous study. Nishi lab analyzed their expression patterns in developing chick ciliary ganglion and found that one of these genes, ChLy6, is upregulated during apoptosis. When this molecule was misexpressed, it rescued neurons from dying. I have identified that ChLy6 is a homologue of mammalian prostate stem cell antigen (PSCA). Sequence alignments of Ly6 domains of avian Ly6SF proteins and whole protein sequences of ChLy6 and mPSCA are shown in figure 11 and figure 12 respectively.

These results identify novel Ly6SF genes in several organisms, and demonstrate the extreme divergence of this gene family in spite of the high conservation of the cysteine residues that form the structural core of the Ly6 domain.

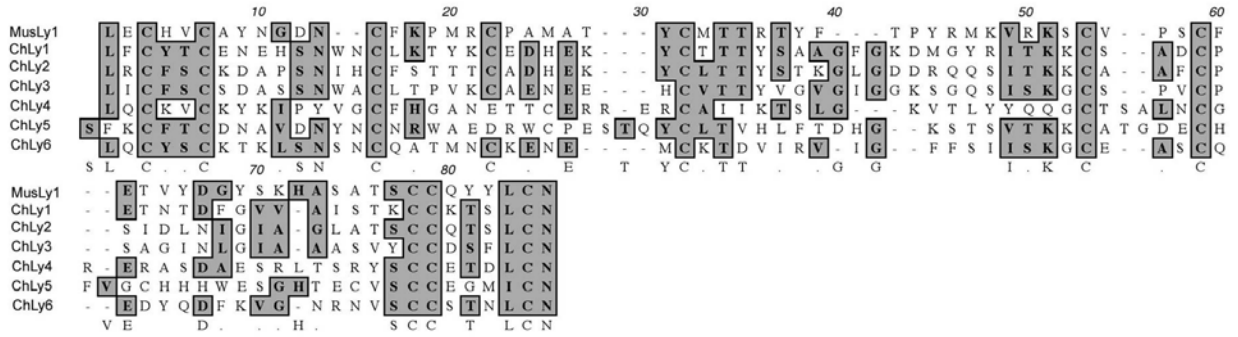


Figure 11: Sequence alignment of Ly6 domains of avian Ly6SF proteins. Six avian Ly6SF proteins were identified according to previously described criteria. Sequence alignment was performed by Nishi lab.

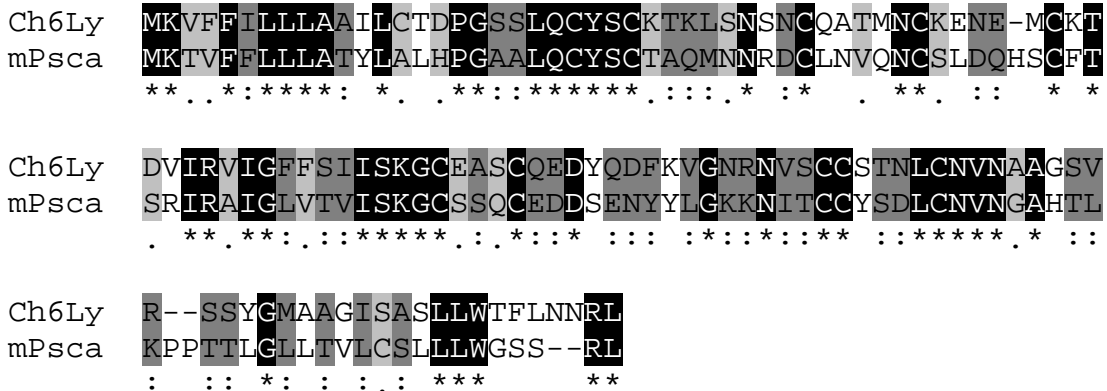


Figure 12: Ch6Ly is a homologue of mPscA. The protein sequences of Ch6Ly and mPscA were aligned with Dialign2 and alignment was analyzed with Boxshade program.

CHAPTER 3:

Expression and Functional Analysis of Lynx1

Homologues

Summary

I have identified 24 mouse Ly6SF genes in our phylogenetic analysis, 11 of which are novel genes. In order to identify lynx homologues that function in nicotinic receptor modulation, I searched expression databases for expression information on mouse and human Ly6SF genes. I further analyzed expression patterns of mouse Ly6SF genes that have little expression information in the databases with RT-PCR (reverse transcriptase-polymerase chain reaction) analysis. Among these genes, CNS expression of lynx2, lynx3, lynx4 and Ly6H were assessed with EGFP expressing-BAC transgenic mice. Lynx2 expression was further investigated with Northern and Western blotting and was compared with lynx1. Since lynx3 is expressed mostly in the periphery, distribution of lynx3 protein in various tissues including stomach, lungs, thymus and olfactory epithelia was analyzed with fluorescent microscopy and immunohistochemistry in lynx3 BAC transgenic mice.

Lynx1 forms stable complexes with $\alpha 4\beta 2$ and $\alpha 7$ nAChRs in mammalian tissue culture cells. I have investigated if lynx2, lynx3 and Ly6H can also form stable complexes with nAChRs through co-immunoprecipitation analysis. I also tested if lynx2, lynx3 and Ly6H can modulate desensitization of nAChRs through voltage clamp recordings in *Xenopus* oocytes.

Expression Analysis of Lynx1 Homologues

Database analysis for expression of human and mouse Ly6 genes

I have analyzed various databases including the Institute for Genomic Research (TIGR), Serial Analysis of Gene Expression (SAGE) and expressed sequence tag (EST) databases for expression information for the novel mammalian genes. Summaries of the preliminary examinations for some of the human and mouse Ly6SF genes are shown in table 2 and table 3.

Table 2: Summary of Expression information of human Ly6SF genes derived from TIGR, SAGE and UNIGENE databases. Ly6SF genes are also expressed in many cancer cell lines. All the proteins whose names start with hCP or mCP are initially identified as protein sequences by Celera and were named with Celera's nomenclature.

| Gene | Chromosomal location | Mouse homologue | Expression in Human tissues according to TIGR, UNIGENE and SAGE databases |
|----------|----------------------|-----------------|--|
| hLynx5 | 2 | mLynx5 | Lung, colon, ear, esophagus, head-neck, ovary, kidney, testis |
| hNG24 | 6p21.33 | mNG24 | Heart, ovary, placenta, brain, skin |
| hG5B | 6p21.3 | mG5B | Placenta, prostate, stomach |
| hG5C | 6p21.33 | mG5C | Breast, CNS, eye, heart, ovary, thymus, testis, lung, tonsil, pancreas, cerebellum, mammary gland, fetal lung |
| hCP49117 | 8 | mCP128173 | Brain, colon, esophagus, lung, head-neck, placenta, kidney, uterus |
| hLynx3 | 8q24 | mLynx3 | No expression information |
| hPSCA | 8q24.2 | mPSCA | Prostate, blood, breast, colon, heart, kidney, pancreas, placenta, skin, stomach |
| GML | 8q24.3 | | Prostate, cerebellum, pancreas, mammary gland |
| hLy6E | 8q24.3 | mLy6E | Widespread expression including: breast, lung, pancreas, placenta, brain |
| hSLURP-1 | 8q24.3 | mSLURP-1 | Keratinocytes, heart, cervix, esophagus, larynx, lung, pancreas, mammary glands, prostate, uterus |
| hLy6D | 8q24.3 | mLy6D | Pancreas, fetal heart |
| hSP-10 | 11p12-q13 | mSP-10 | Sperm, testis, brain |
| hCD59 | 11p13 | mCD59 | Widespread expression including: mammary epithelial cells, skin, brain, placenta, liver, spleen, pancreas, heart, lung, testis, kidney |
| hCP49491 | 19 | AK008654 | Brain, heart, breast, lung, colon |

Table 3: Summary of expression information of mouse Ly6SF genes derived from TIGR, SAGE and UNIGENE databases.

| Gene | Chromosomal location | Human homologue | Expression in Mouse tissues according to TIGR, UNIGENE and SAGE databases |
|----------|----------------------|-----------------|---|
| mSLURP-1 | 15 | hSLURP-1 | embryo |
| mPSCA | 15 | hPSCA | Widespread expression including: prostate, testis |
| AK008851 | 5 | | Embryo, liver, kidney, stomach, tongue. Shares 99% homology with mPSCA. |
| mLy6A/E | 15 | hLy6A/E | Widespread expression including: kidney, T-cells, spleen, embryo, brain, placenta |
| mLy6C | 15 | hLy6C | Colon, embryo, heart, kidney, liver, lung, mammary gland, muscle, placenta, skin, brain, spleen |
| mLy6I | 15 | hLy6I | lung |
| mLy6F | 15 | hLy6F | Kidney |
| mLy6D | 15 | hLy6D | Embryo, lymphocytes, skin, spleen, mammary gland, salivary gland |
| mLy6E | 15 | hLy6E | Brain, colon, salivary gland, liver, stomach, placenta, thymus |
| mCD59 | 2 | hCD59 | Widespread expression |
| mHEMT1 | 15 | hGML | Uterus, testis |
| mLynx1 | 15 | hLynx1 | Brain, embryo, muscle, skin, mammary gland |
| mLy6H | 15 | hLy6H | Embryo, brain, mammary gland |
| AI747831 | 15 | | Kidney, liver |
| BB646386 | 15 | | Uterus, colon, testis |
| AK009303 | 17 | | Embryo, lung, skin |
| AV082481 | 15 | | tongue |
| mSVSVII | 9 | | Urinary bladder |
| AK008654 | 7 | | Embryo, skin, stomach |
| mLynx3 | 15 | hLynx3 | Embryo, kidney |
| mLynx4 | 15 | | Thymus, testis, tongue, placenta |
| mLynx5 | 1 | hLynx5 | Colon, embryo, skin, spleen, kidney, thymus |

RT-PCR Analysis of Ly6 Genes and Northern Blots

Database searches gave us only preliminary information about the expression data of some of the Ly6SF genes. Therefore, I decided to analyze the expression patterns of these genes with Reverse Transcriptase Polymerase Chain Reaction (RT-PCR). I have used total RNA isolated from multiple tissues as template. The genes analyzed through this method and the results of their RT-PCR analysis are described below and shown in figure 13.

AK008654 is located on mouse chromosome 7, and in RT-PCR, I observed that it has a strong expression in lungs, and weak expression in brain and liver. I didn't detect any expression in stomach, kidney, heart or muscle. AK009303 is located in chromosome 17 and its expression was strong in brain, stomach and lung and in weak in liver and kidney. I couldn't detect AK009303 mRNA in heart or muscle.

AI747831 is located on mouse chromosome 15, within the Ly6 locus. I have observed that it has high levels of expression in brain, liver, stomach, kidney and heart and expressed in lower amounts in lung. BB646386 is also located within the Ly6 locus on chromosome 15, and it is expressed strongly in brain and weakly in lung, liver, kidney and heart.

AV082481 is also located in Ly6 locus on chromosome 15, and strong expression of this gene was detected in brain, stomach, kidney, heart and lung. I observed a low level of expression in liver.

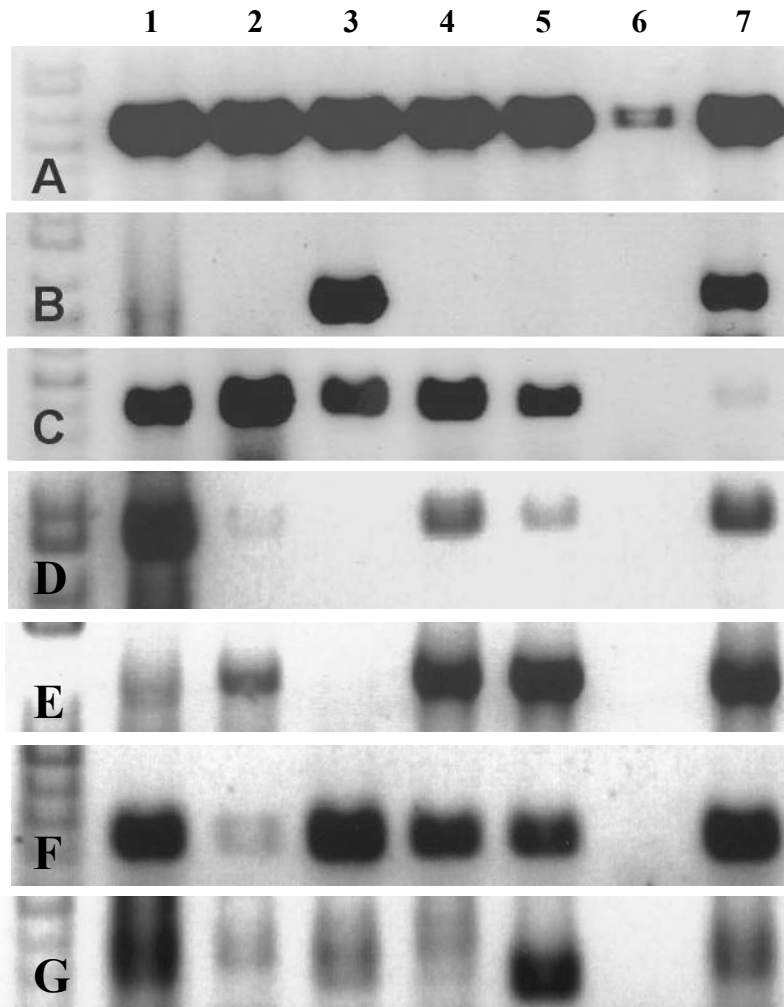


Figure 13: RT-PCR analysis of Ly6 protein in seven different tissues: In all pictures, the order of tissues is as following: 1) Brain, 2) Liver, 3) Stomach, 4) Kidney, 5) Heart, 6) Muscle, 7) Lung. A: B-actin as positive control, is expressed in all seven tissues, however, the amplification in muscle RNA is low, which suggests that muscle RNA was not as good as the other tissues. B: AK008654 is amplified in stomach and lung, and wasn't amplified in other tissues. C: AI747831 is amplified in brain, liver, stomach, kidney and heart. D: BB646386 is expressed in brain, kidney and lung in high amounts (highest in brain), and is expressed in low amounts in liver and heart. E: AK009303 is expressed in high amounts in brain and in stomach and in lower amounts in liver, kidney and lungs. F: AV082481 is expressed in high amounts in brain, stomach, kidney, heart and lung, and in low amounts in liver. G: Lynx5 is expressed in high amounts in brain and heart.

AK009282, which is located close to lynx2 on chromosome 2, is expressed in high amounts in brain and heart and has weak expression in lung and stomach. The results of this preliminary expression analysis are important for finding future targets of study.

The expression analysis of Lynx-2 has been performed with a mouse multiple tissue Northern blot shown in figure 14. Lynx2 cDNA is ~1500bp in size. A specific high level of expression of Lynx-2 was observed in brain whereas I couldn't detect any Lynx2 expression in heart, liver, skeletal muscle, testis, spleen, lung and kidney. In a multiple tissue dot-blot analysis, I observed that Lynx2 is expressed highly in brain, and it has very low levels of expression in submaxillary gland, prostate, epididymis and testis. I also observed that Lynx2 is expressed early in development, having expression in embryos at age E11, E15 and E17 and no expression at age E7 (Figure 15).

Lynx2 expression pattern in embryos and parts of adult CNS has been recently published by Dessaud et. al. [46]. They have shown that at age E10.5 and E12.5, lynx2 is expressed in trigeminal motor nucleus (cranial nerve V), and glossopharyngeal (cranial nerve IX) and vagal (X) cranial ganglia. At age E12.5, lynx2 expression is detected in brachial motor neurons, caudal thoracic motor neurons and few lumbar motor neurons in spinal cord. Lynx2 is also expressed in developing limb buds at age E12.5. Although it is clear that the lynx2 expressing cells in developing limb buds are not muscle cells, the identity of these cells is not known [46].

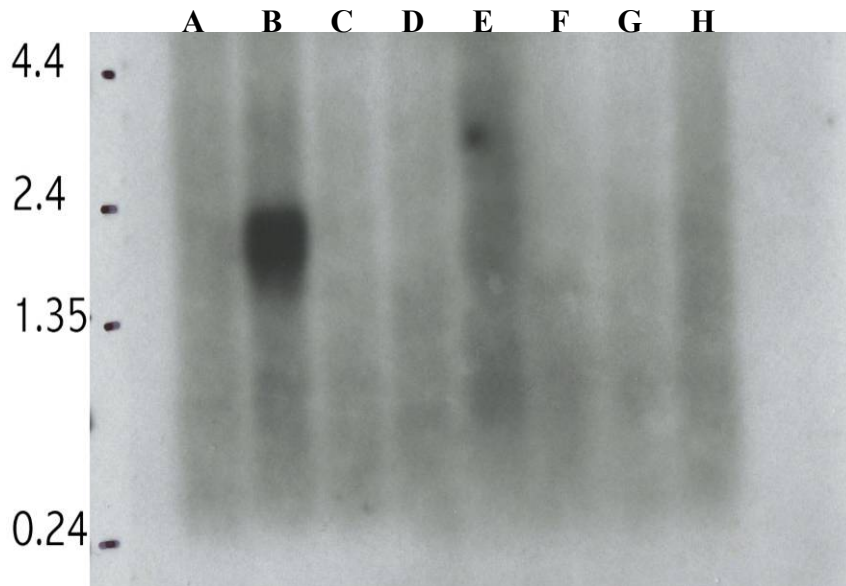


Figure 14: Northern blot analysis of lynx2. lynx2 mRNA expression was higher in brain compared to other organs represented on the blot. **A.** Heart; **B.** Brain; **C.** Spleen; **D.** Lung; **E.** Liver; **F.** Skeletal muscle; **G.** Kidney; **H.** Testis

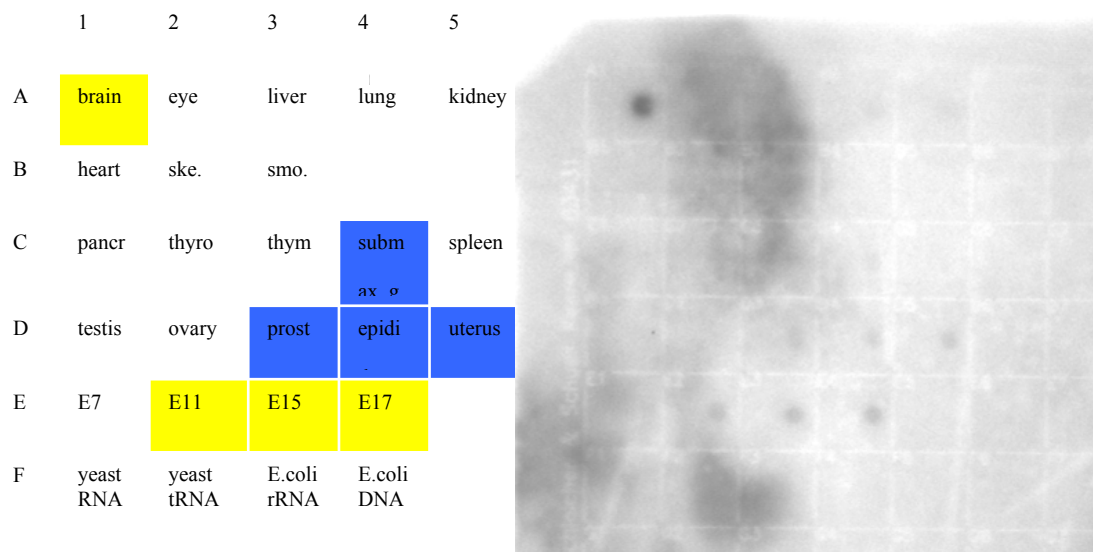


Figure 15: Dot blot analysis of lynx2 expression. Lynx2 is highly expressed in brain and expressed in lower amounts in prostate, epididymis, submaxillary gland and uterus. In embryo, lynx2 expression is observed at age E11, E15 and E17 but is not detectable at E7.

In situ hybridization analysis

As described by Miwa et al. [69], *Lynx1* is expressed in CA2 and CA3 regions of hippocampus, Purkinje cells of cerebellum, and layers V and VI of cortex in the adult mouse brain. Through *in situ* hybridization analysis, I found that mouse *Lynx2* and *Ly6H* are also expressed in the adult brain; however, their expression patterns differ from the one of *Lynx1*. *Lynx2* is expressed in CA1 region of hippocampus, dentate gyrus, Golgi cells of the cerebellum, and in scattered cells in layers IV and V in cortex. *Lynx2* is also observed in amygdala, and specific nuclei in the brainstem (data not shown). *Ly6H* has a more widespread expression, it is expressed in all three CA regions of hippocampus, dentate gyrus, layers I-V in cortex and in the purkinje cell layer of cerebellum. Although I didn't observe any detectable expression of *Lynx3* in adult mouse brain, I detected its expression in olfactory epithelia on E15.5 mouse head sections through *in situ* hybridization. The *in situ* hybridization detection sites match with the expression data from the GENSAT BAC transgenic database for *Lynx3* and *Ly6H*. The *in situ* hybridization results I had also match Allen Brain Atlas Database results for *lynx1* and *lynx2* (Figure 16).

On E15.5 head cryostat sections, *Lynx1* is expressed in specific nuclei in brain stem. *Lynx2* is also expressed in the same region in brain stem however its expression is stronger and the area it's expressed in is larger than *Lynx1*. *Lynx2* is also expressed in migrating interneurons in cerebellum. *Lynx3* is expressed in olfactory tract. *Ly6H* is expressed in cortex, brainstem, olfactory bulb and cerebellum in very low levels so that it was barely detectable through *in situ* hybridization. *Lynx1* and *Lynx2* do not have any expression data on GENSAT server (Figure 17).

Taken together, these results show that Lynx1 homologues have distinct expression patterns in mice.

BAC Transgenic Mice Show Expression Patterns of Lynx Homologues

BAC transgenic animals were prepared by the method described in Gong et al [208]. Lynx3 BAC transgenic mice expressed Enhanced Green Fluorescent Protein (EGFP) under the lynx3 promoter; therefore, the cells that normally express lynx3 also expressed EGFP. The lynx3 BAC transgenic mice were analyzed at three different ages. At age E15.5, immunohistochemistry with anti-EGFP antibodies on frozen embryo head sections revealed lynx3 expression in olfactory cells, respiratory epithelium, developing colliculi, pituitary gland and retina (Figure 18-GENSAT data). When I perfused the whole embryos at age E15.5, and visualized EGFP in the whole embryo, I also detected fluorescence in olfactory epithelia and in palate (Figure 19).

At age P7, lynx3 expression was detected in olfactory bulb, scattered cells in dentate gyrus, olfactory cells, superior colliculus, visual afferents, vestibular nucleus and forebrain on frozen brain sections (Figure 20-GENSAT data). In adult frozen brain sections, lynx3 expression could only be detected in olfactory bulb, probably in the olfactory ensheathing cells surrounding the axons coming to the glomeruli, through immunohistochemistry with anti-EGFP antibodies (Figure 21-GENSAT data).

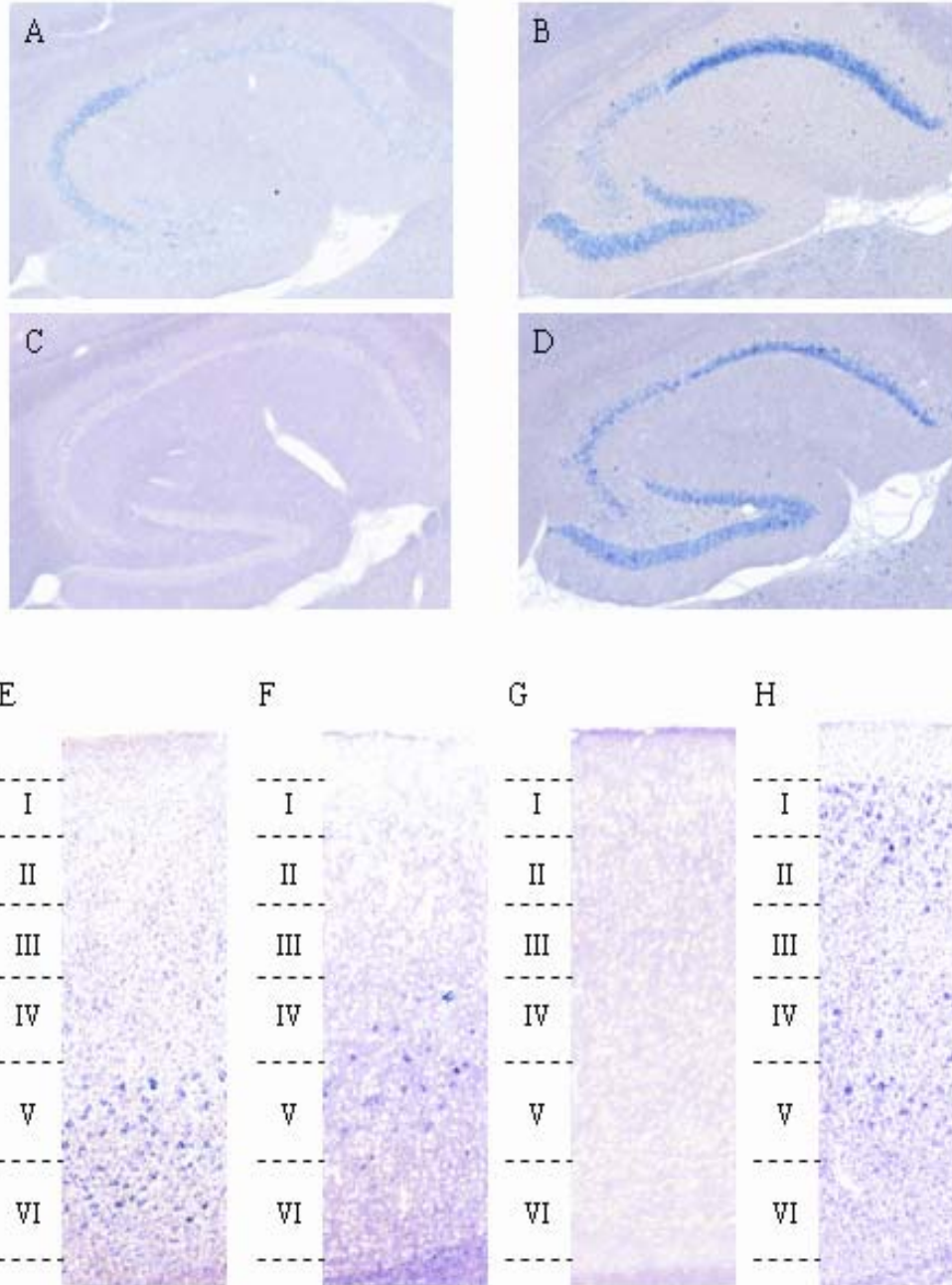


Figure 16: Differential expression of lynx1, lynx2, lynx3 and ly6h in the adult mouse cerebral cortex and hippocampus. In situ hybridization analysis using lynx1, lynx2, lynx3 and ly6h as probes, showed that in hippocampus, lynx1 is expressed in CA2 and CA3 regions (A), lynx2 is expressed in CA1 and dentate gyrus (B), lynx3 is not expressed (C), and ly6h is expressed in CA1, CA2, CA3 and dentate gyrus (D). In cerebral cortex, we observed expression of lynx1 in layers V and VI (E), lynx2 in layers IV and V (F) and ly6h in layers I through V (H). We didn't detect any expression of lynx3 in cerebral cortex (G)

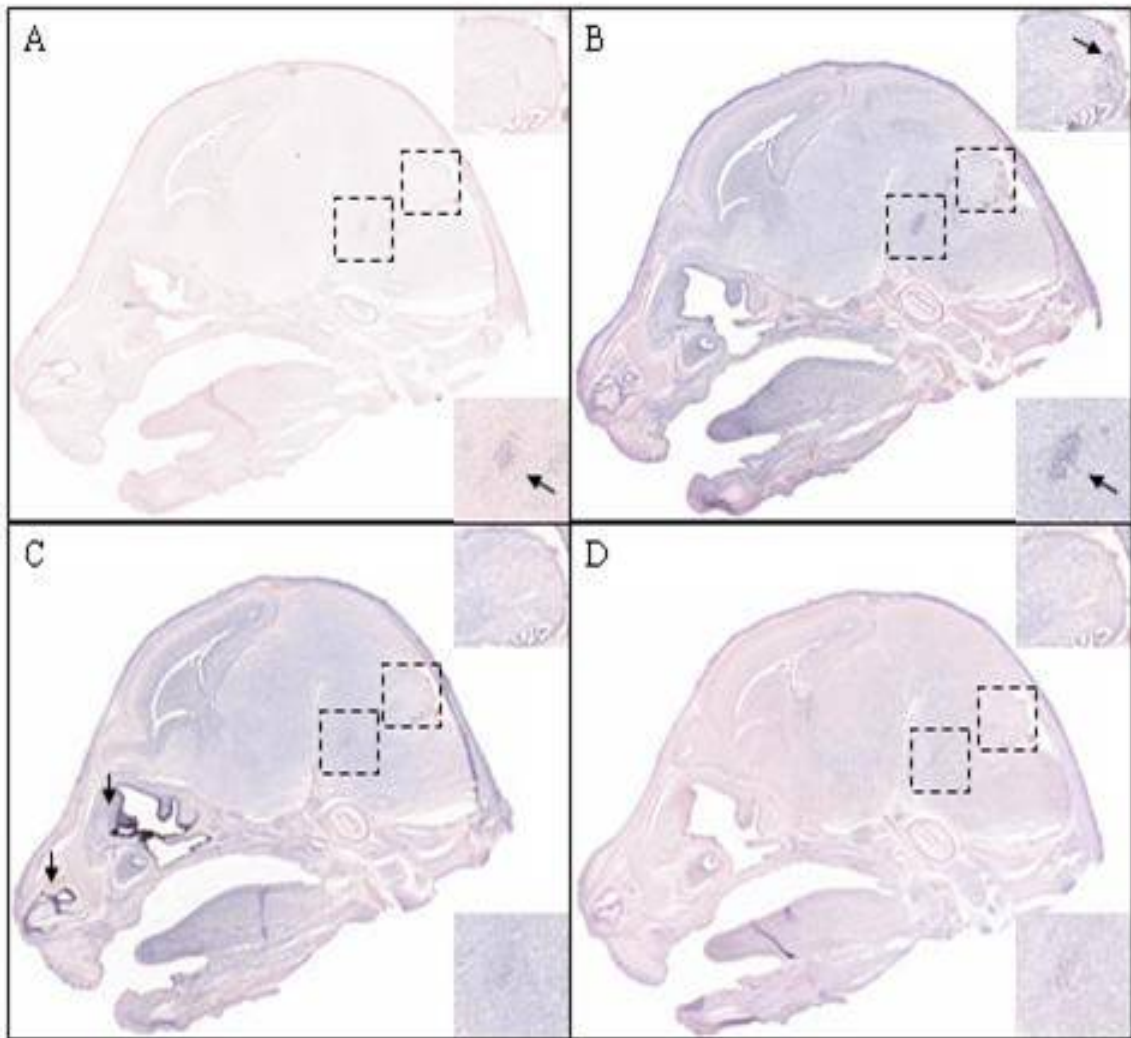
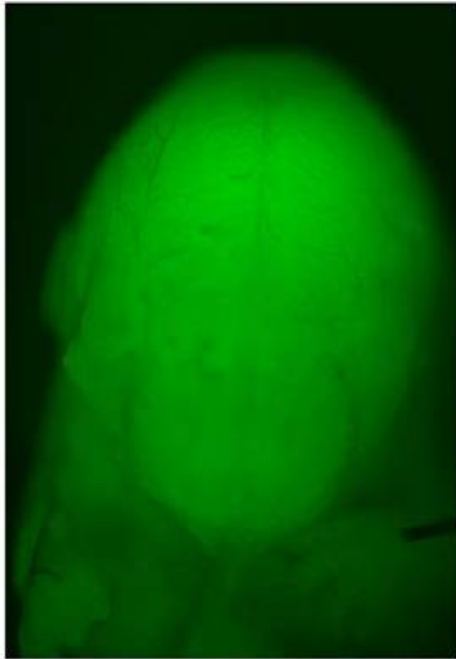


Figure 17: Expression analysis of Lynx1 homologues in brains sections from E15.5 mouse embryos with colorimetric in situ hybridization. **A.** lynx1 expression was detected in low amounts in brain stem. **B.** lynx2 is expressed in high levels in brain stem, cerebellum, and midbrain. **C.** High levels of lynx3 expression was detected in olfactory epithelia and retina (not shown). **D.** ly6H mRNA has a widespread expression in low amounts in many regions of the brain including cortex, cerebellum, midbrain and brainstem.



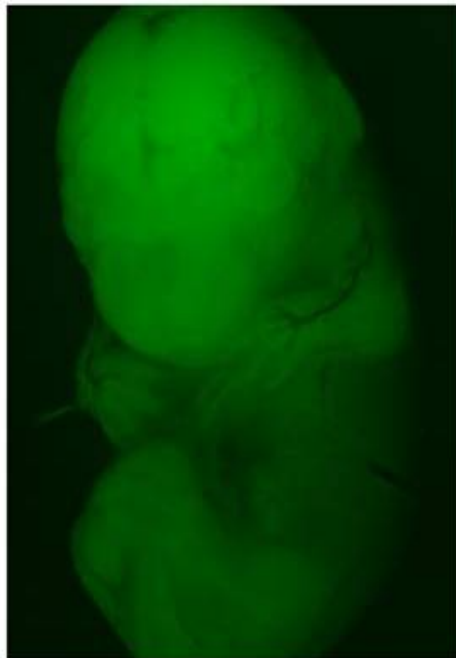
Figure 18: Expression analysis of *lynx3* in heads of BAC-transgenic animals at age E15.5. Expression was detected with immunohistochemistry with anti-EGFP antibodies. *Lynx3* is expressed in olfactory epithelium, respiratory epithelium, retina, pituitary gland, midbrain, colliculi and cortex. (*GENSAT*)



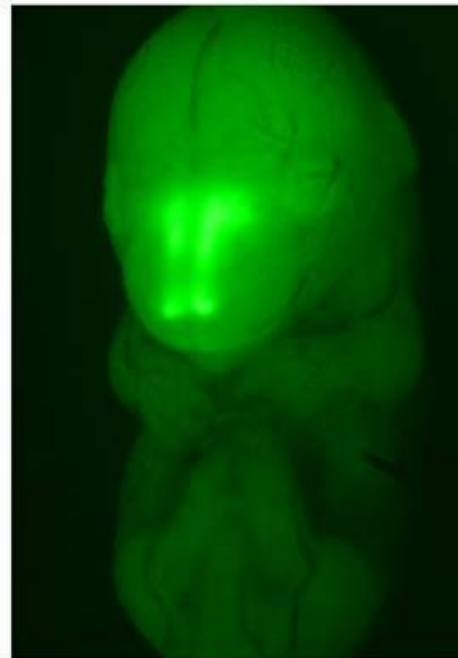
Wild type



Lynx3 BAC transgenic



Wild type



Lynx3 BAC transgenic

Figure 19: Expression of *lynx3* in BAC-transgenic embryos at age E15.5. Whole mount embryos were visualized under fluorescent microscope. *lynx3* is expressed in olfactory epithelia and tongue.

Lynx3 is mainly expressed outside the CNS in BAC transgenic mice. When I looked at the perfused BAC transgenic mice under fluorescent microscope at age P10, I have observed that lynx3 is expressed in many tissues including anterior nasal cavity, lungs, stomach, thymus, reproductive organs and spleen, so I decided to analyze the expression pattern of lynx3 in these tissues in more detail. lynx3 is found in mostly epithelial cells in these tissues, and I haven't observed any significant expression in kidneys, prostate and heart.

In anterior nasal cavity, lynx3 is expressed in both stratified squamous epithelium that lines the beginning of the anterior nasal cavity and the nostrils and the respiratory epithelium, which is composed of ciliated pseudostratified columnar epithelium that lines the rest of the trachea (Figure 22).

In lungs, lynx3 expression was observed through both direct immunofluorescence and through immunohistochemistry with anti-EGFP antibodies. Lynx3 is expressed in the respiratory ciliated pseudostratified columnar epithelium in trachea. Trachea is bifurcated into primary bronchi, which subsequently branches into smaller intrapulmonary bronchi, terminal bronchioles and respiratory bronchioles. Lynx3 is expressed throughout the bronchial tree in various types of epithelia, so that under fluorescent microscope, the bronchial tree lights up like two small green trees. In intrapulmonary bronchi, lynx3 is expressed in respiratory ciliated pseudostratified columnar epithelium. Lynx3 is expressed in ciliated simple columnar epithelium in smaller bronchi and in cuboidal epithelium in bronchioles (Figure 23).

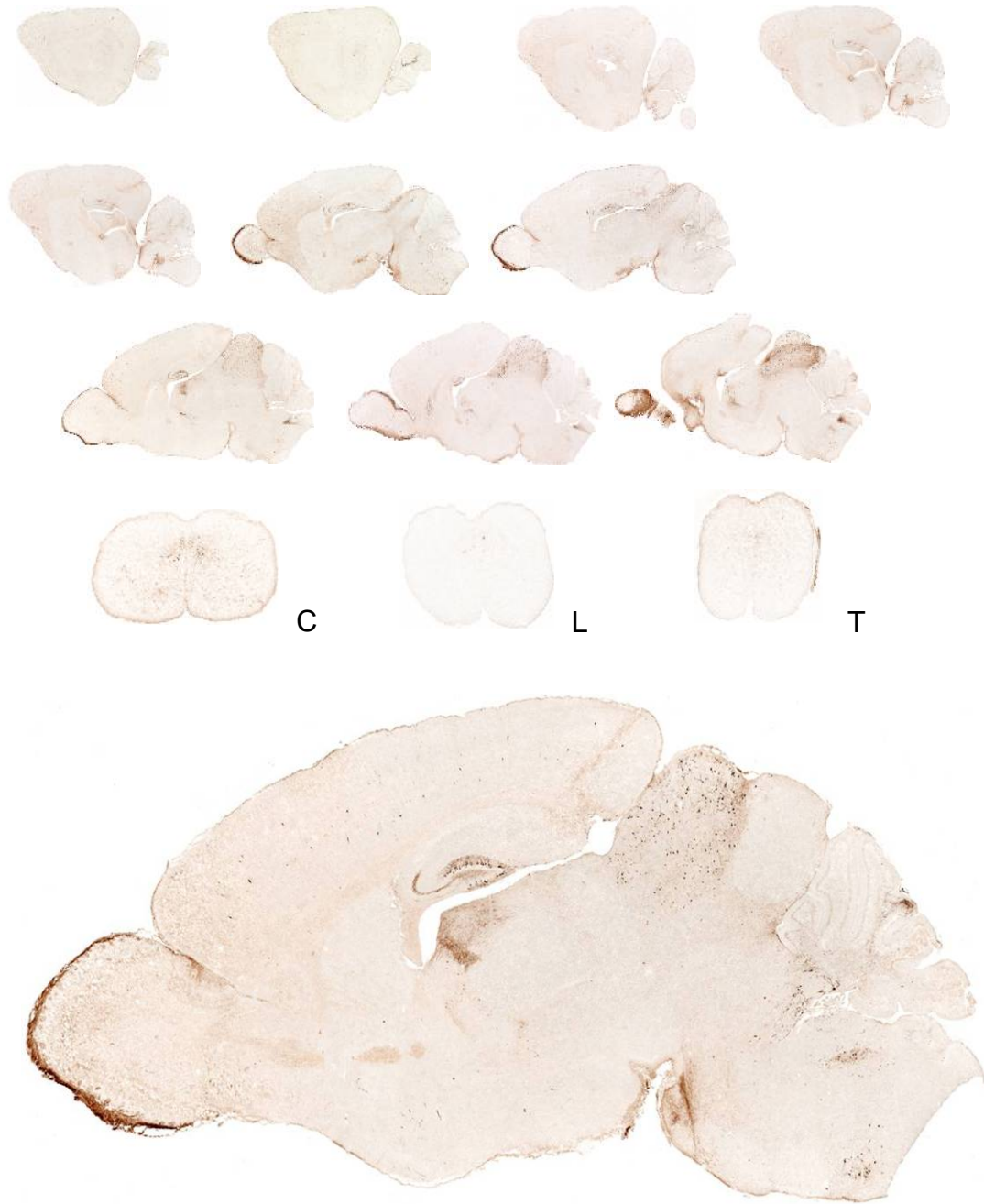


Figure 20: Expression of *lynx3* in BAC-transgenic mice at age P7. *lynx3* expression was analyzed through immunohistochemistry with anti-EGFP antibodies. At age P7, high levels of *lynx3* expression is observed in the olfactory bulb, hippocampus, thalamus, superior colliculus and brain stem. (*GENSAT*)

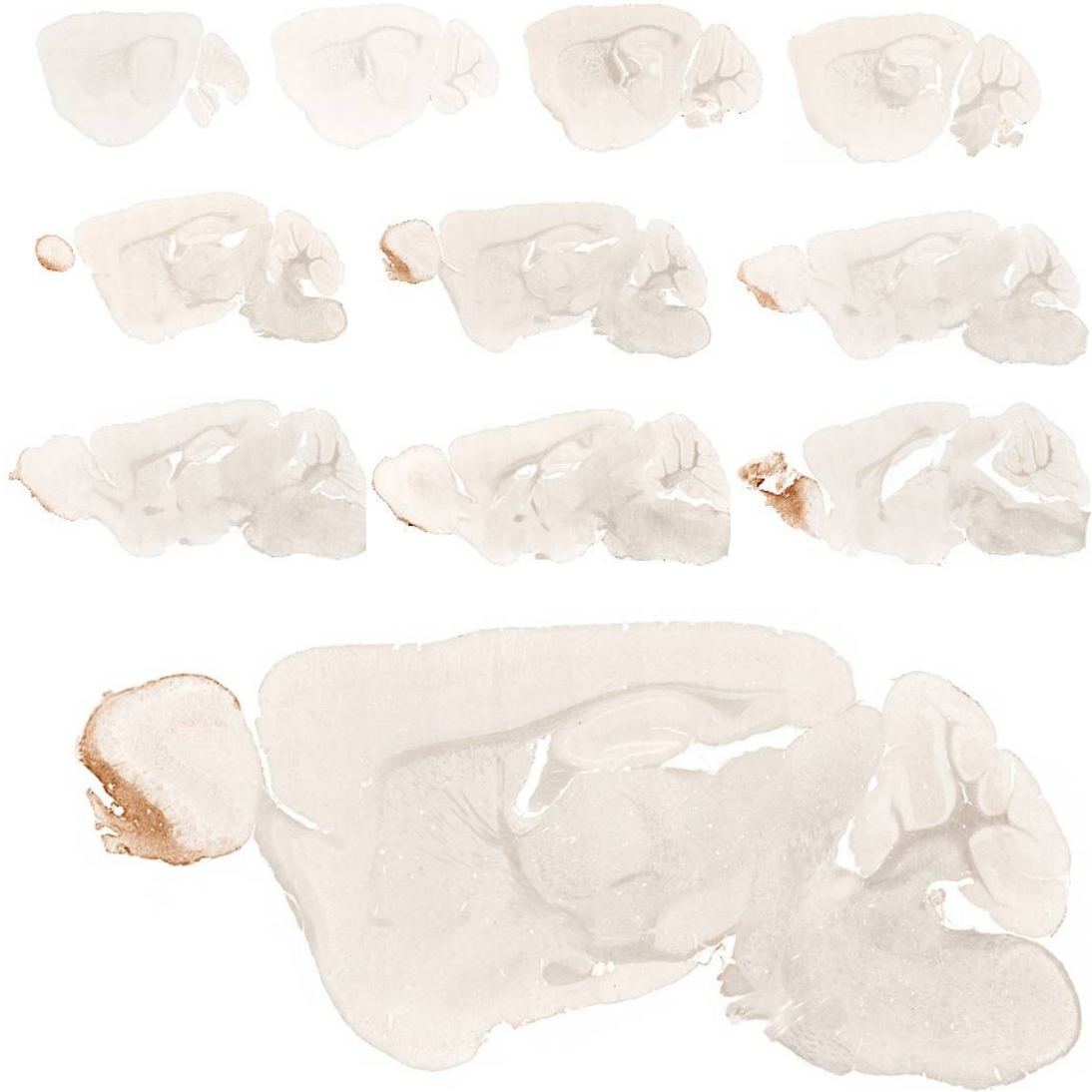


Figure 21: Expression of *lynx3* in brain sections from the adult BAC-transgenic mice. *lynx3* expression was analyzed through immunohistochemistry with anti-EGFP antibodies. *lynx3* expression was only detected in olfactory bulb.
(*GENSAT*)

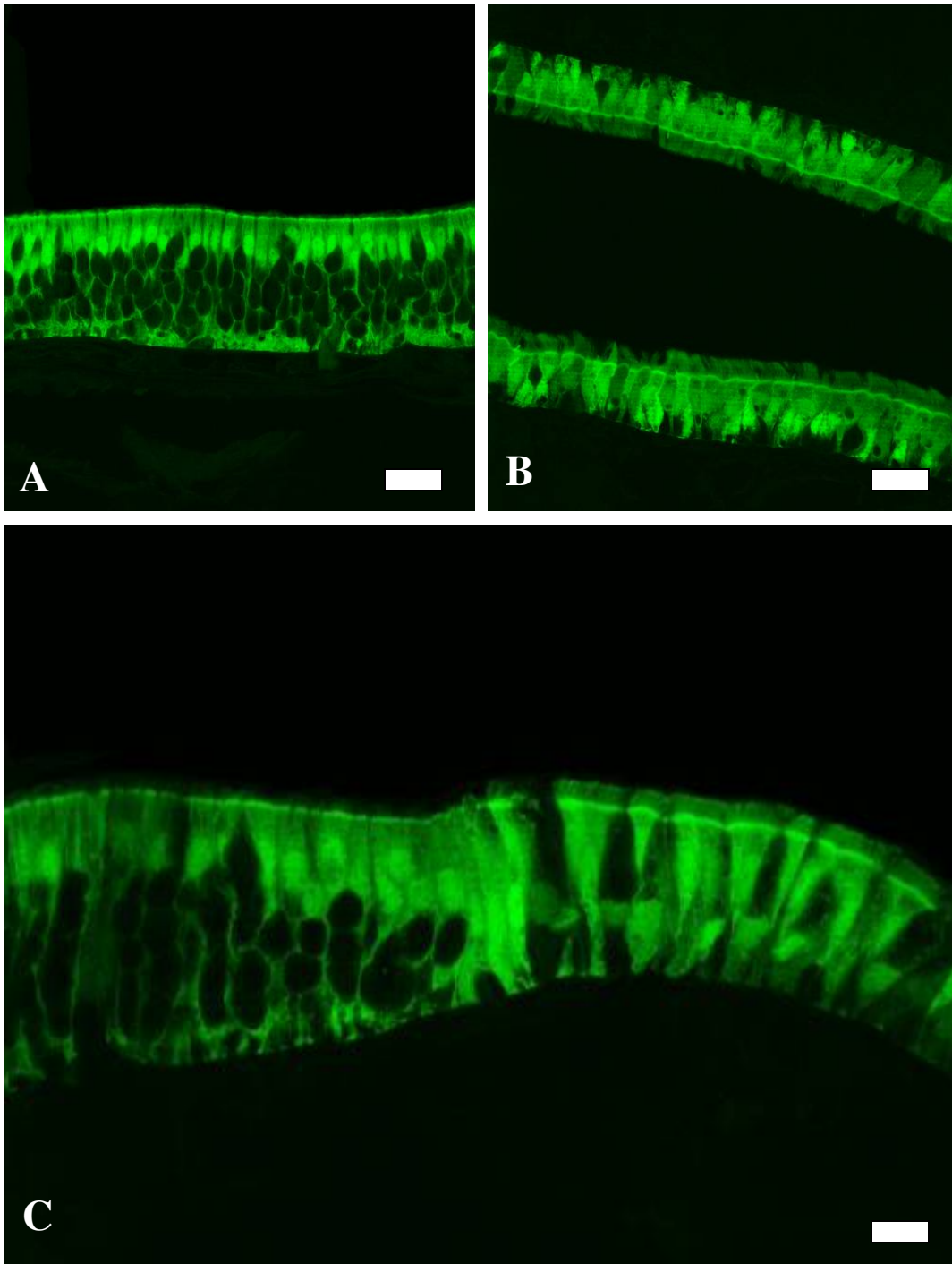


Figure 22: lynx3 is expressed in olfactory epithelia and respiratory epithelia, EGFP expression in Lynx3 BAC transgenic mice (A) Lynx3 expression detected in anterior nasal cavity, stratified squamous epithelium is labelled. Bar=25 μ m. (B) Lynx3 expression is detected in ciliated pseudostratified columnar respiratory epithelium. Bar=25 μ m. (C) Lynx3 expressed in the transition between the olfactory epithelium and the respiratory epithelium. Bar=10 μ m.

Mouse stomach has two well-defined parts that are separated with a ridge. The first part is non-glandular forestomach, which is similar to esophagus, and the second part is the glandular stomach. Lynx3 is expressed in stratified squamous epithelium that lines up the esophagus and the fore-stomach; however, it is not expressed in the stratified squamous epithelium in glandular stomach (Figure 24). In thymus, scattered epithelial cells and some lymphocytes had revealed lynx3 expression with immunohistochemistry and direct fluorescent microscopy (Figure 25). In female reproductive organ, lynx3 is expressed in the squamous stratified epithelium in vaginal mucosa (Figure 26).

There were two tissues in which I have observed lynx3 expression in neurons. One of them was the brain sections in which I observed a subset of olfactory sensory neuron axons coming to glomeruli. The other one was in the spleen, where I observed lynx3 expression in nerve axons surrounding the blood vessels (Figure 27).

BAC transgenic mice that express EGFP under lynx4 promoter control were also made by GENSAT. Transgenic mice were analyzed at three different stages. At age E15.5, Lynx4 is expressed in non-keratinized stratified squamous epithelia in palate, and various epithelial cells in vibrissa (Figure 28). At age P7, lynx4 is expressed in scattered cells in pons, geniculate and cerebellum (Figure 30), and in adult brain sections lynx4 expression was not detected.

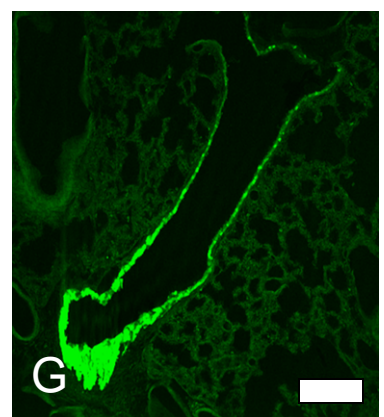
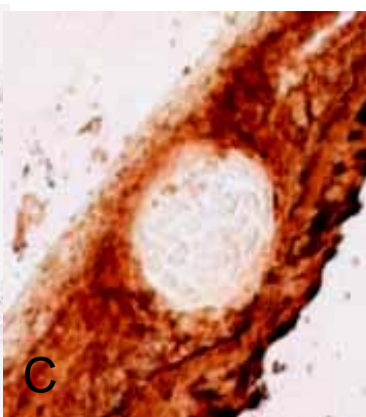
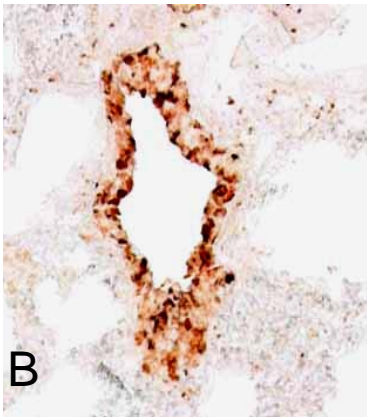
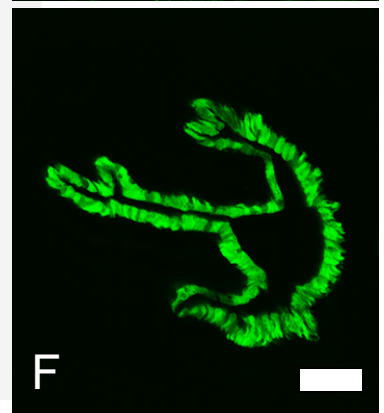
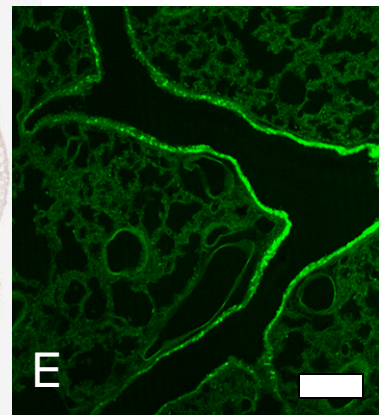
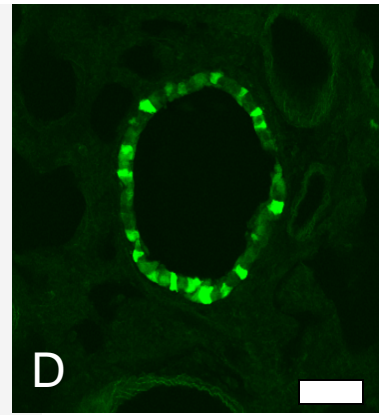
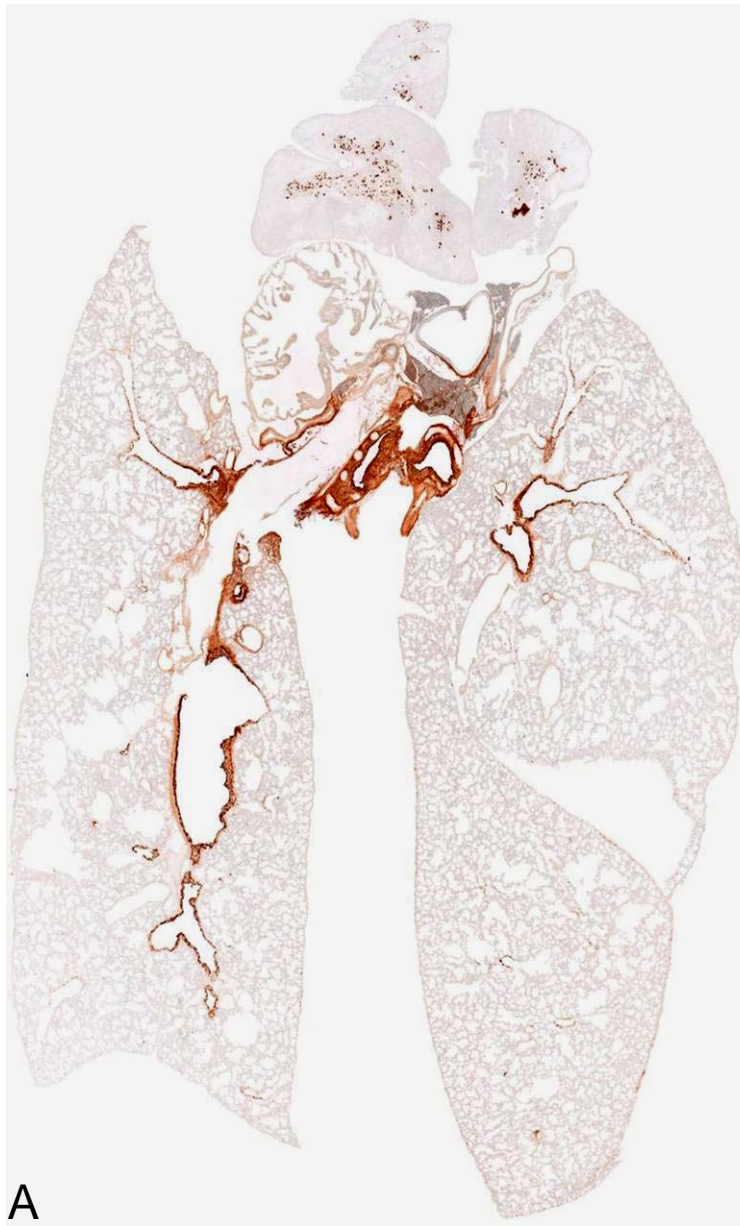


Figure 23: lynx3 expression in trachea and lungs in Lynx3 BAC transgenic mice visualized with immunohistochemistry with EGFP-antibodies and direct immunofluorescence. Lynx3 is expressed in ciliated pseudostratified columnar respiratory epithelium in trachea and ciliated simple columnar epithelium in bronchi, cuboidal epithelium in bronchioles. **A.** Lung section of adult Lynx3 BAC-transgenic mice. Higher magnification pictures of **B.** bronchi, **C.** cartilage in lung, **D,** *Bar=30 μ m*, **E,** *Bar=80 μ m*, **F,** *Bar=40 μ m*, **G,** *Bar=80 μ m*. bronchi and bronchioli,

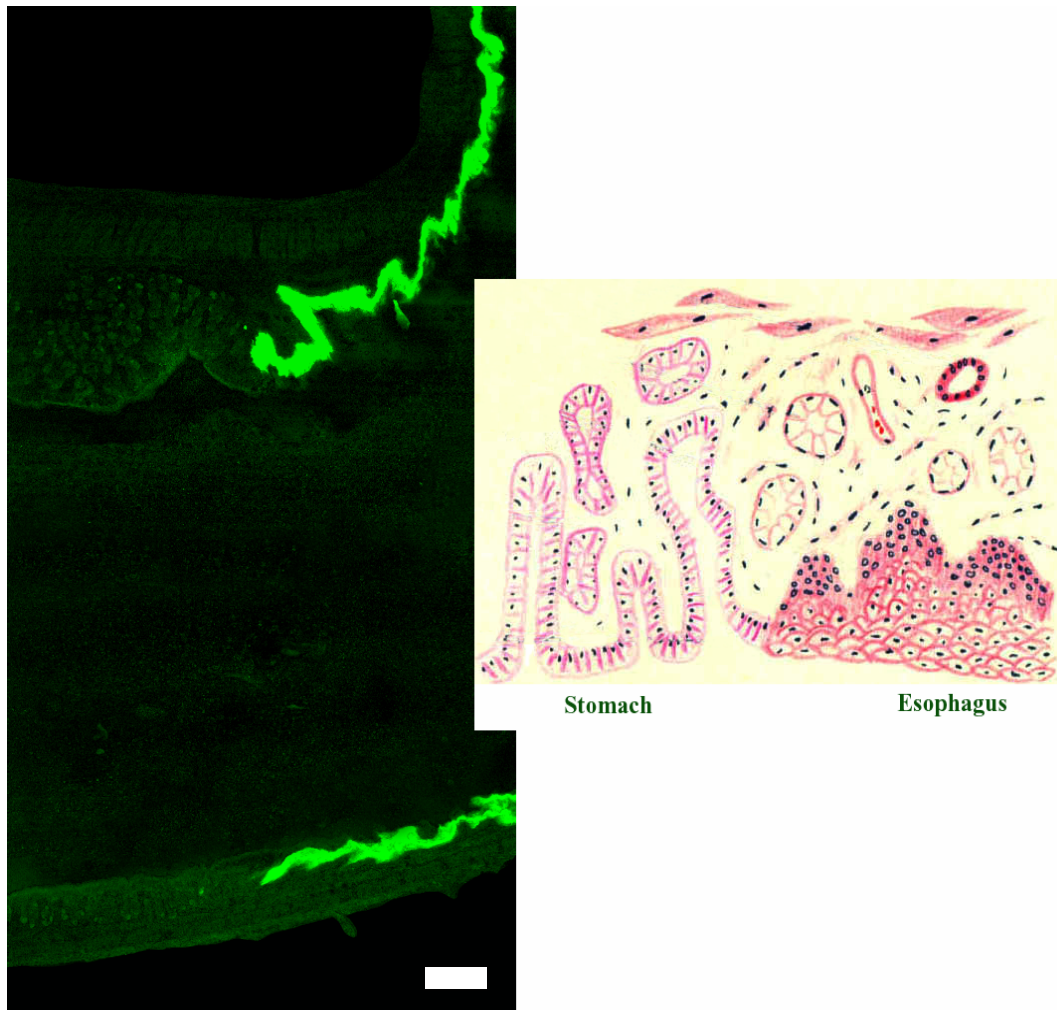


Figure 24: lynx3 expression esophageal epithelium in Lynx3 BAC transgenic mice visualized with direct immunofluorescence. Lynx3 is expressed in stratified squamous epithelium in esophagus and non-glandular forestomach. *Bar=40 μ m.*

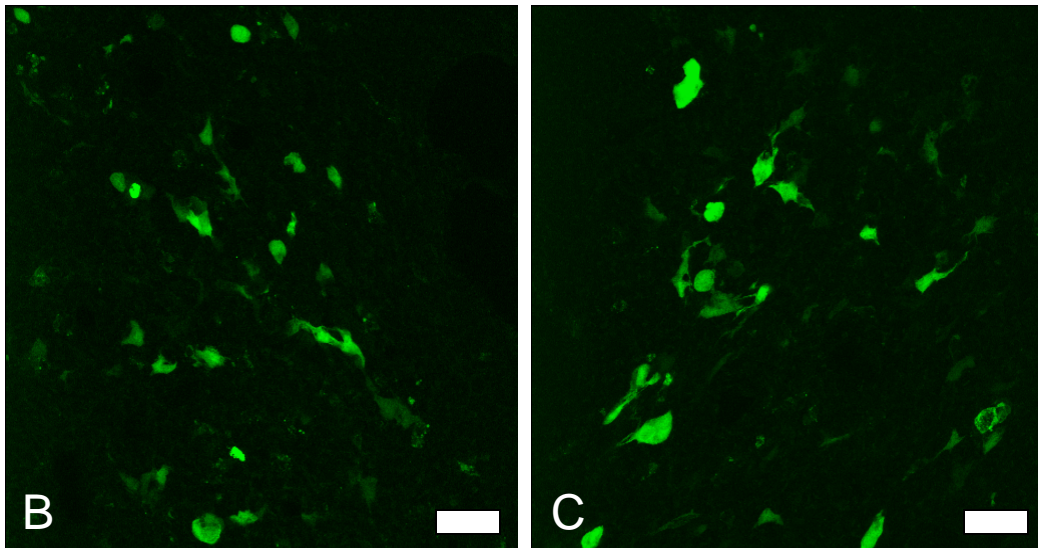
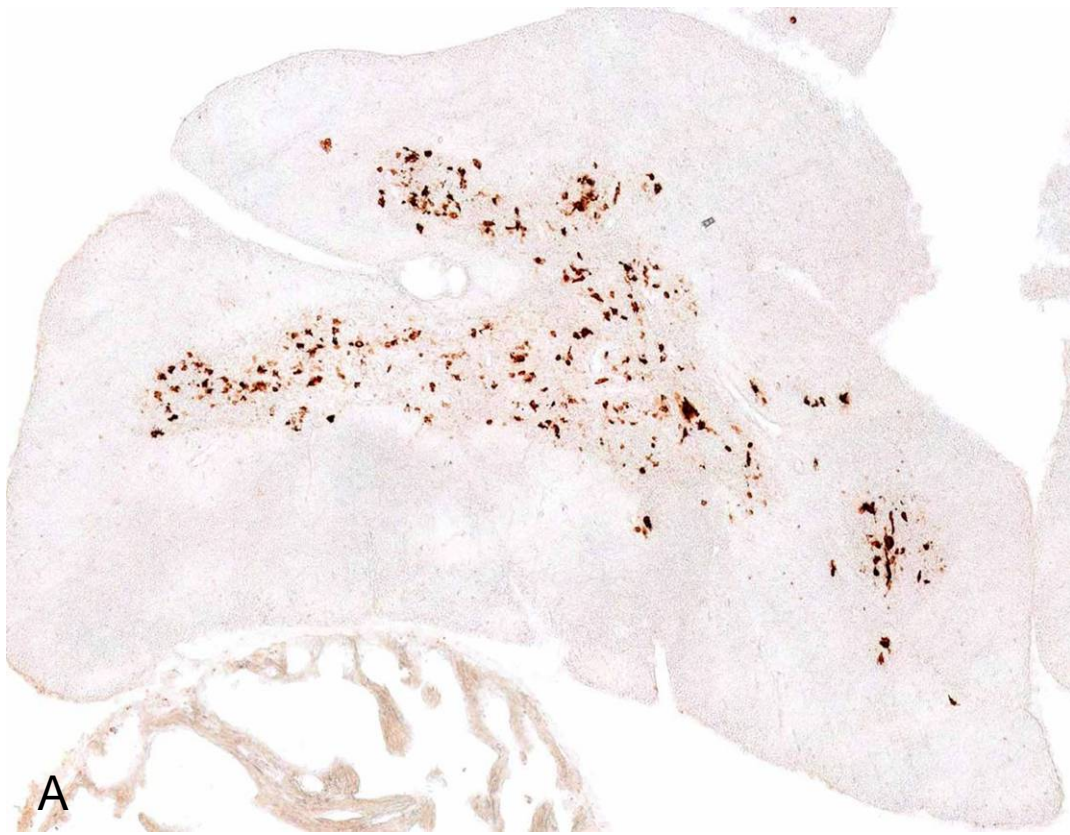


Figure 25: lynx3 expression in thymus of BAC-transgenic mice. Expression visualized with immunohistochemistry with anti-EGFP antibodies and direct fluorescence. Lynx3 is expressed in the epithelial cells and lymphocytes. *Bar= 15 μ m*

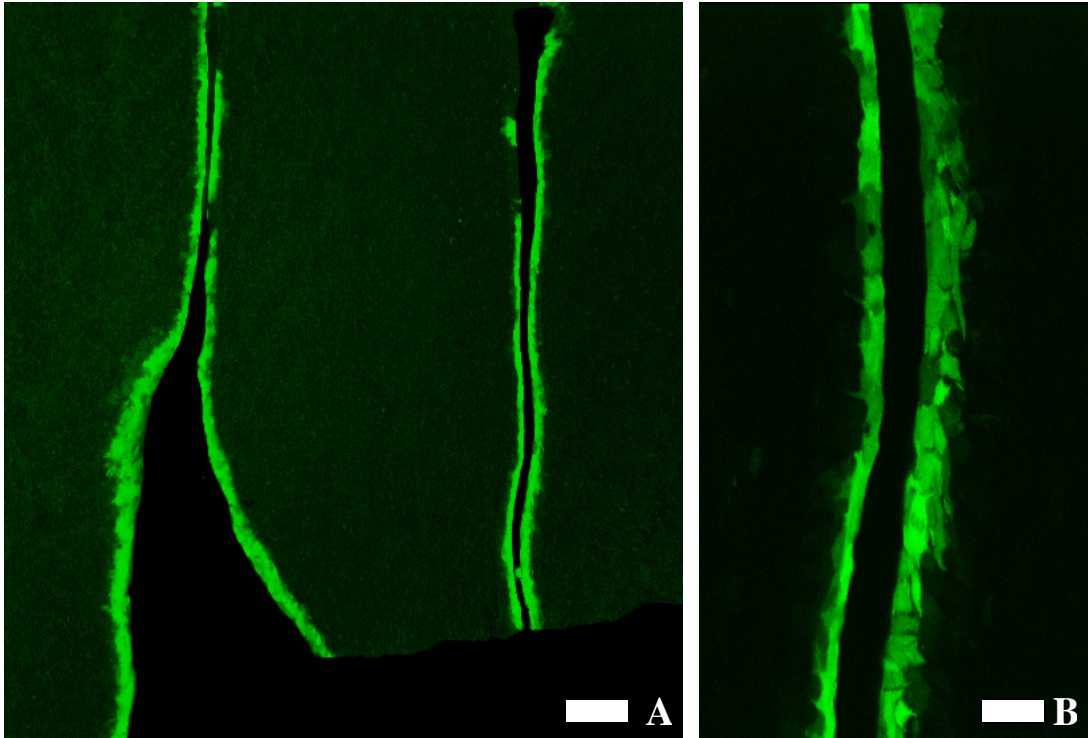


Figure 26: Expression of lynx3 in vaginal mucosa of BAC-transgenic mice shown by direct fluorescence microscopy. Lynx3 is expressed in squamous stratified epithelium. A. *Bar=40 μ m* B. *Bar=10 μ m*

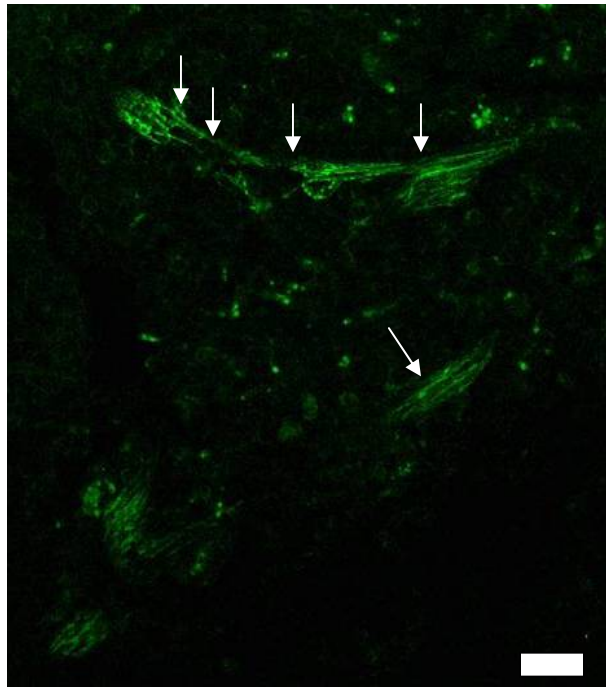


Figure 27: Expression of lynx3 in neurons surrounding blood vessels in spleen. Direct fluorescence microscopy was used to visualize lynx3 expression in spleen of BAC-transgenic mice. *Bar=10 μ m*



Figure 28: lynx4 expression analyzed in BAC-transgenic mice at age E15.5. EGFP-lynx4 expression was detected through immunohistochemistry with anti-EGFP antibodies. Lynx 4 is expressed in whiskers at high levels. No significant level of expression was detected in brain. (*GENSAT*)

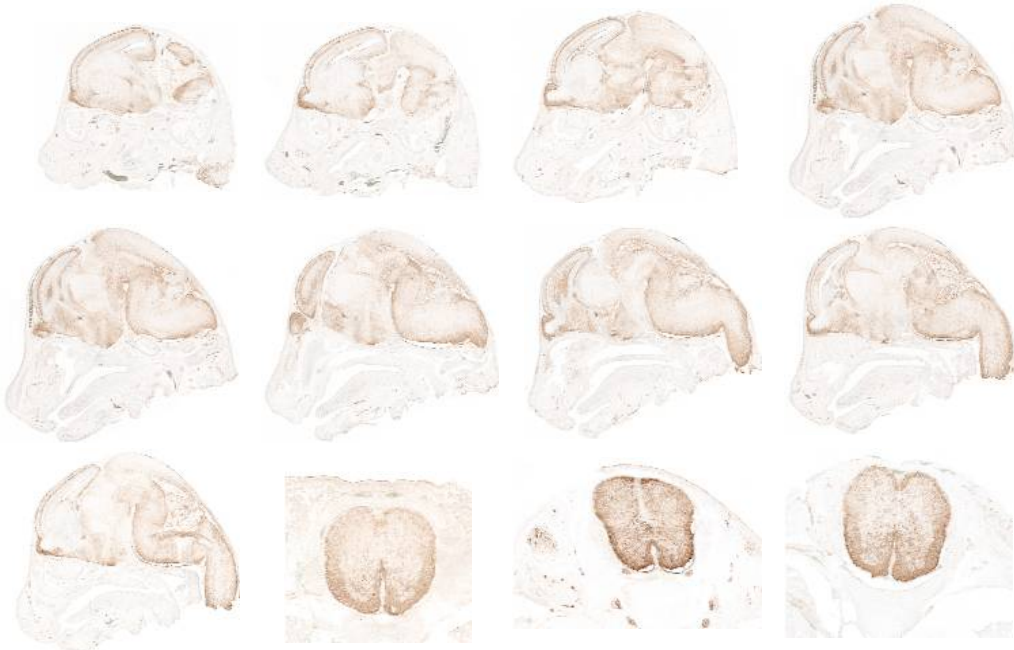


Figure 29: Expression of ly6H at age E15.5 in BAC-transgenic mice. Ly6H expression was detected with anti-EGFP antibodies. Ly6H has a widespread expression in brain and spinal cord at E15.5. (*GENSAT*)



Figure 30: lynx4 expression analyzed in BAC-transgenic mice brain sections. Immunohistochemistry was performed with anti-EGFP antibodies. Lynx4 is expressed in thalamus, cerebellum and brain stem. (*GENSAT*)

Ly6H expression pattern was also analyzed in BAC transgenic mice. BAC transgenic mice that express EGFP under Ly6H promoter were perfused, their brains were dissected and sectioned and immunohistochemistry was performed on these brain sections with anti-EGFP antibodies. The results revealed that Ly6H has a widespread expression pattern in neurons in brain and spinal cord at all three stages analyzed, E15.5, P7 and adult mice (Figure 29, 31, 32). The expression pattern observed in Ly6H BAC transgenic mice correlates with the expression information I have gathered through *in situ* hybridization studies.

The last BAC transgenic mouse line that was made by GENSAT was lynx2 BAC transgenic line. Although the sites where EGFP expression was observed are also positive in lynx2 *in situ* hybridization studies, not all brain regions that express lynx2 according to *in situ* hybridization studies show EGFP expression in BAC transgenic mice. For example, lynx2 expression is detected in CA1 region of the brain, subiculum, and post-subiculum in both BAC transgenic mice and *in situ* hybridization analysis, however, lynx2 expression is very strong and widespread in amygdala according to *in situ* hybridization results, but BAC transgenic mice show EGFP expression in scattered cells in amygdala. Since the expression was not complete, I have not included pictures of the lynx2 BAC transgenic mouse brain sections. The pictures can be found at GENSAT website at www.gensat.org.

Western Blot Analysis

A peptide that has the sequence of the second loop of the three-finger structure in lynx2 was synthesized and injected into two rabbits. The serum taken from those rabbits were purified with IgG purification columns. The purified antibodies bound to a single

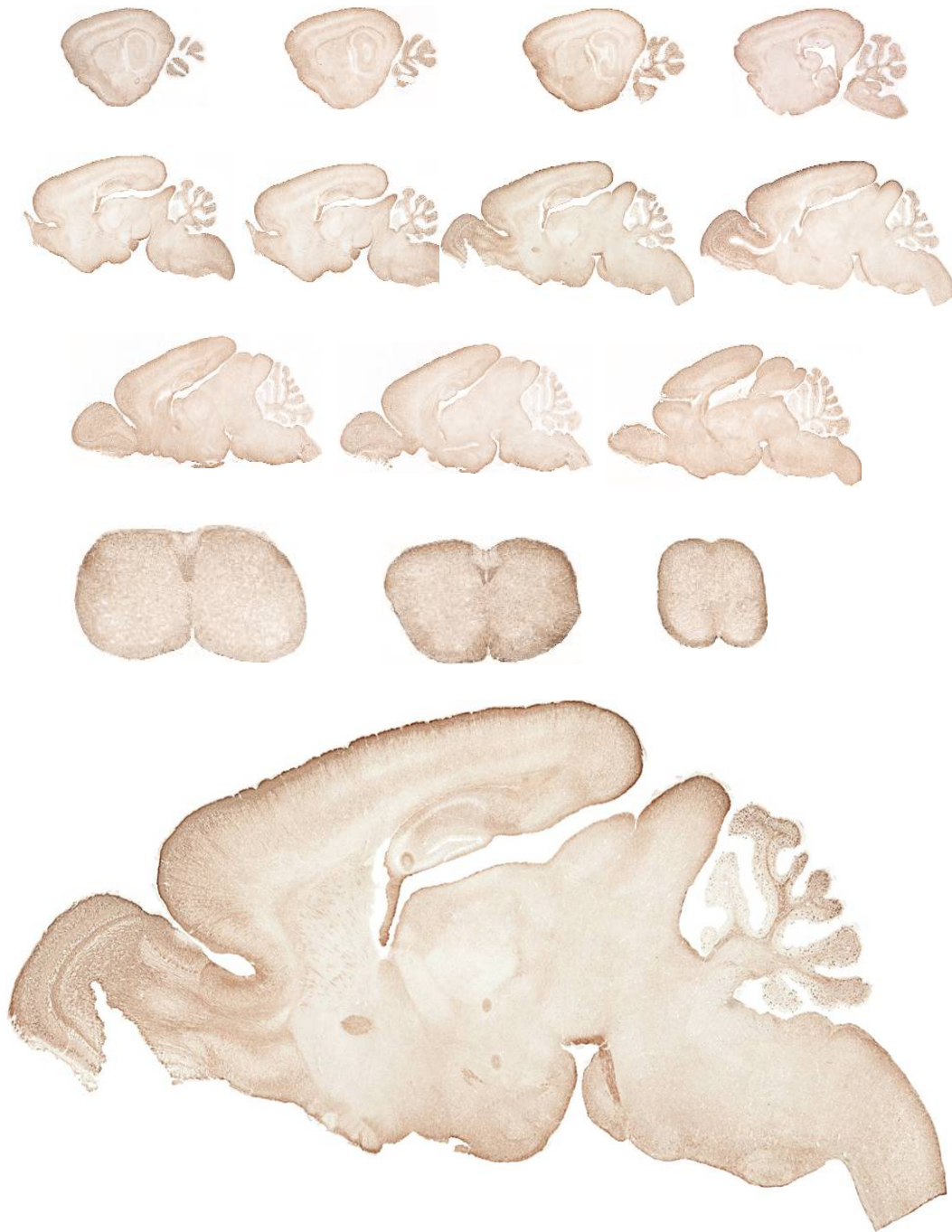


Figure 31: Expression of ly6H in BAC-transgenic mice at age P7. A widespread ly6H expression was detected in neurons in brain and spinal cord with anti-EGFP antibodies. (*GENSAT*)



Figure 32: ly6H expression analyzed in the adult brain and spinal cord sections in BAC transgenic mice. Ly6H has a widespread expression in brain except for cerebellum. It is also expressed in the dorsal horns of the spinal cord.

(GENSAT)

band with a size of ~16 kDa on brain extract western blots. ~16 kDa is the expected size for lynx2 protein. This purified antibody was used for further western blots at 1:2000 dilution.

For multiple tissue western blot, protein extracts were prepared from brain, heart, spleen, kidney, lung, liver and muscle tissues from C57Bl6 mice with a solution that contained 8M Urea to completely linearize the proteins. Equal amounts of protein extracts from each tissue were run on a bis-tris gel and blotted on a membrane. Western blotting was performed on this membrane with anti-lynx2 antibody. Among these tissues, the highest lynx2 expression was detected in brain. Lynx2 expression was also observed in spleen and kidney and a lower level in liver (Figure 33).

In order to analyze the developmental expression patterns of lynx1 and lynx2, I extracted proteins from embryos at age E8.5 and E15.5, heads of embryos at age P1 and brains of mice at ages P4, P7, P10, P15, P19 and P30. C57Bl6 mice were used for all ages and extraction solution contained 8M Urea to linearize all proteins. Equal amounts of protein extracts from each sample were run on a 4-12% bis-tris gel from Invitrogen and blotted with a semi-dry gel blotting system from BioRad. The blots were incubated with Lynx1 polyclonal antibody 1:100 and with Lynx2 polyclonal antibody 1:2000. HRP-conjugated anti-rabbit antibodies were used as secondary antibodies. As a result of our analysis, I have observed that lynx1 is expressed late in development after age P10 and continues to be expressed in adulthood whereas Lynx2 is expressed in all developmental stages that I looked at, from E8.5 to adulthood (Figure 34).

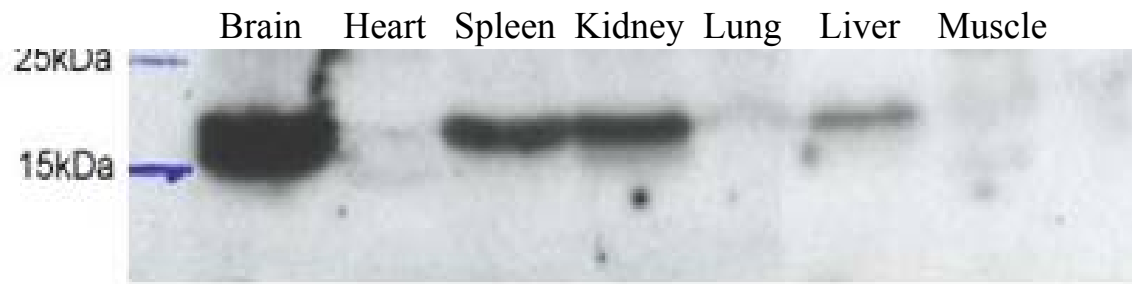


Figure 33: lynx2 expression analyzed in multiple tissue Western blot: Lynx2 is very highly expressed in brain, expressed in lower amounts in spleen, kidney and liver

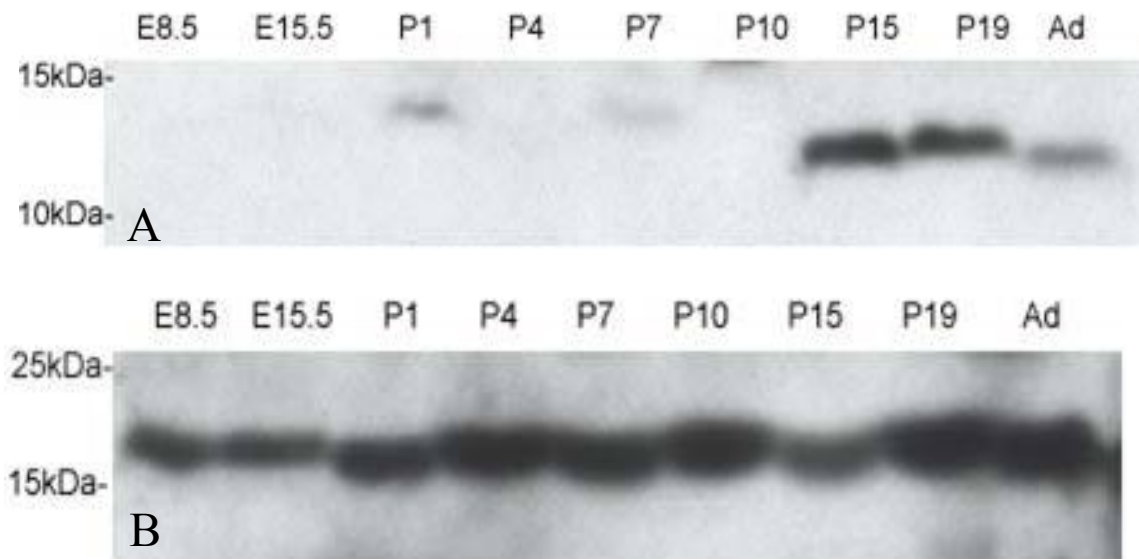


Figure 34: Analysis of developmental expression of lynx1 and lynx2. **A.** Western blot using lynx1 polyclonal antibody showed that lynx1 is expressed very late in development after P10 and is expressed in adult brain. **B.** Lynx2 is expressed throughout the development, expression starting as early as E8.5.

Lynx2 is a membrane protein

Polyclonal Lynx2 antibody was made against a 15 amino acid long peptide on the second finger of Lynx2 protein. The serum was affinity purified and was used for immunocytochemistry on Lynx2 transfected HEK 293T cells, non-transfected control cells and cells that were transfected with an intracellular protein, pacsin. The cells that were transfected with pacsin, were stained with anti-rabbit fluorescence conjugated antibodies when there was detergent in the solution. However, they were negative for fluorescence when there was no detergent in the staining solution, since the antibodies couldn't pass the cell membrane in the absence of detergents, confirming that pacsin is an intracellular protein. Non-transfected cells were incubated with anti-lynx2 antibodies and later with anti-rabbit fluorescence conjugated antibodies in the presence or absence of detergent. In both cases, non-transfected cells were not stained, showing that anti-lynx2 antibodies do not bind to other proteins on HEK293T cells. Lynx2 transfected cells were also incubated with anti-lynx2 polyclonal antibodies and later with anti-rabbit fluorescence conjugated antibodies with and without detergent. Lynx2 transfected cells were positive for fluorescence in the presence and absence of detergent meaning that lynx2 antibodies do not need membrane permeabilization with detergents to bind to lynx2 proteins. These results confirm that lynx2 is a membrane protein (Figure 35).

Immunohistochemistry

The same polyclonal antibody that was used for immunocytochemistry was used for immunohistochemistry studies. 1:100 ratio of the purified antibody was used on free-floating brain cryostat-sections. Lynx2 polyclonal antibodies have stained CA1 region of

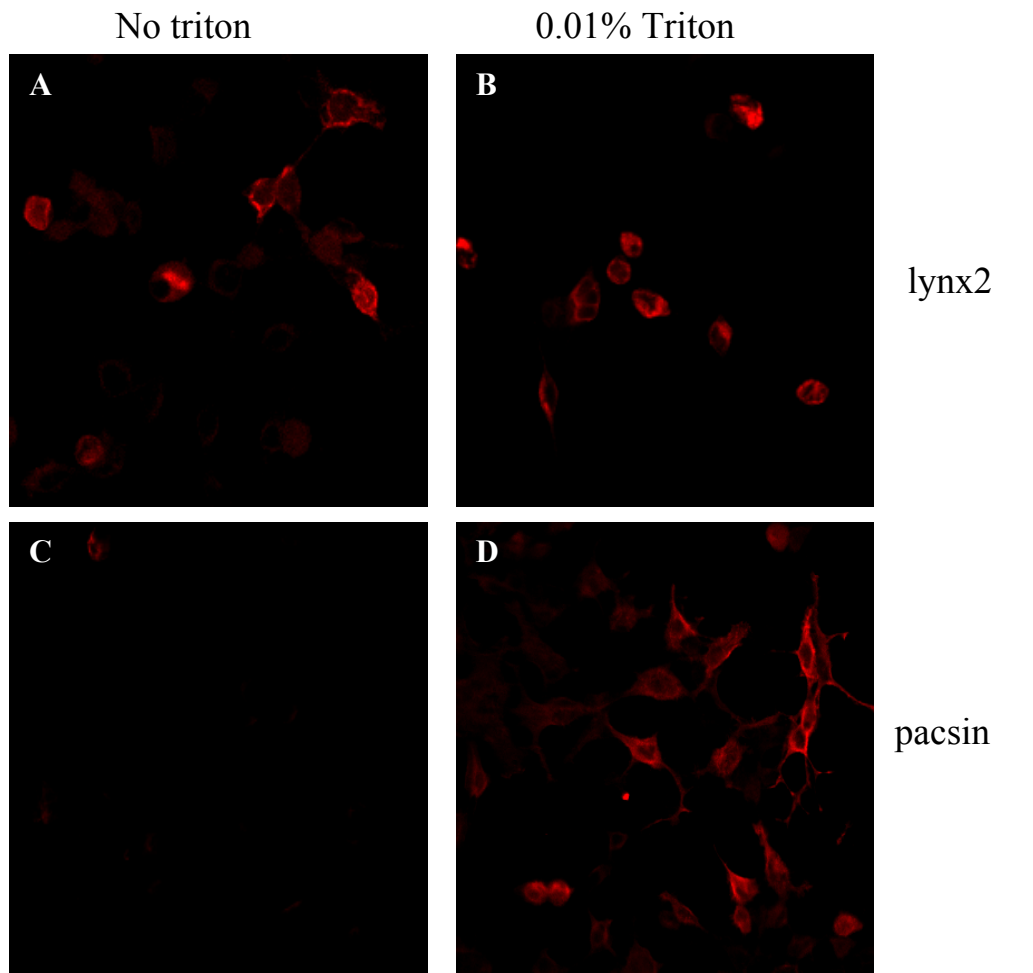
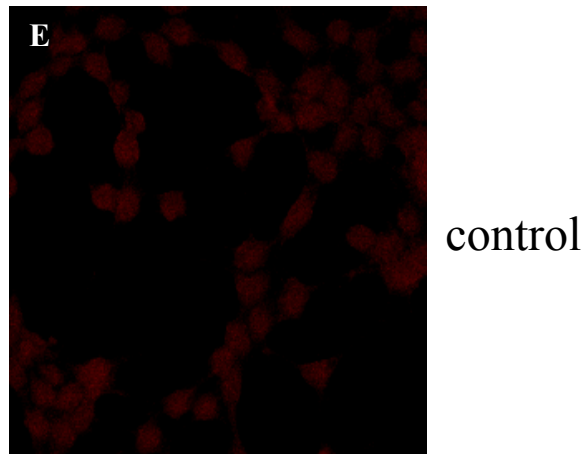


Figure 35: lynx2 is a membrane protein. **A, B:** lynx2 transfected cells stained with affinity purified anti-lynx2 pAb (1:1000) and anti-rabbit Alexa Ab in blocking solutions with **(B)** and without **(A)** triton.

C, D: pacsin (myc tagged) transfected cells stained with anti-myc (1:200) and anti-rabbit Alexa Ab in blocking solutions with **(D)** and without **(C)** triton. **E:** none transfected cells stained with anti-lynx2 pAb (1:1000) and anti-rabbit Alexa Ab in blocking solution with triton.



the hippocampus, however, did not bind to CA2 or CA3 regions which correlate with the in situ hybridization analysis. In addition, scattered neurons in deep nuclei and cortex also showed lynx2 expression (Figure 36). I have tried many different perfusion conditions and sectioning conditions as well as staining solutions to improve these results, and have a more clear immunohistochemistry result, however, they haven't worked well enough. Optimization of this polyclonal antibody for immunohistochemistry still needs more analysis.

Since the polyclonal antibody did not work well with immunohistochemistry, I have made another polyclonal antibody against a peptide with the sequence of the first finger of the three-finger domain of lynx2. The 10 week and 14 week bleeds of this polyclonal antibody didn't work on western blots and worked very poorly in immunocytochemistry compared with Lynx2-second-finger-pAb.

I have made two polyclonal antibodies against lynx3 as well. The first one was against a peptide that the sequence of the second loop of lynx3, but it did not work either on western blots or with immunocytochemistry on lynx3-transfected cells. The second polyclonal antibody against lynx3 was made against the third finger peptide, and I am on the process of analyzing its binding affinity to lynx3 on western blots and immunocytochemistry.

In conclusion, I have observed that Lynx1, Lynx2, Lynx3 and Ly6H have distinct expression patterns in mice. Dissimilarity in their expression patterns suggests that they may have similar or complementary functions in different cell types. Since their expression patterns match expression patterns of nAChRs,

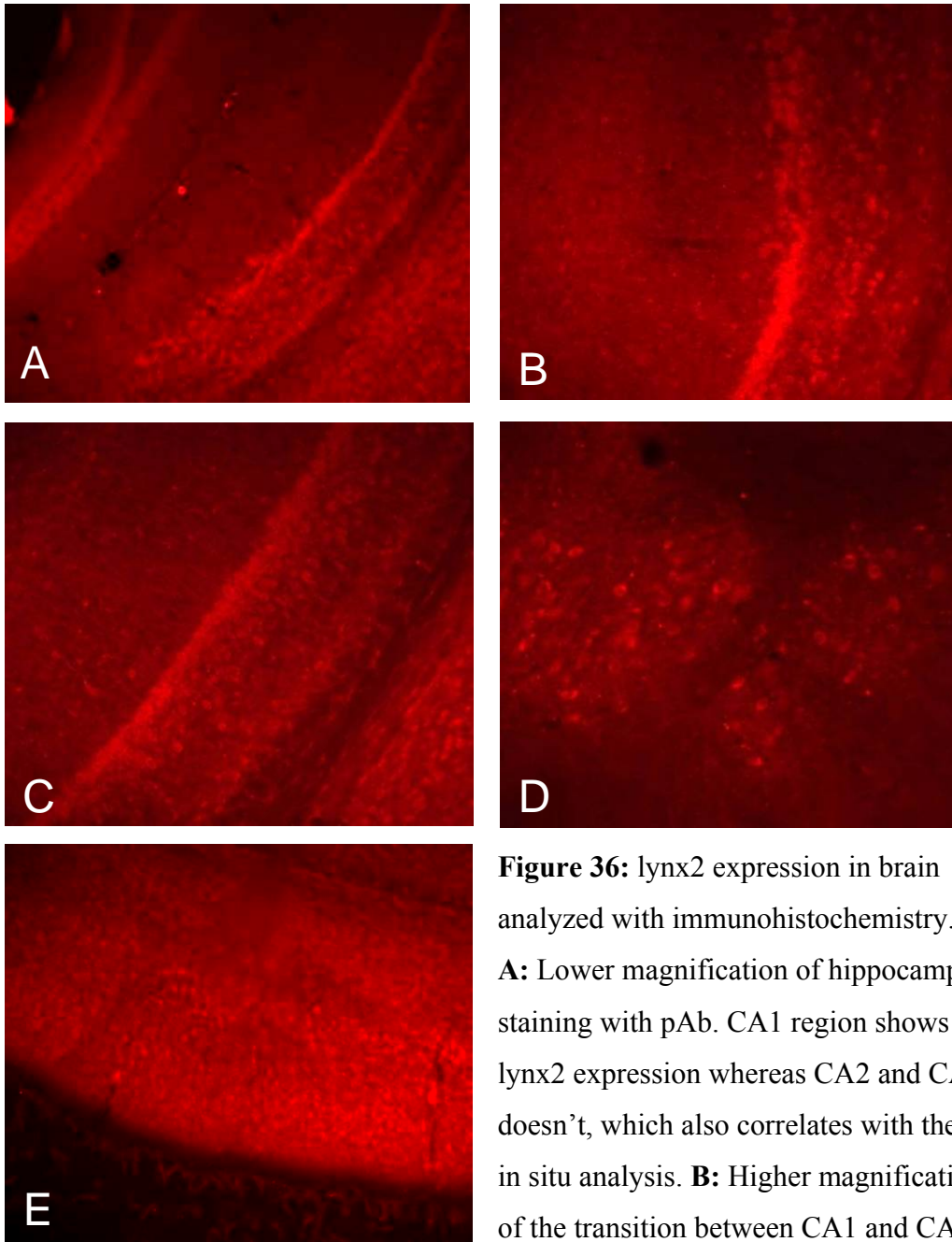


Figure 36: lynx2 expression in brain analyzed with immunohistochemistry.

A: Lower magnification of hippocampal staining with pAb. CA1 region shows lynx2 expression whereas CA2 and CA3 doesn't, which also correlates with the in situ analysis. **B:** Higher magnification of the transition between CA1 and CA2 regions of hippocampus. **C:** Higher magnification of CA1 region of hippocampus. **D:** lynx2 also showed expression in deep nuclei, which also correlates with the in situ hybridization analysis results. **E:** Although not as clear as in situ hybridization analysis, lynx2 pAb showed staining in scattered neurons of cortex.

and lynx1 was already shown to modulate and form stable complexes with nAChRs, I decided to check whether lynx1 homologues behave similarly.

Functional Analysis of Lynx1 homologues

Co-immunoprecipitation analysis

In the recent paper by Ibanez-Tallon et. al. [67], Lynx-1 was shown to co-immunoprecipitate with nAChR subtypes $\alpha 4\beta 2$ and $\alpha 7$. These experiments were performed with avian nAChR subunits. Lynx2 also co-immunoprecipitates with avian $\alpha 4\beta 2$ receptors, however Ly6H doesn't. In order to find out if there is any specificity in binding of Lynx1 and Lynx2 to different nAChR subtypes, mouse and rat nAChR subunits were cloned into expression vectors and Flag-tags were added at C-terminus. Flag-tagged and myc-tagged constructs of Lynx1, Lynx2 and Ly6H were also prepared. The following receptor subunits were subcloned with Flag-tags, and the following subunit compositions were transfected to HEK293T cells:

muscle nAChR subunits: $\alpha 1\beta 1 \gamma \delta$

neuronal nAChR subunits: $\alpha 2, \alpha 3, \alpha 4, \alpha 5, \alpha 6, \alpha 7, \alpha 9, \alpha 10$

$\beta 2, \beta 3, \beta 4$

Receptor combinations: $\alpha 2\beta 2 \quad \alpha 3\beta 2 \quad \alpha 4\beta 2 \quad \alpha 6\beta 2$

$\alpha 2\beta 4 \quad \alpha 3\beta 4 \quad \alpha 4\beta 4 \quad \alpha 9\alpha 10$

$\alpha 7 \quad \alpha 1\beta 1\gamma \delta$

The HEK 293T cell extracts were incubated with either subunit specific antibody or Flag antibody (in that case myc-tagged Lynx proteins are expressed instead of Flag-

tagged constructs) coated protein G beads overnight and the samples were run in PAGE gels and western-blot was performed with anti-Flag-HRP antibody or anti-myc-HRP antibody. As negative control, I transfected HEK cells with myc-tagged lynx constructs and performed immunoprecipitations with anti-Flag antibodies. Unfortunately, I have observed that anti-flag antibodies pulled down myc-tagged lynx subunits, which suggested that we shouldn't use anti-flag antibodies for the immunoprecipitations to eliminate false positive results. Therefore, we decided to use nicotinic receptor subunit specific antibodies for the pull down assays. Since there aren't any good antibodies against some of these subunits, after trying to Co-IP all of these for a while, I decided to narrow the combinations to the following widely expressed nicotinic receptors: Flag-tagged $\alpha 4\beta 2$, chick- $\alpha 7$, Flag-tagged $\alpha 1\beta 1 \gamma \delta$ and the Flag-tagged $\alpha 4\beta 4$ receptor combination (Figure 37).

Membrane fractions were prepared from cells co-expressing $\alpha 7$ -lynx1, $\alpha 7$ -lynx2, $\tilde{\alpha} 7$ -lynx3 and $\alpha 7$ -Ly6H. For immunoprecipitation studies, membrane fractions were incubated with protein G beads bound to $\alpha 7$ monoclonal antibody. Immunoblot analysis with another $\alpha 7$ monoclonal antibody demonstrated that $\alpha 7$ was specifically immunoprecipitated. Immunodetection on the same fractions with an antibody against flag-tag showed that lynx1 and lynx2 immunoprecipitate with $\alpha 7$ receptor, however, lynx3 and Ly6H do not. Same experimental set-up was used for $\alpha 4\beta 2$, $\alpha 1\beta 1\gamma \delta$ and $\alpha 4\beta 4$ receptors and lynx1 and its homologues. For immunoprecipitating $\alpha 4\beta 2$ and $\alpha 4\beta 4$ receptors, we used protein G beads bound to $\alpha 4$ monoclonal antibody, and for immunoprecipitating $\alpha 1\beta 1\gamma \delta$, we used $\beta 1$ monoclonal antibody bound protein G beads. Through immunoblot analysis with an antibody against flag-epitope, we showed that

$\alpha 4\beta 2$, $\alpha 1\beta 1\gamma\delta$ and $\alpha 4\beta 4$ receptors were specifically immunoprecipitated. We also demonstrated that lynx1 and lynx2 immunoprecipitate with all three of these receptor subtypes and Ly6H does not immunoprecipitate with any of them. Lynx3 immunoprecipitates with $\alpha 4\beta 2$ and $\alpha 4\beta 4$ receptors, however, does not immunoprecipitate with $\alpha 1\beta 1\gamma\delta$ receptor. Control experiments with membrane fractions from cells that are transfected with only lynx1 or its homologues demonstrated that lynx1 or its homologues were not precipitated with protein G beads bound to any of the $\beta 1$, $\alpha 1$, or $\alpha 7$ antibodies in the absence of the receptors. Our results are consistent with previous findings for both $\alpha 7$ and $\alpha 4\beta 2$ co-immunoprecipitations with lynx1 [67]. lynx1 also immunoprecipitates when co-expressed with $\alpha 4\beta 4$ and muscle nAChRs. lynx2 acts similar to lynx1 in co-immunoprecipitation experiments with all four nAChR subtypes tested. Interestingly, lynx3 forms stable complexes with $\alpha 4\beta 2$ and $\alpha 4\beta 4$ nAChRs, but does not co-immunoprecipitate with neither $\alpha 7$ nor muscle nAChRs. Ly6H does not form stable complexes with any of the four nAChR subtypes that were tested (Table 4).

These results demonstrate that lynx1 homologues form stable complexes with specific nAChR subtypes. Although their target nAChR subtypes are the same, lynx1 and lynx2 do not function redundantly since their expression sites are distinct and even complementary in hippocampus (lynx1 is expressed in CA2 and CA3 regions, whereas lynx2 is expressed in CA1 region). lynx3, however, co-immunoprecipitates with only $\alpha 4\beta 2$ and $\alpha 4\beta 4$ nAChR subtypes and does not form stable complexes with neither $\alpha 7$ nor muscle type of nAChRs. This suggests that lynx3's effect on modulation of nAChRs is more specific than its homologues. The expression patterns of lynx3 and $\alpha 4\beta 2$ nAChRs

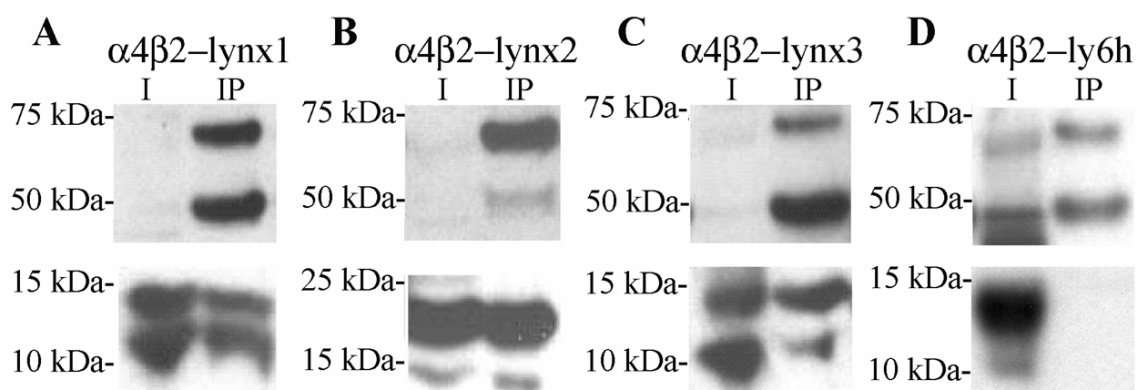


Figure 37: Distinct interactions of lynx1, lynx2, lynx3 and ly6h with nAChRs.

Membrane extracts from HEK293 cells expressing $\alpha 4\beta 2$ -lynx1 (**A**), $\alpha 4\beta 2$ -lynx2 (**B**), $\alpha 4\beta 2$ -lynx3 (**C**), and $\alpha 4\beta 2$ -ly6H (**D**) were analyzed. All of the constructs, $\alpha 4$, $\beta 2$, lynx1, lynx2, lynx3 and ly6h, were flag-tagged. The first lane in each blot show a sample of the membrane extract input and indicated with letter I. The second lane in each blot contain the immunoprecipitation fractions incubated with protein G beads bound to a4 monoclonal antibody. The blots were probed with anti-flag-epitope monoclonal antibody. The upper panels show that a4 (~69kDa) and b2 (~45kDa) subunits were immunoprecipitated with protein G beads bound to a4 monoclonal antibody (upper panels, **A**, **B**, **C** and **D**). lynx1, was also immunodetected with anti-flag antibody in the precipitate fraction (~11-13 kDa), demonstrating that lynx1 forms stable complexes with $\alpha 4\beta 2$ nAChRs (A, lower panel). lynx2 was immunodetected in the precipitate fraction, showing that lynx2 also co-immunoprecipitates with $\alpha 4\beta 2$ nAChRs (B, lower panel). Immunoblot analysis showed that lynx3 also immunoprecipitated with $\alpha 4\beta 2$ nAChRs (C, lower panel). Although ly6h could be detected in the membrane extract input fraction, I, it could not be detected in the precipitate fraction, IP, showing that ly6h does not immunoprecipitate with $\alpha 4\beta 2$ nAChRs (**D**, lower panel).

Table 4: Summary of co-immunoprecipitation analysis with nAChRs and lynx

homologues. lynx1 and lynx2 both form stable complexes with $\alpha 4\beta 2$, $\alpha 4\beta 4$, $\alpha 7$ and muscle nAChRs. Lynx3 binds to $\alpha 4\beta 2$ and $\alpha 4\beta 4$ nicotinic receptors, but does not bind to $\alpha 7$ or muscle receptors. Ly6H does not bind to any of the four nicotinic receptors we have assayed.

| nAChR | $\alpha 4\beta 2$ | $\alpha 4\beta 4$ | $\alpha 7$ | $\alpha 1\beta 1\gamma\delta$ |
|-------|-------------------|-------------------|------------|-------------------------------|
| Lynx1 | √ | √ | √ | √ |
| Lynx2 | √ | √ | √ | √ |
| Lynx3 | √ | √ | – | – |
| Ly6H | – | – | – | – |

overlap in tissues like bronchial epithelium suggesting that Lynx1 homologues might also be modulating nAChR subtypes in non-neuronal tissues.

Electrophysiology

Lynx1, Lynx2 and Lynx3 modulate desensitization kinetics of alpha4-beta2 nAChRs whereas Ly6H does not

It was previously shown that co-expression of lynx1 modulates the rate and extent of desensitization of ACh-evoked responses through $\alpha 4\beta 2$ nAChRs [67]. To assess whether lynx1 homologues share similar functional traits with lynx1, we performed two-electrode voltage clamp recordings in *Xenopus* oocytes expressing $\alpha 4\beta 2$ nAChRs alone, or in combination with lynx1, lynx2, lynx3 and ly6H. Oocytes were exposed to acetylcholine (ACh) for 20 seconds and the evoked currents were analyzed. In oocytes expressing the receptor alone, ACh elicited a fast peak current followed by a slow biphasic desensitization phase during ACh application. At the end of the ACh exposure, the currents quickly returned to baseline. In contrast, in oocytes expressing either lynx1, lynx2 or lynx3 with $\alpha 4\beta 2$ nAChRs, the ACh evoked responses after the initial peak showed a significantly faster desensitization in the first biphasic component before reaching the second biphasic component or plateau (Figure 38A). This effect on desensitization is not observed when $\alpha 4\beta 2$ receptors are co-expressed with ly6H. To measure these differences in desensitization, two exponential component equations were fitted to the desensitizing currents during ACh application, and fast (Figure 38B) and slow (Figure 38C) time constants were calculated as described in [67]. Figure 38B and 38C shows the average values of these time constants for ACh responses. As shown in

Figure 38B, the fast time constant is significantly faster in oocytes co-expressing lynx1, lynx2 and lynx3, and is not affected in oocytes co-expressing ly6H. No differences in the slow time constant during the plateau phase were observed (Figure 38C). These results indicate that lynx1, lynx2 and lynx3 share similar modulatory properties on nAChRs.

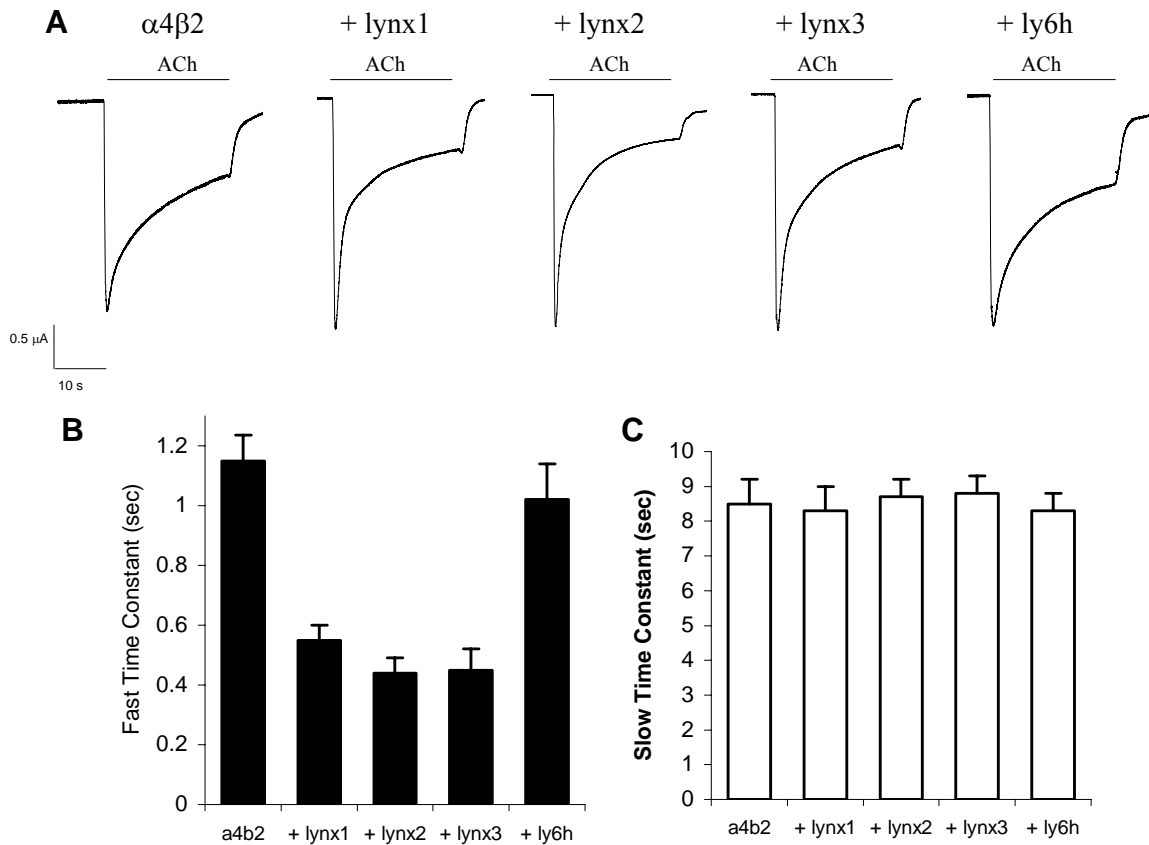


Figure 38: lynx1, lynx2 and lynx3 enhance desensitization of ACh-evoked currents mediated through $\alpha 4\beta 2$ nAChRs in oocytes. **A.** Representative recordings of voltage clamped oocytes expressing $\alpha 4\beta 2$ nAChRs alone, or in combination with lynx1, lynx2, lynx3 and ly6H. The inward currents were evoked by 20 sec periods of superfusion (horizontal calibration bar) with external saline containing 1mM ACh. ACh evoked responses in oocytes coexpressing $\alpha 4\beta 2$ nAChRs with lynx1, lynx2 or lynx3 showed significantly faster desensitization during agonist application immediately after the initial peak. ly6h had no effect on desensitization when coexpressed with a4b2 receptors. **B** and **C.** The differences in desensitization are shown with bar graphs. As described in (2), two exponential equations were fitted to the desensitization currents during ACh application. Using these equations, fast (**B**) and slow (**C**) time constants were calculated and the average values of these constants for ACh responses are shown in **B** and **C**. In oocytes coexpressing $\alpha 4\beta 2$ nAChRs with lynx1, lynx2 or lynx3, the fast time constant is significantly faster, while the slow time constant during the plateau phase remained the same. Both constants are unaffected in oocytes coexpressing Ly6.

CHAPTER 4:

Gene-targeted Deletion Analysis for Lynx2 and Lynx3

Summary

Nicotinic receptors are involved in many biological processes in the CNS and in the periphery. Some of these processes are learning and memory and modulation of anxiety in the CNS and cell-to-cell adhesion and signaling in the periphery. lynx2 and lynx3 modulate nicotinic receptor desensitization in vitro and they form stable complexes with specific nAChRs in mammalian cell cultures. The expression patterns of both lynx2 and lynx3 correlate with nAChR expression as well.

In order to find out which nicotinic receptor mediated biological process lynx2 and lynx3 might be effecting, we have generated lynx2 and lynx3 null mutant mice. As a result of phenotypical analysis of *lynx2*^{-/-} mice, we have observed that there are no gross anatomical differences between brain sections of *lynx2*^{-/-} and WT mice till the age of 8 months. However, *lynx2*^{-/-} mice exhibited abnormal anxiety related responses, motor strength, motor coordination, motor learning and associative learning. Our results are described below.

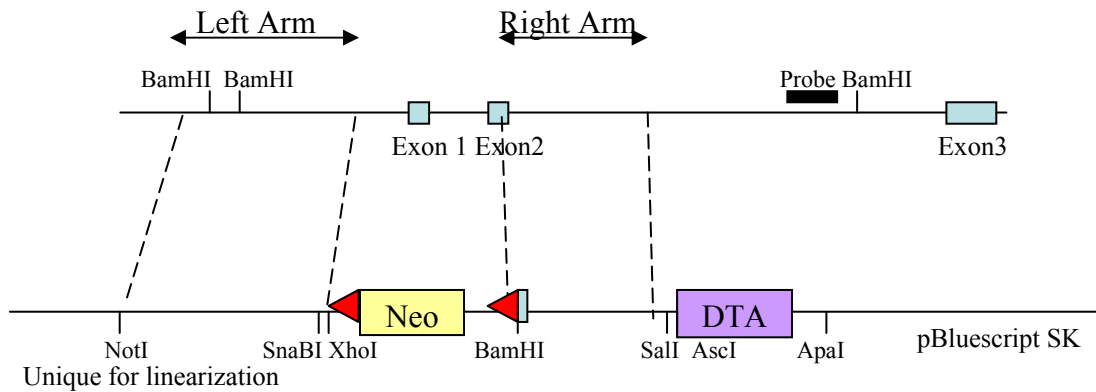
Lynx2

Straight KO Construct Preparation

Three different KO constructs were prepared with C57Bl6 genomic DNA. The arms for homologous recombination were cloned by subcloning a Bacterial Artificial Chromosome (BAC) and Expand long-template PCR reaction from a *lynx2* containing BAC. The first construct aimed to delete the first exon, which has the start codon and had a neomycin (neo) cassette with a poly-A tail sequence in it. Since we could only get less than 10 ES clones as a result of the electroporation, and no homologous recombination, we chose to prepare another construct with a different neo cassette. The second construct had the same properties as the first one, but had another neo cassette in it. The electroporation of this construct yielded about 50 colonies and no homologous recombination, which is still less than average (~200 colonies is the average). To solve this problem, I prepared a third construct which contained a longer homology arm, a neo cassette without a poly-A tail and a diphtheria toxin (DTA) sequence at the end of the second homology arm for increased selection. This construct aimed to delete first and the second exon of *lynx2*, since the second exon had two in frame ATG sequences, which might be targeted for translation. Third construct is shown in figure 39.

Chimeras and Breeding:

KO constructs were electroporated into Bruce4 ES cells 5 times total (first and second construct once, the third one three times). Out of ~800 colonies picked up 4 were positive for homologous recombination. These 4 positive colonies were injected into



Neo cassette has TK promoter and LoxP sites at both ends
 Linearization enzyme is NotI
 For Southern analysis, RE enzyme is BamHI, KO~8kb, WT~12kb

Figure 39: Lynx2 KO construct. Homologous recombination arms of the KO construct were prepared with C57Bl6 genomic DNA, and a modified version of the pBluescript SK vector was used as the backbone of the construct.

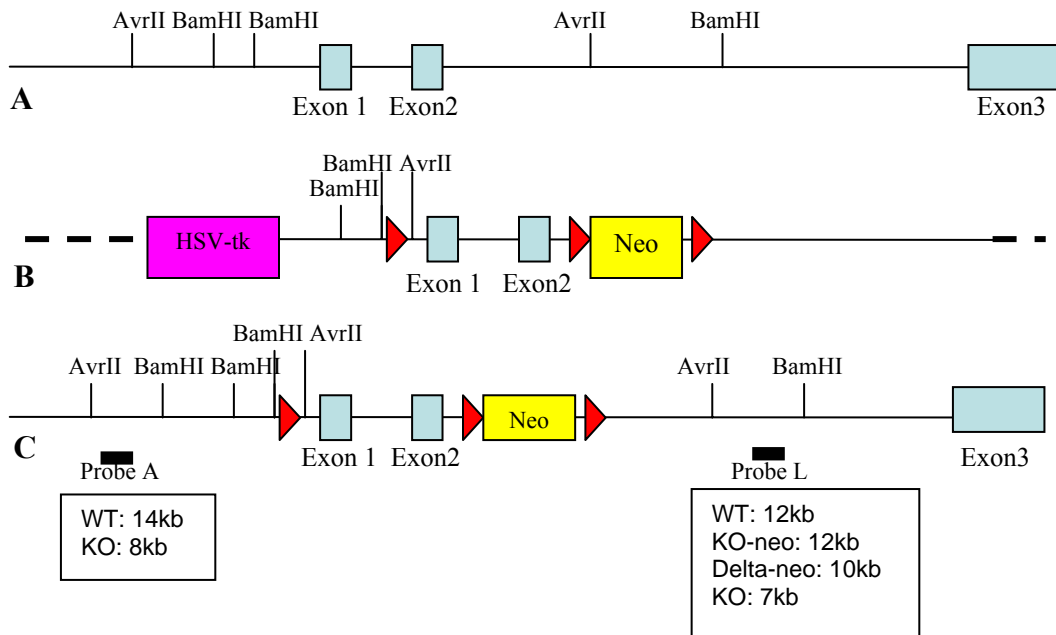


Figure 40: Lynx2 Conditional KO construct. A. Scheme of the genomic structure of Lynx2 gene. B. Lynx2 KO construct scheme. C. Scheme of result of homologous recombination of the KO construct with genomic DNA. (*Construct designed and prepared by Dr. Ivo Lieberam*)

FVB, Balb/C and AlbinoB6 blastocytes. We had 7 chimeras which were three 5% chimeric males, and four females (with 10%, 85%, 80% and 40% chimerism). After breeding the chimeras to C57Bl6 males and females for at least 6 generations, we had ~600 pups but no germline transmission.

Conditional KO construct properties

The construct for the conditional KO was prepared by Dr. Ivo Lieberam in Jessell Lab at Columbia University. These constructs were also prepared by using C57Bl6 genomic DNA. Two different constructs were prepared since the first construct failed to yield any positive clones for homologous recombination among ~600 colonies after electroporation into Bruce4 ES cells. The second construct had two short homology arms and one long homology arm and there were three lox-P sites that separates the first and the second homology arms, the second homology arm and the neo cassette and at the end of the neo cassette. The construct was designed to be able to yield in three different deletions after being processed by cre. The construct and the results of possible deletions are described in the figure 40.

Chimeras and Breeding

The conditional KO construct was electroporated into Bruce4 ES cells at Columbia University, which resulted in two colonies with homologous recombination. These two ES cell colonies were injected into C57Bl6 blastocysts in Columbia University and into Albino B6 and Balb/C blastocysts at Rockefeller University Gene Targeting Facility. As a result of the injections at Rockefeller University, we had 10 chimeras from 3 different injections of 2 separate ES clones: 6 males (5%, 90%, 5%, 1%, 95%, 60%

chimeric), and 4 females (50%, 45%, 10%, 90% chimeric). We had success in germline transmission with these chimeras and have crossed the heterozygotes to EIIa-cre transgenic mice on C57Bl6 genetic background. We have had both total deletions and partial deletion of neo cassette, which resulted in conditional KO allele. Both heterozygotes and homozygotes for the total deletion of lynx2 are viable.

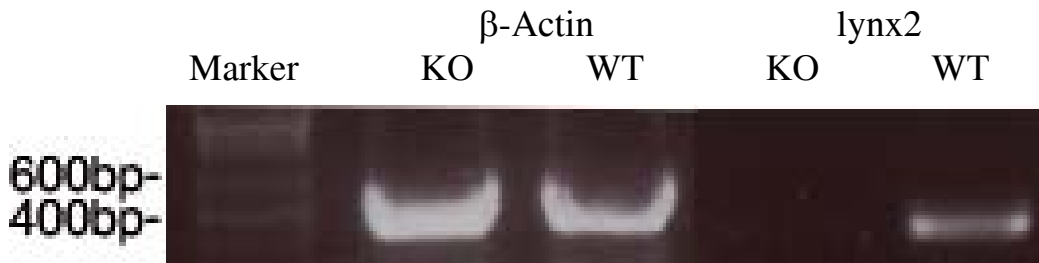


Figure 41: RT-PCR analysis shows lynx2 mRNA is absent in *lynx2*^{-/-} mice. mRNA was isolated from brains of WT and *lynx2*^{-/-} mice with Trizol reagent. RT-PCR analysis was done with primers for amplifying β-actin mRNA and lynx2 mRNA with single-step RT-PCR kit from Invitrogen. β-actin control band was amplified in both samples. Lynx2 mRNA was amplified in WT sample but not in the null mutant mRNA sample. The primers were chosen from two different exons to exclude amplification from genomic DNA contamination.

Anatomical Analysis of *lynx2*^{-/-} Animals

As a result of preliminary analysis, we have not observed any major anatomical differences between the brain sections from the WT and mutant mice around 6-8 months of age. The body weights and sizes of the mutant mice are also similar to the WT animals. All the *lynx2*^{-/-} and WT animals are on pure C57Bl6 background, which minimizes the problems that are associated with genetic background. Pictures of hippocampus and cortex from the WT and *lynx2*^{-/-} mice brain sections are in the following figure 41. The mice brains were perfused, dissected and embedded in paraffin and sectioned and stained with Hemotoxylene-Eosine (H&E) staining (figure 42).

Behavioral Phenotyping of *lynx2*^{-/-} Mice

Using expression pattern of Lynx2 mRNA and protein as a guide, we analyzed behavioral phenotypes of *lynx2*^{-/-}. Some of the major expression sites of Lynx2 in the mouse brain are regions associated with emotional behavior including: amygdala, stria terminalis, CA1 region of hippocampus, subiculum, cortex, ventromedial hypothalamic nucleus and mammillary body; motor functions and learning: interneurons in cerebellum and deep nuclei, caudate putamen; sites associated with olfaction: olfactory bulb, olfactory tubercle, anterior olfactory cortex, piriform cortex and entorhinal cortex; nociception: anterior pretectal nucleus; and several motor nuclei in medulla and pons: motor trigeminal nucleus (jaw movement control), parabrachial nucleus (cardiovascular regulation, pain conduction and vasopressin release regulation), gigantocellular reticular nucleus (part of sensory innervation of the arm-touch, pain), nucleus ambiguus (pharynx, larynx, thoracic organ control).

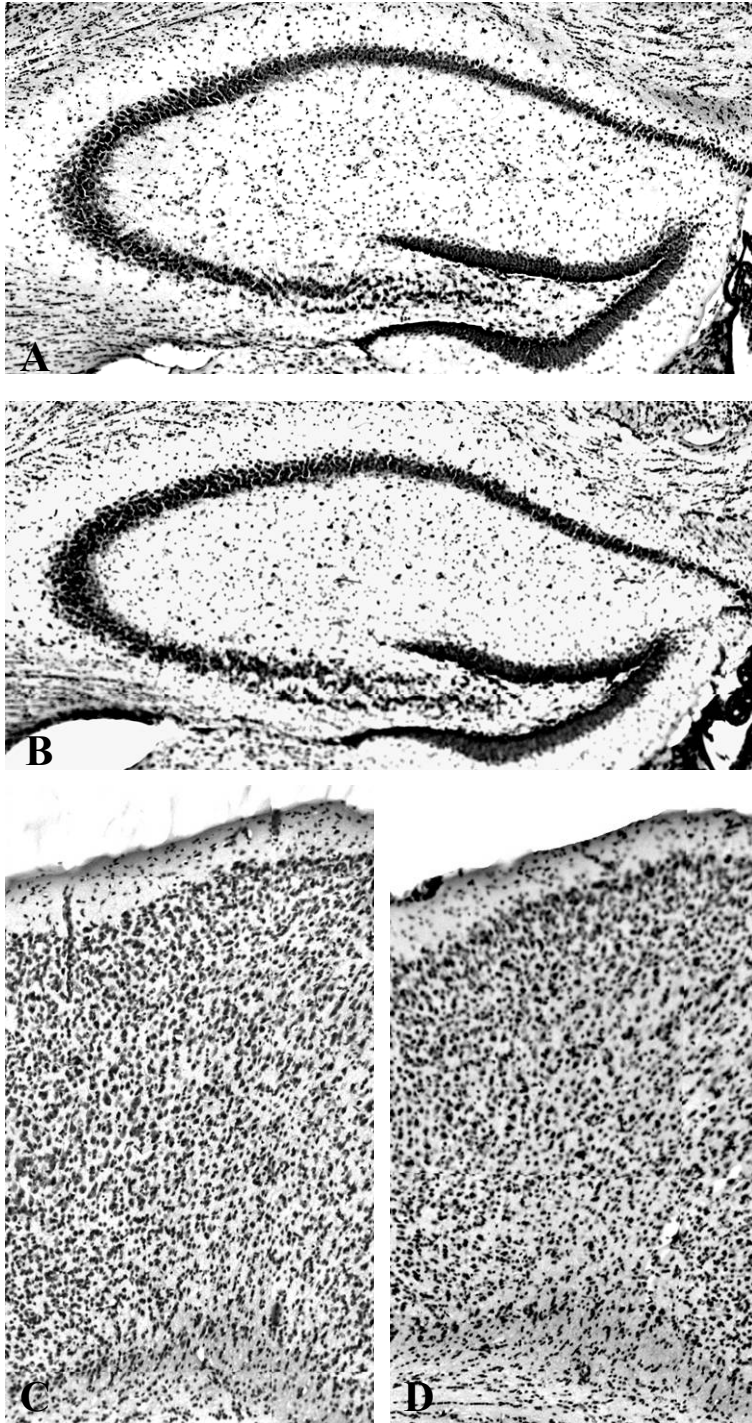


Figure 42:

Representative pictures of hippocampus and retrosplenial cortex in *lynx2*^{-/-} and WT mice.

There were no gross anatomical differences

between brain sections of WT and *lynx2*^{-/-} mice at 7 months of age.

Hematoxyline-eosine stained sections. **A.**

lynx2^{-/-} hippocampus, **B.**

WT hippocampus, **C.**

lynx2^{-/-} cortex, **D.** WT

cortex.

In order to check if there were any major motor abnormalities in the *lynx2*^{-/-} mice, we first observed and analyzed their behavior in open-field exploration test. 12 male *lynx2*^{-/-} mice and 12 male WT mice were tested at 22 weeks of age. The WT and *lynx2*^{-/-} mice behaved similarly in terms of the distance moved, percentage of time they spent moving, mean velocity and percentage of time spent in the center. Both the WT and *lynx2*^{-/-} mice jumped during the trial, however, the *lynx2*^{-/-} mice jumped significantly more than the WT mice (Student's-T-Test performed, p-value < 0.01). The results are shown in figure 43.

The mice were then tested for ear-twitch and eye-blink reflexes, and both the WT and *lynx2*^{-/-} mice behaved in the same way. Following the reflex tested, the *lynx2*^{-/-} and WT mice were analyzed for motor strength. The *lynx2*^{-/-} animals have less motor strength than the WT mice assessed by hanging wire test, during which the latency of the animals to fall from a wire cage, where they hang with their paws, is measured. The results are shown in figure 44.

Since *lynx2* is expressed in various regions that are associated with motor coordination and learning, I also tested them with a rotarod task during which the latency of the mice to fall from a cylindrical accelerating rod is measured. The *lynx2*^{-/-} animals exhibited a superior motor coordination with respect to the WT mice on the first day of experiment (Mixed effects ANOVA, p-value < 0.01). The *lynx2*^{-/-} mice continued to perform better than the WT mice in the following 3 days that the test was performed, which shows that the *lynx2*^{-/-} mice have enhanced motor learning (Repeated measures ANOVA, p-value<0.001, on all days collectively). The results of this test are shown in figure 45.

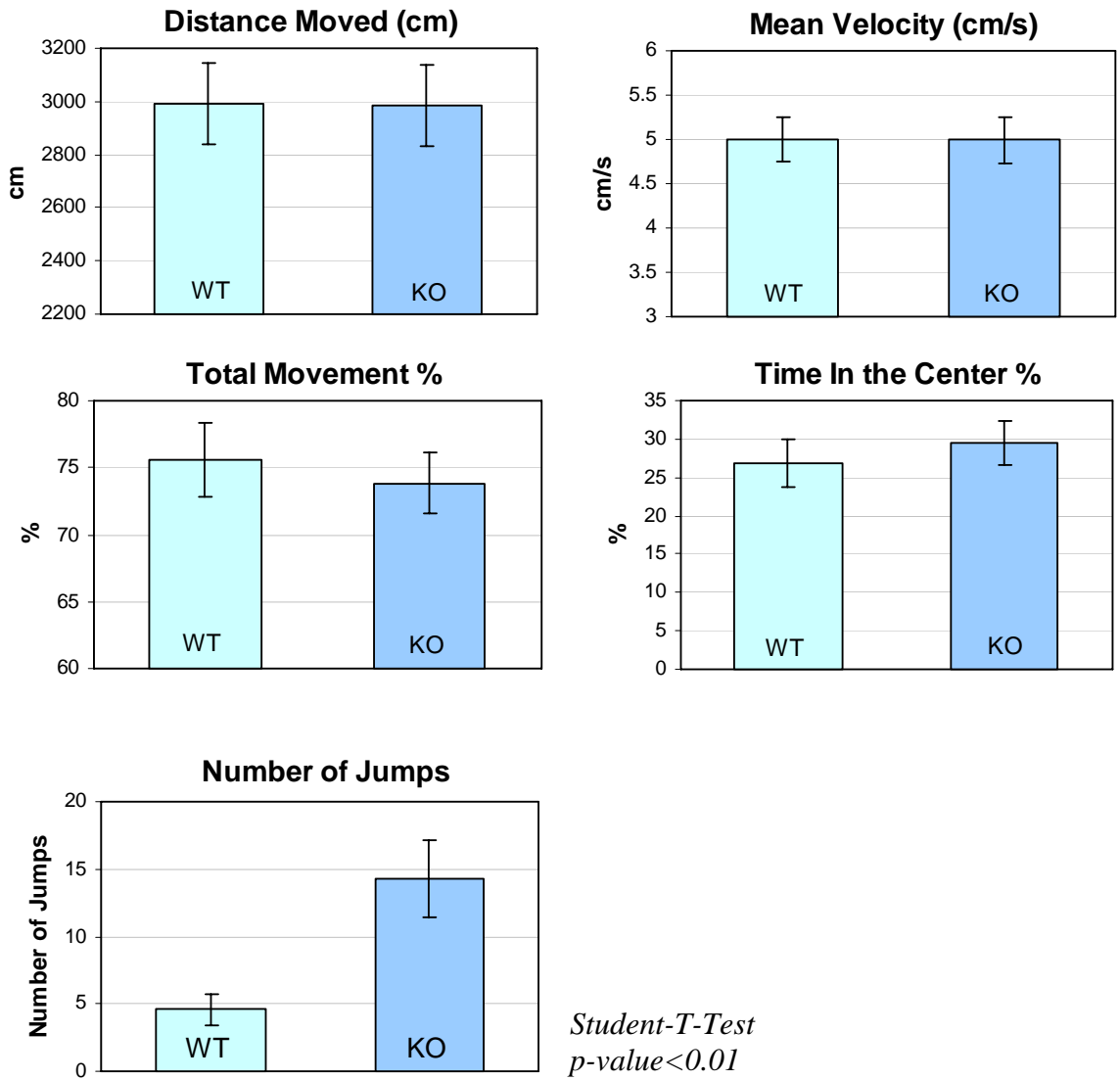


Figure 43: Open Field Exploration Test. *lynx2^{-/-}* mice and WT mice were tested to compare their gross motor skills. *lynx2^{-/-}* mice and WT mice had similar mean velocities, moved similar amount of distances and moved for similar durations. They spent similar amount of time in the center, too. However, *lynx2^{-/-}* mice jumped significantly more times than WT mice. *N=12 male mice per genotype. Age: 22 weeks*

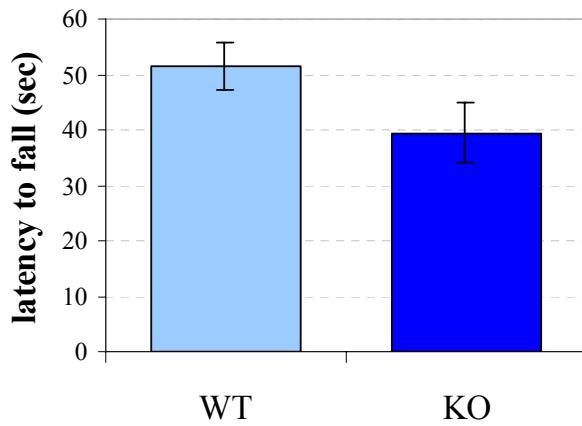


Figure 44: Hanging wire test. Motor strengths of *lynx2*^{-/-} mice and wild type mice were compared with hanging wire test. Latency to fall from a wire cage was measured with a cut off of 60 seconds since WT mice should easily be able to stay on the wires for that period. *lynx2*^{-/-} mice tended to fall off earlier than wildtype mice.

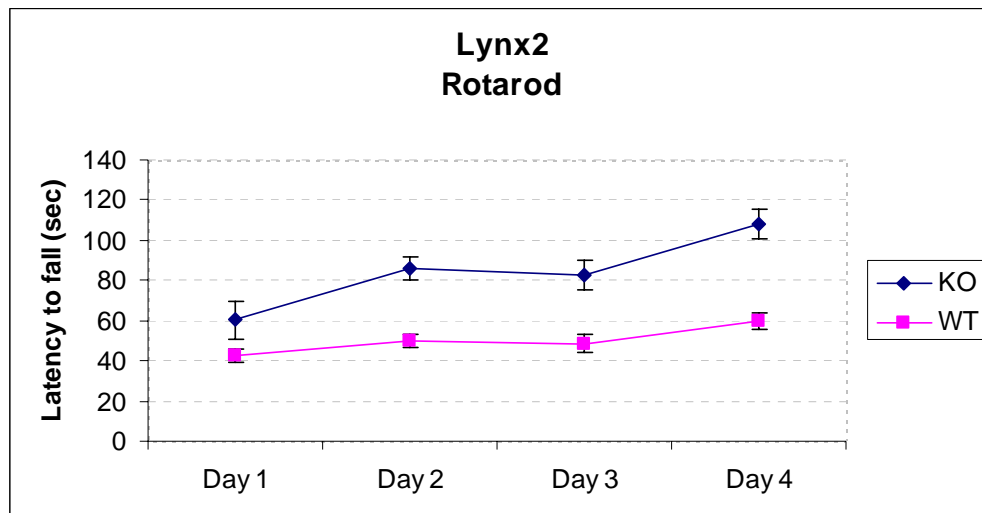


Figure 45: Rotarod test. Motor coordination and learning of *lynx2*^{-/-} mice and wild type mice were compared with an accelerating rotarod for four consecutive days. *lynx2*^{-/-} mice performed significantly better than wild type mice on day one and on the following days. (Repeated measures ANOVA, p-value < 0.001)

Activation of the nicotinic receptors through intraperitoneal nicotine injections has been shown to deteriorate motor coordination in the WT animals [209]. In order to assess the effects of nicotine on motor coordination of the *lynx2*^{-/-} animals, they were tested on rotarod assay. I observed that motor performance of the *lynx2*^{-/-} animals is not affected by nicotine, however the WT mice perform worse than saline injected control the WT mice (Mixed effects ANOVA, p-value=0.06).

Mecamylamine is an antagonist of nicotinic receptors and it was previously shown that nicotinic receptor antagonists impair rotarod performance [209]. In my experiments, injection of mecamylamine, an antagonist of nAChRs that affects both central and peripheral nicotinic receptors, also causes a decrease in motor coordination and motor learning for the WT mice when compared with the control WT mice. Intraperitoneal injection of mecamylamine also deteriorates motor coordination and motor learning in the *lynx2*^{-/-} mice with respect to saline injected the control *lynx2*^{-/-} mice. These results confirm my previous data that shows modulatory effect of *lynx2* on nicotinic receptors in vivo (Mixed effects ANOVA, p-value = 0.06).

In order to assess whether the effect of *lynx2* on motor coordination is due to the nicotinic receptors in the peripheral or central nervous system, we injected the *lynx2*^{-/-} and WT mice with saline and hexamethonium, which is a nicotinic receptor antagonist that blocks receptors expressed in peripheral nervous system that does not pass blood-brain barrier. Hexamethonium didn't affect the motor coordination of either the WT mice or the *lynx2*^{-/-} animals, which suggests that *lynx2* effect on rotarod performance is through its action on nAChRs in CNS (Mixed effects ANOVA, p-value ~ 0.2)

Another test that I have done using rotarod assay was using mecamylamine injection followed by nicotine injection. Animals injected with both of these drugs performed like animals injected only with nicotine. The results of the rotarod test are shown in figures 46 and 47.

lynx2 is expressed very highly in brain regions involved in emotional behaviors, including amygdala, stria terminalis and hippocampus. Therefore, I used several tests to investigate if the *lynx2*^{-/-} mice perform differently than the WT mice in emotional behavior. Basolateral amygdala, in which *lynx2* is very highly expressed, has been associated with auditory-cue-associative and context-associative learning in the fear conditioning test [210]. When the *lynx2*^{-/-} mice and the WT mice were analyzed with fear conditioning test, on the first day, mice were trained to associate a mild electric shock to a tone, a conditioned cue (Figure 49).

On the second day, mice are placed in the training environment without any auditory-cue, and they were observed every 10 seconds to count the number of times they freeze. The *lynx2*^{-/-} mice demonstrated similar contextual-associative learning to the WT mice as a result of comparison with Student-T-test (p-value=0.55) (Figure 49).

In the second part of the day 2, the mice were placed in a novel environment and the number of freezes were recorded every 10 seconds, with or without the auditory cue. The *lynx2*^{-/-} mice exhibited a significant higher number of freezes to the tone than the WT mice, which might suggest that the *lynx2*^{-/-} mice show better auditory-cued-associative learning than the WT mice or have increased fear due to the auditory-stimulus. (results analyzed with Student-T-test, p-value<0.01) (Figure 49).

Anatomical regions of the brain that are associated with anxiety are not very well characterized; however, amygdala, hippocampus, stria terminalis and cortex have been implicated as major sites for regulating anxiety [189, 211, 212]. Since *lynx2* is heavily expressed in amygdala, stria-terminalis, CA1 region of hippocampus and layer 4 and 5 of cortex, and nicotinic receptor activation have been implicated in several forms of anxiety, I have tested the *lynx2*^{-/-} animals on various anxiety-related assays. In light-dark box test, where the amount of time spent in light and dark compartments of a test box is measured, I observed that the *lynx2*^{-/-} animals spent less time in light with respect to the WT mice (Student's-T-Test, p-value < 0.05) (Figure 50).

Intraperitoneal injections of nicotine have been shown to have an anxiolytic effect in light dark box test [213]. Since *lynx2* modulates nicotinic receptors and lack of *lynx2* increases anxiety related responses in mice, I wanted to test the effect of nicotine on the *lynx2*^{-/-} mice in light-dark box test. The WT and KO mice were injected with saline or 1mg/kg nicotine and were tested 40 minutes after injection. I have observed that indeed nicotine injections have an anxiolytic effect on the WT mice, since it increases the time spent in the light compartment of the light dark box, with respect to the mice that were injected with saline. However, nicotine injections had no significant effect, on anxiety related behaviors of the *lynx2*^{-/-} mice. The *lynx2*^{-/-} mice injected with nicotine behaved similarly to the *lynx2*^{-/-} mice injected with saline. This result suggests that *lynx2* modulates nicotine-mediated anxiety (Figure 51) (Two-way ANOVA, p-value < 0.05 for genotypic variance, and p-value = 0.08 for treatment variance).

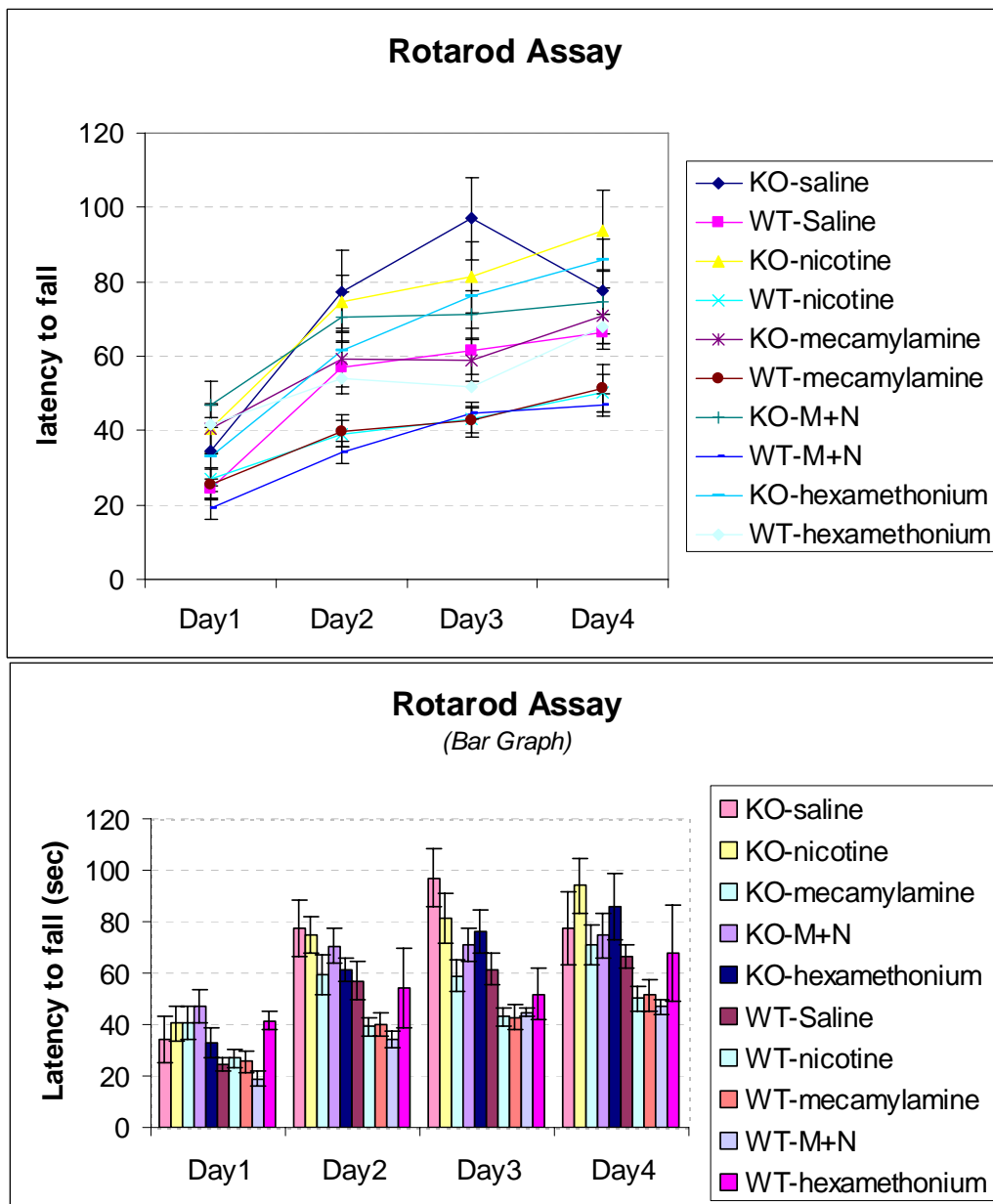


Figure 46: Effects of nAChR agonists and antagonists on rotarod performance of WT and *lynx2*^{-/-} mice. *lynx2*^{-/-} mice and WT mice were injected with 1mg/kg nicotine, saline, 4 mg/kg mecamylamine, 4 mg/kg mecamylamine followed by 1mg/kg nicotine, and 4 mg/kg hexamethonium. Tests were performed 5 minutes after nicotine or saline injections, and 15 minutes after mecamylamine or hexamethonium injections. 4 consecutive tests were done with 5-minute intervals on each test day for 4 days. The results are shown as bar graphs and line graph as means of four trials per day for each test days. At least 8 age matched male mice were tested for each group.

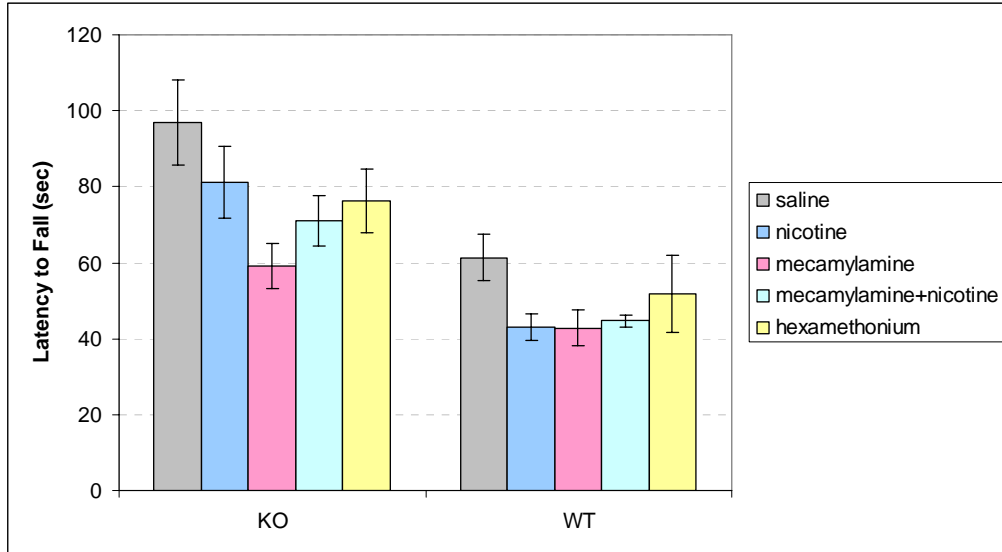


Figure 47: Effects of nicotine and nAChR antagonists on the motor skills of *lynx2*^{-/-} mice and WT mice. Nicotine injections impair motor coordination of WT mice, however, it has no significant effect on *lynx2*^{-/-} mice. Mecamlamine injection impairs motor coordination of not only WT mice, but also *lynx2*^{-/-} mice. Hexamethonium injections have no effect on either WT or *lynx2*^{-/-} mice. Mecamlamine injections followed by nicotine injections have similar effect to nicotine injections in both

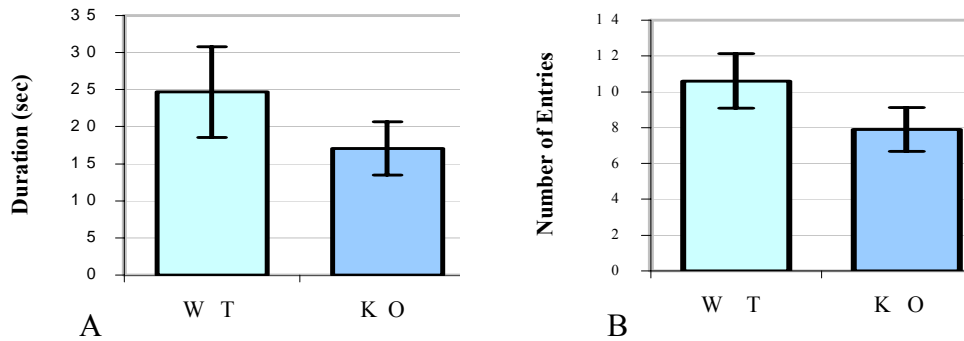


Figure 48: Elevated Plus Maze test. In another anxiety related test, elevated plus maze, *lynx2*^{-/-} mice and wild type mice performed similarly. **A.** Duration of stays of wild type and *lynx2*^{-/-} mice in open arms were measured. **B.** Number of entries into open arms are shown.

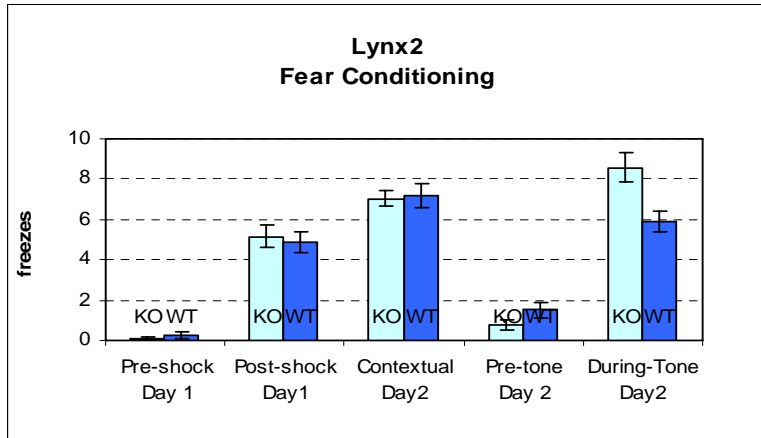


Figure 50: Fear Conditioning test. *lynx2*^{-/-} mice and WT mice were for their contextual and associative learning abilities. *lynx2*^{-/-} and WT mice showed similar fear responses on training day, before and after being exposed to a tone followed by a mild electric shock. On test day, when mice were placed in the training environment, *lynx2*^{-/-} and WT mice exhibited similar freezing responses to the context without any tone. On the second part of the test day, mice were placed in a novel environment, *lynx2*^{-/-} and WT mice showed similar fear responses before tone. However, *lynx2*^{-/-} mice froze significantly more times to the tone than the WT mice, showing they demonstrated better associative learning (for auditory-cued conditioning, Student's-T-test, p-value < 0.05).

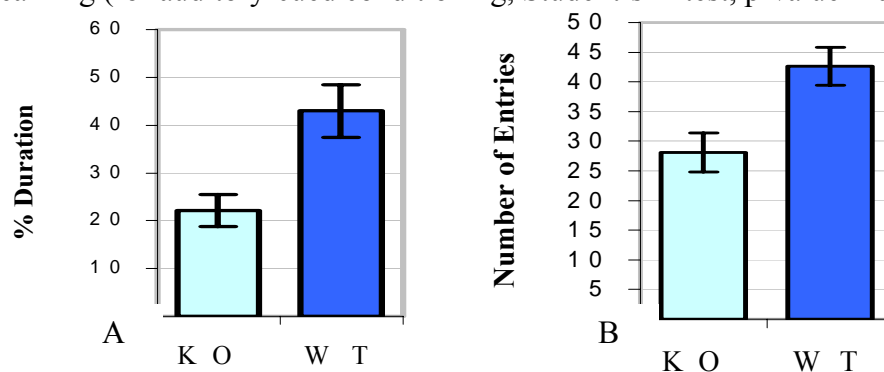


Figure 51: Light-Dark Box Test. As a measure of anxiety related behavior, *lynx2*^{-/-} mice and wild type mice were tested on light-dark box. **A.** *lynx2*^{-/-} mice entered light compartment significantly less times than wild type mice. **B.** Percentage of time that the *lynx2*^{-/-} mice spent in light compartment was significantly less than wild type mice (Student's-T-Test, p-value < 0.05 for both measures).

Another test that is related to anxiety-associated behavior is social interaction test. In social interaction test, the tendency of spending time with a novel mouse with respect to an empty cage is tested. A diagram of the test apparatus and the labeled areas in the apparatus are shown in figure 52. In the first part of this test, mice are kept in the middle region, with doors closed for 10 minutes. After 10 minutes, the doors are opened and test mouse starts to freely explore the apparatus. The time spent in the compartment where the caged-mouse is present is named as Sniff1-stranger1. The time spent in the compartment, where there is an empty cage, is named Sniff2-empty cage. The close areas around the cages, where the test mouse sniffs the cages, are labeled as Sniff1 and Sniff2. In this test, we observed that the *lynx2*^{-/-} spends significantly less time with the novel mice than the WT mice. Instead, the *lynx2*^{-/-} mice prefer to spend time in the compartment where there's an empty cage (Figure 53). Our results from this test and the light-dark box test show that the *lynx2*^{-/-} mice exhibit more anxious behavior than the WT mice. Statistical comparison was performed with Student-T-test, p-value<0.05)

During the second part of social interaction test, another novel mouse was placed in the empty cage, and the previous novel mouse, which is familiar to the test mouse now, is kept in the same cage. After rehabilitation in the middle compartment for two minutes, the doors are opened again, and the test mouse roamed freely between the compartments. On this part of the test, there were no significant differences between the WT and *lynx2*^{-/-} mice in terms of the time spent with the familiar mouse or novel mouse, according to Student's-T-test comparison (Figure 54).

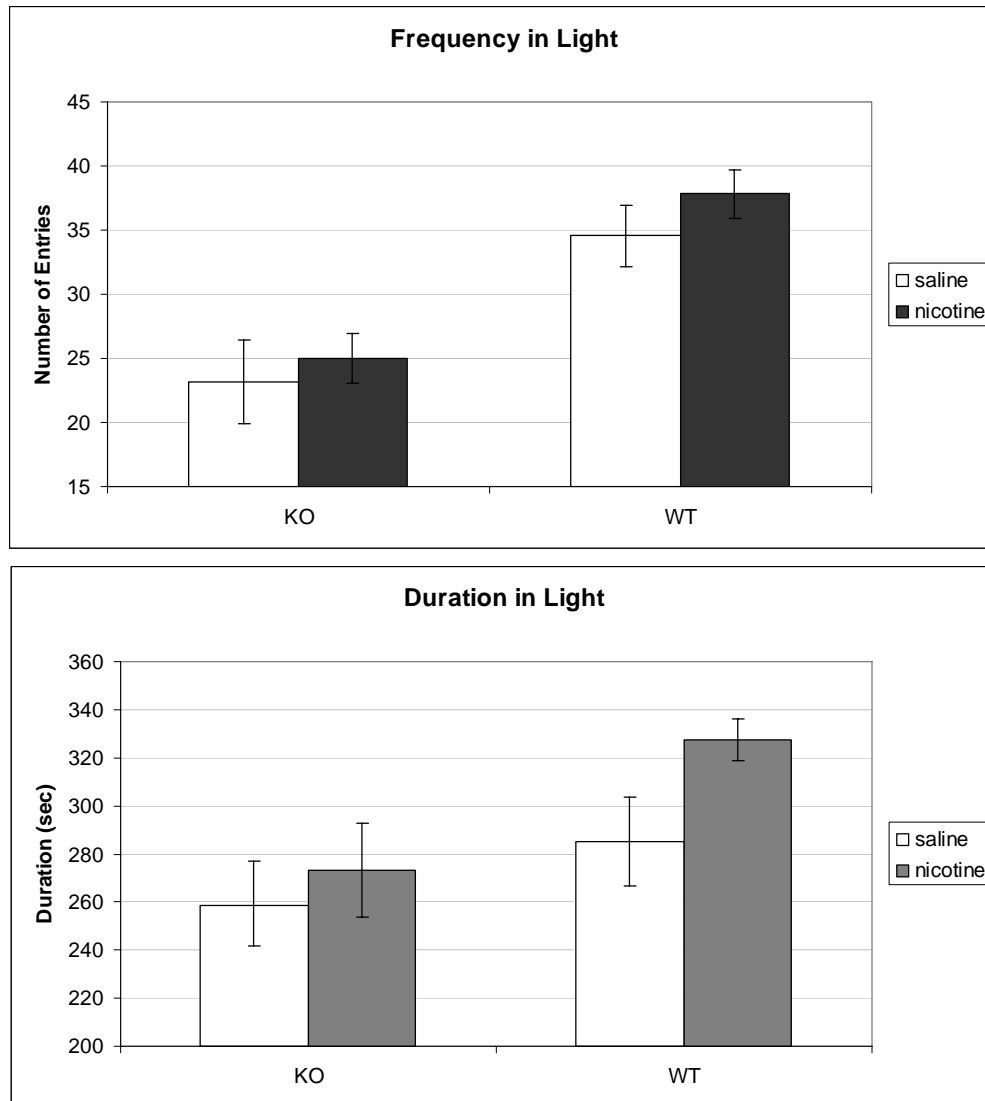


Figure 51: Effect of nicotine on anxiety related behavior. *lynx2^{-/-}* mice and wild type mice were tested with light dark box 40 minutes after being injected with saline or 1mg/kg nicotine. I did not observe a statistically significant difference in the number of entries in to light compartment between saline or nicotine injected wild type or *lynx2^{-/-}* mice. However, wildtype mice injected with nicotine spent more time in light than saline injected wild type mice. *lynx2^{-/-}* mice injected with nicotine or saline spent similar durations in light compartment (Two-way ANOVA, p-value < 0.05 for genotypic variance and p-value = 0.08 for treatment variance).

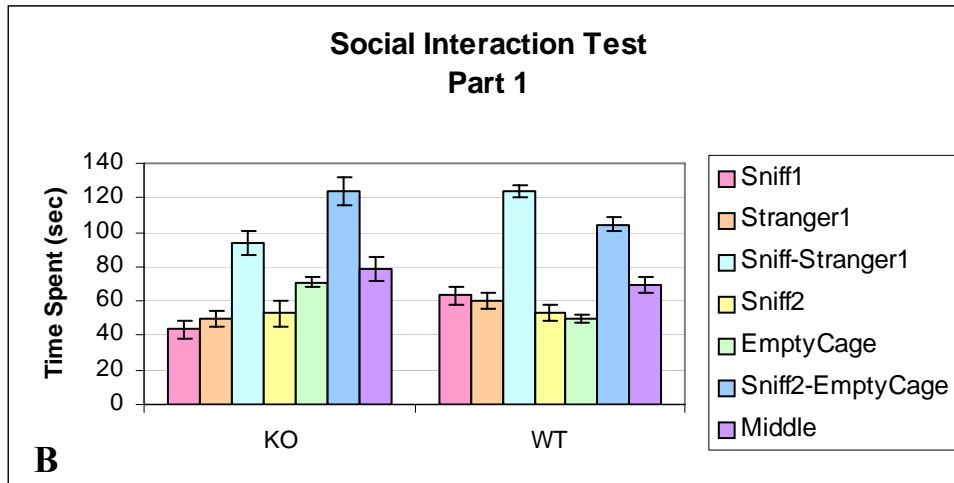
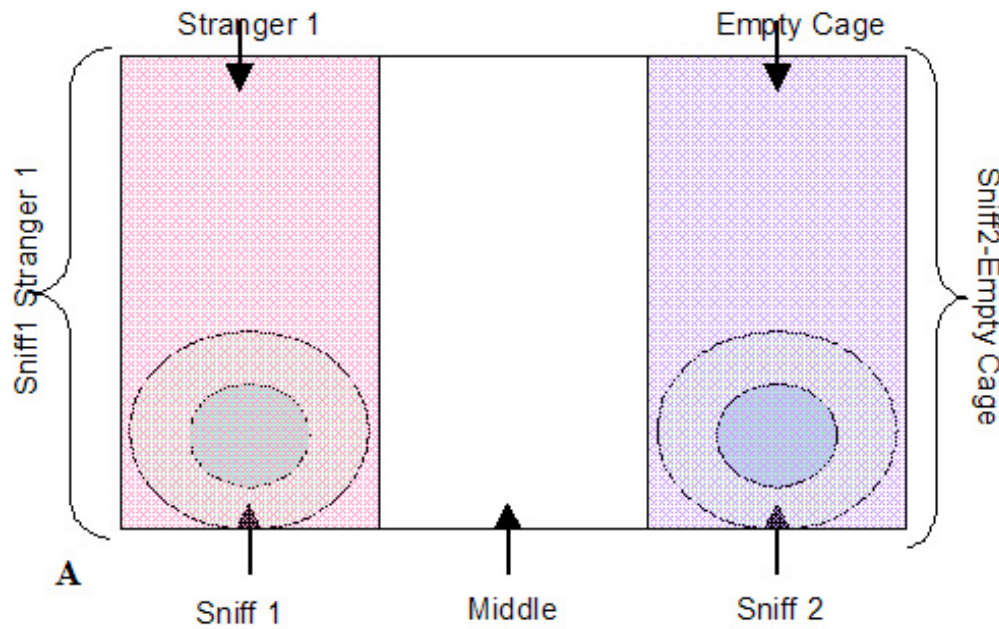


Figure 52: *lynx2^{-/-}* mice were tested for anxiety related behavior with the Social Interaction test. **A.** A scheme of the test box used for the social interaction test. There were three compartments divided with removable doors; middle compartment was used for habitation, for the first Part of this test, a novel mouse was put in a round cage in the Stranger 1 compartment in the blue circle. The close area around the cage was counted as interaction area with the novel mouse and was named Sniff 1. The cage in the Empty Cage compartment was empty, and it was also placed in the blue circle. The time spent around the empty cage, in Sniff 2 area, was counted as interaction with the empty cage. **B.** The results of the first part of the social interaction test are shown.

In another test for anxiety, elevated plus maze, where a different aspect of anxiety is measured, mice are placed in a cross shaped elevated platform. Two of the arms have walls and named closed arms, and two of the arms don't have walls and are named open-arms. The time spent in the closed arms, open arms and center are measured. In this test, the *lynx2*^{-/-} mice performed similarly to the WT mice (Student's-T-test, p-value>0.05 for both number of entries into open arms and duration in open arms). Since elevated-plus maze and the other two anxiety tests that I have performed are testing different measures of anxiety in mice, this result does not contradict with our previous results (Figure 48).

Since *lynx2* is expressed in many regions of the brain that are associated with olfaction, I performed a basic olfaction test, called buried-food retrieval test. In this test, mice are starved for 18 hours and the next day they are placed in a clean empty mouse cage in which a food pellet is buried approximately 1cm under the bedding. The time interval between placing the mouse in the cage and the time mouse starts eating the pellet or holds it with its two front paws is measured. The mice then are fed for 6 hours and starved for another 18 hours for testing in four consecutive days. On the first day of the buried-food-retrieval test, the *lynx2*^{-/-} animals performed similar to the WT animals, showing that they don't have any olfactory deficiencies (Figure 56). However, they performed differently when the test was repeated two days later in 3 consecutive days. The *lynx2*^{-/-} mice, found the food pellets which were buried in random places better than the WT mice on the first day of the 3 day series (Repeated Measures ANOVA, p-value<0.05), but didn't improve their finding abilities in the following trials, whereas the

WT mice performed better than before in consecutive days of trials (Figure 57) (Repeated measures ANOVA, p -value >0.05).

Anterior pretectal nucleus have been associated with pain [214]. Nicotinic receptors have also been shown to be important for nociception [156]. Since *lynx2* is very highly expressed in the anterior pretectal nucleus and modulates nicotinic receptors, we tested the *lynx2*^{-/-} mice on hot plate test. In this test, the animal is placed on a 55°C plate and its latency to jump or lick paws is measured. In hot-plate test, KO mice and WT mice had similar latencies responding to pain (Student's-T-test, p -value >0.05) (Figure 55).

As a result of our behavioral phenotyping analysis of the *lynx2*^{-/-} mice, I conclude that, like *lynx1*^{-/-} mice, *lynx2*^{-/-} mice performed different than the WT mice in audio-cued-associative learning task. Unlike *lynx1*^{-/-} mice, *lynx2*^{-/-} mice exhibit more anxiety behavior than WT mice in light-dark box test. *lynx2*^{-/-} mice also show increased anxiety in social interaction test but not in elevated-plus maze test. In motor coordination and learning tests, *lynx2*^{-/-} mice show superior motor coordination and learning than WT mice. However, the *lynx2*^{-/-} mice had less motor strength than the WT mice as assessed by the hanging-wire test. I couldn't detect any significant effect of *lynx2* on olfaction, contextual learning, pain perception, eye-blink and ear-twitch reflexes or basic motor tasks. The results of the behavioral analysis of *lynx2*^{-/-} mice are summarized in table 5.

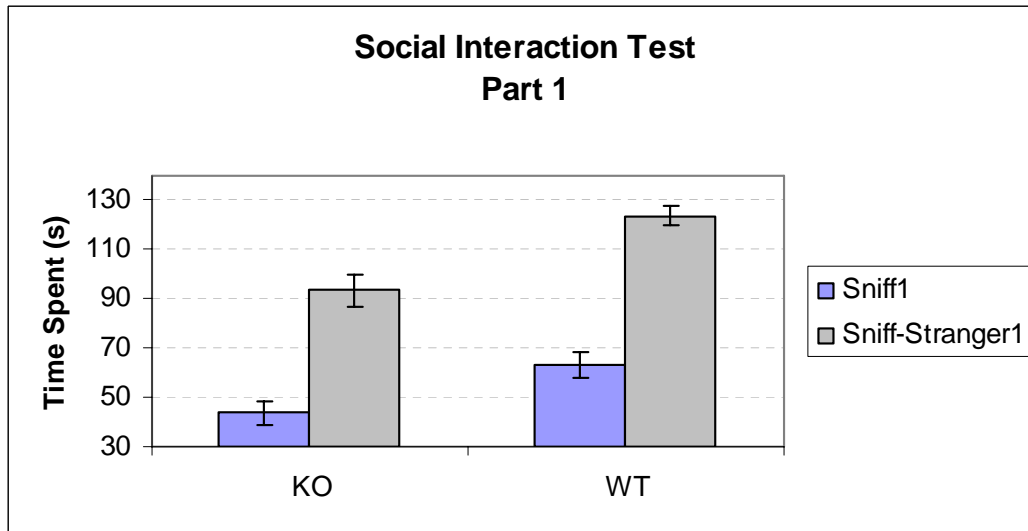


Figure 53: *lynx2^{-/-}* mice and wild type mice behave differently in Part 1 of Social Interaction Test. Among the various behaviors measured, the time spent with the novel mice for the *lynx2^{-/-}* and WT mice were significantly different from each other. *lynx2^{-/-}* mice spent less time interacting with the novel mouse than WT mice. They also spent less time in the compartment where there is a mouse than WT counterparts.

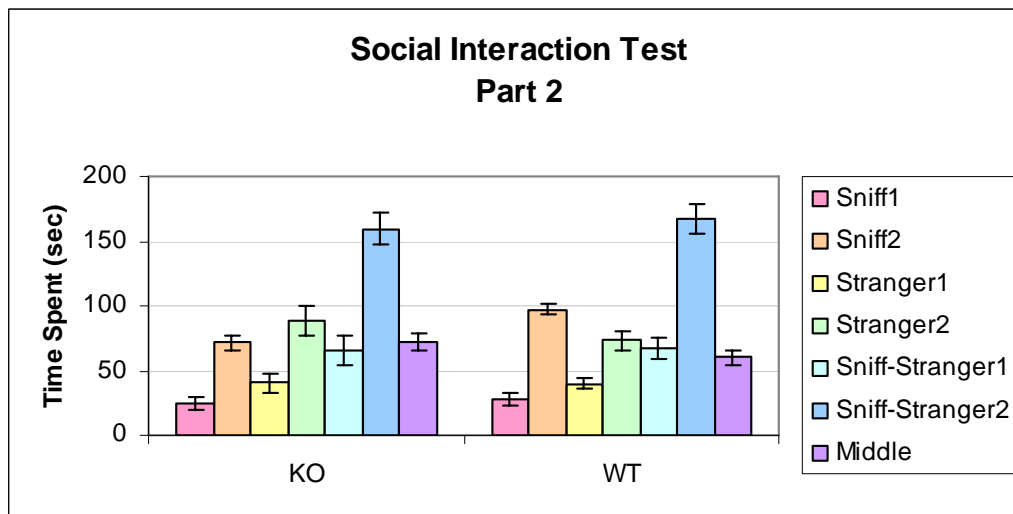


Figure 54: *lynx2^{-/-}* and WT mice behaved similarly in the Social Interaction test Part 2. In Part 2, a novel mouse was placed in the Empty cage, and the novel mouse from part 1, which is not novel to the test mouse anymore, was kept in its initial cage. WT mice and *lynx2^{-/-}* mice behaved similar in every measure that I have checked in this part of the test.

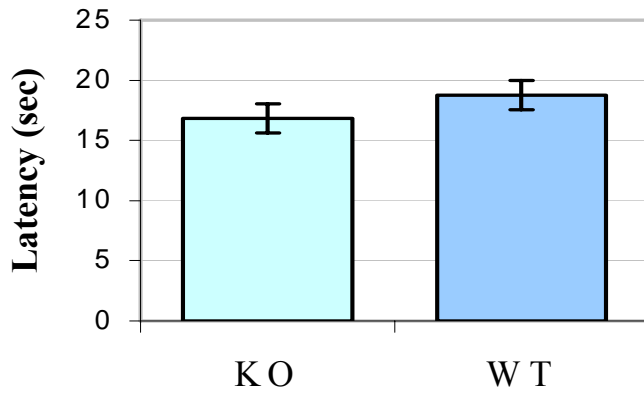


Figure 55: Hot Plate test. Antinociception properties of *lynx2^{-/-}* mice and wild type mice were compared by measuring their latencies to respond to heat in hot plate test. *lynx2^{-/-}* mice performed similar to wild type mice.

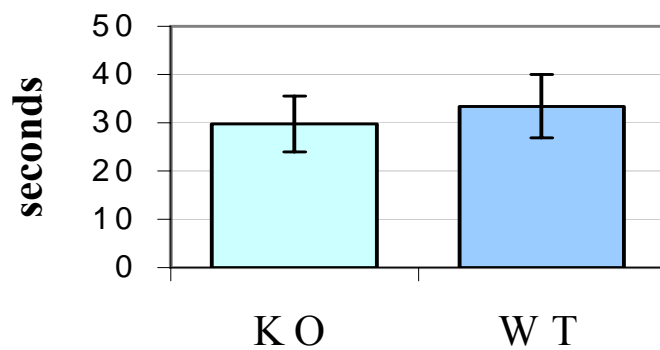


Figure 56: Finding Buried Food Test. The latencies of wild type and *lynx2^{-/-}* mice for finding buried food were measured. *lynx2^{-/-}* mice performed similar to wild type mice.

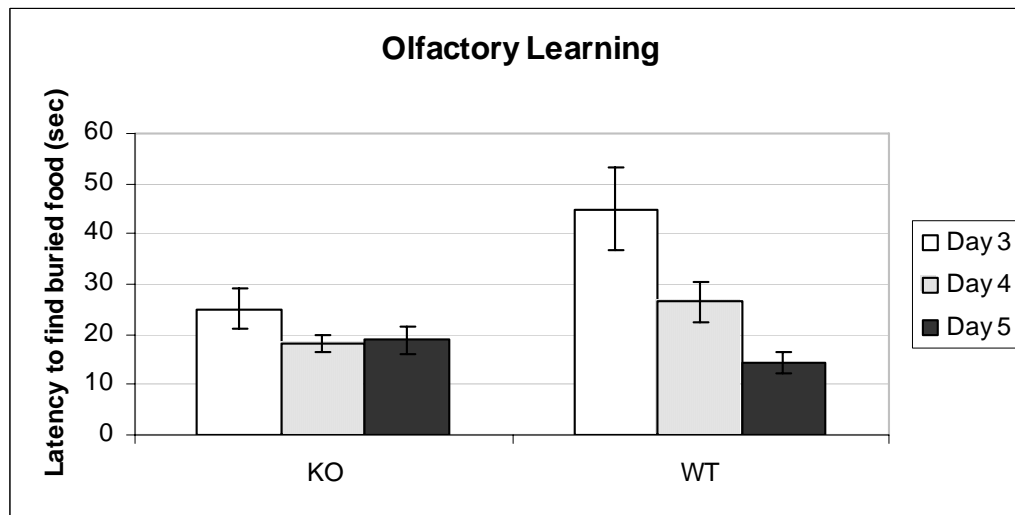


Figure 57: Olfactory learning tested with buried food finding test. One day after the first day of finding buried food pellet test, the same test was performed for 3 consecutive days. *lynx2^{-/-}* mice found the pellet faster than WT mice on first day of the consecutive days, but their performances

Table 5: Summary of behavioral phenotyping of *lynx2*^{-/-} mice. At least 10 age-matched male mice per genotype were used for each test. All our results are statistically significant.

| Behavior | Test | Are WT and <i>lynx2</i>^{-/-} different ? |
|--------------------------------------|--|---|
| Gross motor skills | Open-field exploration | No. Only difference is <i>lynx2</i> ^{-/-} jump more times than WT. |
| Basic reflexes | Eye-blink and ear-twitch | No. |
| Motor strength | Hanging wire (will repeat without a cut-off point) | Yes. <i>lynx2</i> ^{-/-} are weaker than WT. |
| Motor coordination | Rotarod- Day 1 | Yes. <i>lynx2</i> ^{-/-} are superior to WT. |
| Motor learning | Rotarod-4 Days | Yes. <i>lynx2</i> ^{-/-} learn better than WT. |
| Contextual-cued Associative learning | Fear conditioning-Part 1 | No. |
| Audio-cued Associative learning | Fear conditioning-Part 2 | Yes. <i>lynx2</i> ^{-/-} freeze more than WT. |
| Anxiety | Light-dark box | Yes. <i>lynx2</i> ^{-/-} more anxious than WT. |
| Anxiety | Social interaction | Yes. <i>lynx2</i> ^{-/-} more anxious than WT. |
| Anxiety | Elevated-plus maze | No. |
| Nociception | Hot-plate | No. |
| Olfaction | Finding buried food-Day1 | No. |

Lynx3

KO construct preparation

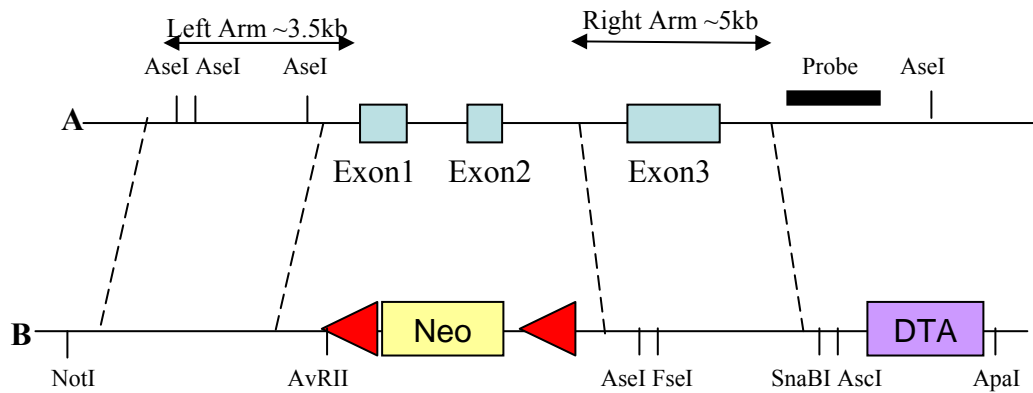
Lynx3 is expressed in a few neuronal and mostly epithelial tissues and its expression is distinct from that of *Lynx1* and *Lynx2*. *Lynx3* also binds to and modulates $\alpha4\beta2$ nicotinic receptors, but it does not bind to $\alpha7$ nicotinic receptors, which makes it a more specific nicotinic receptor modulator. Nicotinic receptors have been implicated in various important functions including cell-to-cell adhesion and signaling in epithelial tissue. In order to analyze the function of *lynx3* in vivo, I made a targeted-deletion for *Lynx3* gene. The KO construct has been prepared with C57Bl6 genomic DNA and it was electroporated to Bruce4 and C2J cells in Rockefeller University's Gene Targeting Facility (Figure 58).

Chimeras and Breeding

Electroporation of the KO construct to Bruce4 cells yielded 2 positive ES clones for homologous recombination. These clones were injected into FVB blastocysts and out of 3 injections, we had 5 female chimeras with 40%, 30%, 15%, 10% and 5% chimerism and 2 male chimeras with 20% and 10% and three males with 5% chimerism. None of these chimeras went germline.

Electroporation to C2J cells, which are derived from albino C57Bl6 mice, resulted in 3 ES cell colonies with homologous recombination. These colonies were injected into C57Bl6 blastocysts and out of 5 injections, we had two 100% male chimeras, one 90% male chimera, one 70% male chimera and ~10 more male chimeras with lower chimerism

rates. I had germline transmission in the first breeding from multiple chimeras, the heterozygote mice have been bred together to get homozygous mice. I have multiple male and female *lynx3*^{-/-} mice that are viable and will require further tests to assess any phenotypical abnormalities.



Neo cassette has *pgk* promoter and *LoxP* sites at both ends
 Linearization enzyme is *NotI*

Figure 58: *lynx3* KO construct. A. Scheme of genomic organization of *lynx3* coding exons. The probe for analyzing homologous recombination is shown as a black bar. The first and second coding exons, which encoded the translation-start and most of the ly6 domain were deleted by the null mutation. The homologous arms were 3.5kb and 5kb long and were sub-cloned from C57Bl6 genomic DNA containing clones. B. Scheme of the KO construct with a Neomycin cassette with *LoxP* sites, and DTA cassette outside the homology arms.

CHAPTER 5:

Lynx3 Modulates A Novel *Xenopus* Oocyte Channel

Summary

Lynx3 binds to and modulates nAChRs, and it has a specific expression pattern in epithelia and neurons. When lynx3 is overexpressed in *Xenopus* oocytes, the cells die in two days compared to fourteen days when other lynx proteins are expressed. Also, in voltage clamp recordings, we observed that lynx3 expressing oocytes have leak currents associated with opening of an endogenous oocyte channel, suggesting that the death is caused by continuous activation of an ion channel. We hypothesized that this channel might be conserved in mammals, and it might be regulated by lynx3. Next, we analyzed electrophysiological properties of the lynx3-affected *Xenopus* channel. We identified a novel *Xenopus* channel with unique pharmacological properties. We are now cloning this *Xenopus* channel and its mammalian homologue by using different methods.

Characterization of Lynx3 Affected Channel

When expressed in *Xenopus* oocytes, lynx3 elicits leak currents in oocytes and the oocytes die after two days of lynx3 expression. I overcame this problem by using less Lynx3 mRNA for injection for analyzing the effect of Lynx3 on $\alpha 4\beta 2$ nAChRs, however I thought that this was a curious event and might reveal another target channel for lynx3. The identity of this target channel would be very helpful in identifying another target channel in mammals; therefore, I continued analyzing. I speculated that Lynx3 was interacting with an oocyte channel causing it to stay open and thus the leak. In order to find out what type of a channel this was, I subjected the lynx3 expressing oocytes to different open channel blockers. One day after injecting the oocytes with 0.5ng lynx3

mRNA, we applied different channel blockers for 20 seconds and analyzed the differences in the current that is passed through the oocyte membrane.

To test for Na⁺ Permeability, NMG⁺ was replaced with Na⁺ in the Ringer solution. After oocytes were perfused with this solution for 20 secs, the currents elicited by channels effected by lynx3 were reduced due to lack of Na⁺, meaning that these channels pass through Na⁺ ions. This experiment was repeated with different lynx3 transcripts and multiple oocytes and the results are consistent (Figure 59).

Ba²⁺ is a blocker for K⁺ channels. When perfused with a Ringer solution that contained 4mM Ba²⁺ for 20 seconds, the channels that are activated by lynx3 are partially blocked by Ba²⁺. This experiment was also repeated with multiple oocytes (Figure 60).

Since lynx3 target channel passes through both K⁺ and Na⁺, I wanted to see if it was more permeable to K⁺ or Na⁺. To test this, we used a ringer solution in which Na⁺ ions were replaced by K⁺ ions. When lynx3 expressing oocytes were perfused with this solution, the leak current increased; this means that the channel that is causing this leak current has a preference for K⁺ ions over Na⁺ ions. This experiment was repeated with multiple oocytes with similar results (Figure 61).

In order to investigate whether lynx3 target channel was permeable to divalent cations, a ringer solution in which Ca²⁺ ions were replaced with Mg²⁺ ions was used to perfuse lynx3-expressing oocytes. During the 20 second perfusion, the leak current caused by lynx3 affected channels increased by 76%, whereas the current increased by only 44% in non-injected oocytes. This experiment was done on multiple lynx3 expressing oocytes and the results were consistent. To see if this result was due to

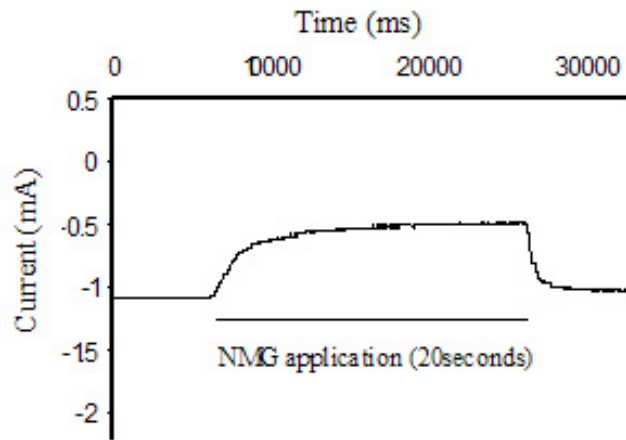


Figure 59: A representative recording demonstrating the effect of NMG containing Ringer solution exposure to the leak current in lynx3 in expressing oocytes.

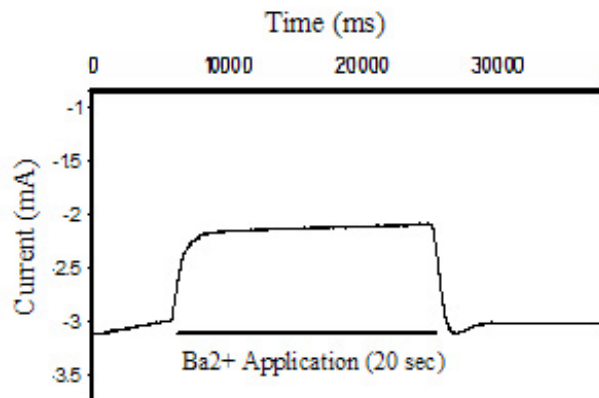


Figure 60: Ba^{2+} partially blocks lynx3-effected channel. A representative recording showing the effect of perfusing the lynx3 expressing oocyte with Ba^{2+} containing Ringer solution.

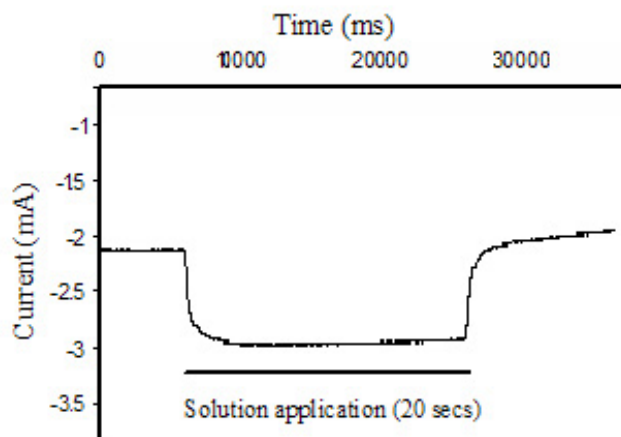


Figure 61: Na^+ vs K^+ . Replacing Na^+ ions with K^+ ions increase the current passed through the lynx3-effected channels.

removal of Ca^{2+} or addition of Mg^{2+} , I have prepared another Ca-free solution with EDTA and flufenamic acid (FFA) to block the hemi-gap channels [215] and perfused the lynx3-expressing oocytes for 20 seconds. I have observed a 10% increase in the leak current. I then used another solution where Ca^{2+} was replaced with Mg^{2+} and added flufenamic acid, and the leak current increased by 39%. This further supports that the channels affected by lynx3 pass through Mg^{2+} and are inhibited by Ca^{2+} (Figure 62) (Table 6).

Non-selective cation channels are blocked by La^{3+} ions, so I decided to check whether lynx3 target channel would also be blocked by La^{3+} . To test this, I added La^{3+} to the Ringer solution and perfused un-injected and lynx3-injected oocytes to this solution for 20 seconds. I observed that the channel was ~90% blocked (Figure 63).

These results demonstrate that the channels that are effected by lynx3 in oocytes and cause leak currents are non-selective cation channels that are blocked by the following ions: $\text{La}^{3+} \gg \text{Ba}^{2+} > \text{Ca}^{2+}$.

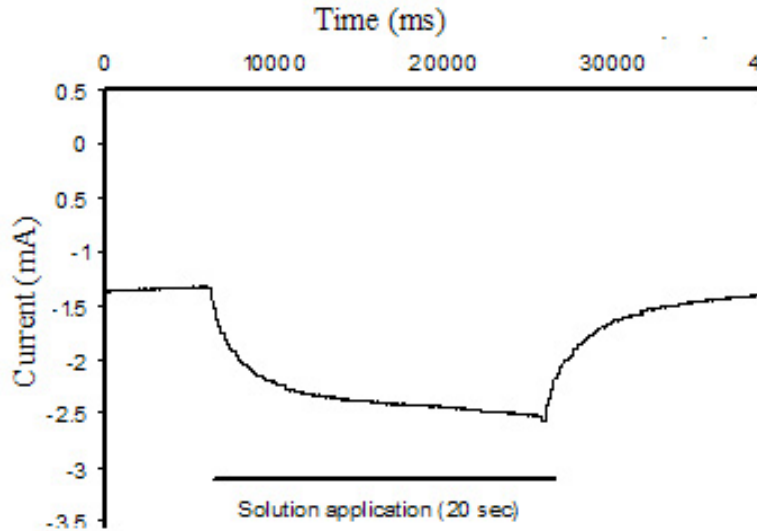


Figure 62: Replacing Ca^{2+} ions with Mg^{2+} ions increase the current passed through the lynx3-effected channels. There's no FFA to block Ca^{2+} inhibited hemi-gap channels in this solution.

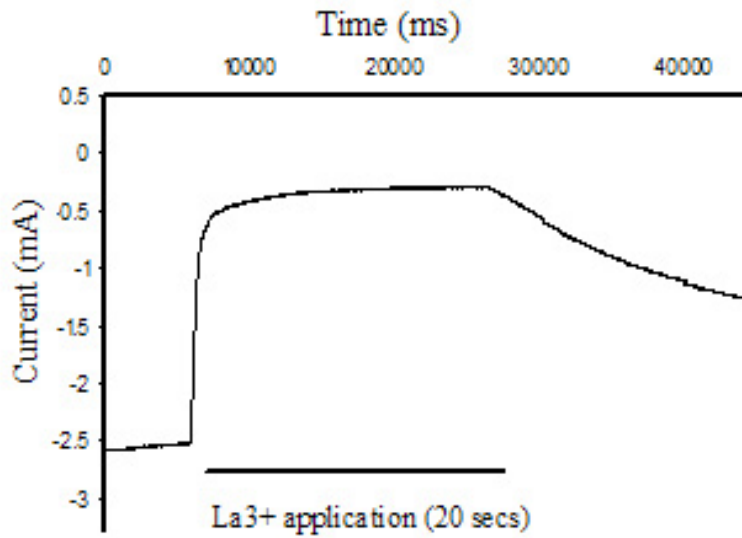


Figure 63: La^{3+} ions inhibit the currents elicited by lynx3 expression in *Xenopus* oocytes. Whole cell currents measured while perfusing the lynx3-expressing oocytes with Ringer solution containing 0.1 mM La^{3+} blocked most of the leak current.

Table 6: Currents elicited by lynx3 expression were further augmented by presence of Mg^{2+} and absence of Ca^{2+} . In the EDTA, which chelates Ca^{2+} ions, and when hemi-gap channels are blocked by FFA, the leak currents elicited by lynx3 expression increases 10%, and in the presence of high calcium the current is increased by 29%. When Ca^{2+} ions are replaced with Mg^{2+} ions, and hemi-gap-channels are blocked with FFA, the current increases by 39%.

| Solution (Ringer solution with) | Percentage of Augmentation in lynx3 expressing oocytes | Percentage of Augmentation in control oocytes |
|-------------------------------------|--|---|
| Mg^{2+} , no Ca^{2+} | 75% | 44% |
| Mg^{2+} , no Ca^{2+} , with FFA | 39% | 0% |
| high Ca^{2+} (40mM) with FFA | 29% | -39% |
| Ca-free with EDTA and FFA | 10% | 0% |

Table 7: Currents in lynx3 expressing oocytes were blocked by the chemicals below.

La³⁺ blocks leak currents by 83%, while benzamil blocks 59%, Ringer solution containing NMG instead of Na, blocks it by 53%, Ba²⁺ containing ringer blocks by 27%, 1mM amiloride blocks 22%, 2mM SITS blocks by 11%, SKF-963654 blocks by 9.7% and a low pH Ringer blocks by 21%.

| Solution (Ringer solution with) | Percentage of Current Reduction in lynx3 expressing oocytes | Percentage of Current Reduction in control oocytes |
|------------------------------------|---|--|
| 0.1mM La ³⁺ | 83% | 0% |
| 1mM benzamil | 59% | 5.5% |
| NMG | 53% | 0% |
| Ba ²⁺ | 27% | 0% |
| 1mM amiloride | 22% | 0% |
| low pH Ringer | 21% | 0% |
| 2mM SITS | 11% | 0% |
| 100mM SKF-963654mM | 9.7% | 0% |

Finding the reversal potential of the channel

I-V curves of the lynx3-injected oocytes were linear; therefore, lynx3-induced currents were mostly voltage independent. The reversal potential was ~15mV in average, which shows that this is a non-selective cation channel (Figure 64).

Pharmacological Characterization of Lynx3 Target Channel

I searched the literature to find if the channel that is modulated by lynx3 has been identified before. I made a list of the endogenous *Xenopus* channels that were studied, and compared the lynx3-effected channel to these channels to see if this is a novel channel, by utilizing various chemicals that were used in previous studies. The effects of 20-second perfusion of the oocytes with these chemicals are shown in table 7.

A similar non-selective cation current was published by Arellano et. al [216] in 1995, and this current was suggested to be due to hemi-gap channels by Ebihara later [217]. One type of channel that fits the above description is the hemi-gap channel. Connexin38, which is expressed in the *Xenopus* oocytes, is a candidate for those hemi-gap channels, so we decided to investigate this further. Hemi-gap channels are blocked by carbenoxolone and flufenamic acid. We perfused lynx3-injected oocytes with Ringer solution containing 100 μ M Carbenoxolone for 20 seconds and I didn't observe any significant blockage. When I perfused the lynx3-injected oocytes with Ringer solution that contains 50 μ M flufenamic acid (FFA), there was no significant difference in the lynx3-induced current. So I concluded that the lynx3 target channels are not hemi-gap channels [218].

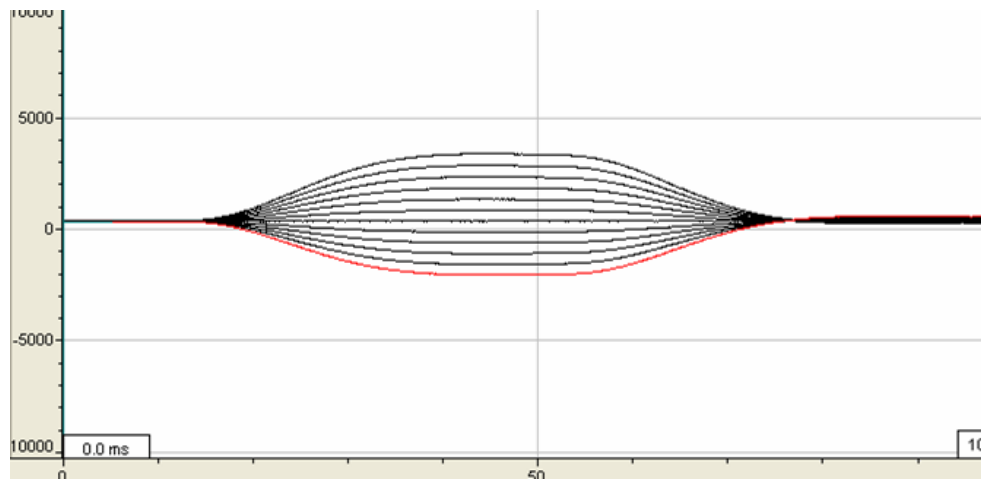
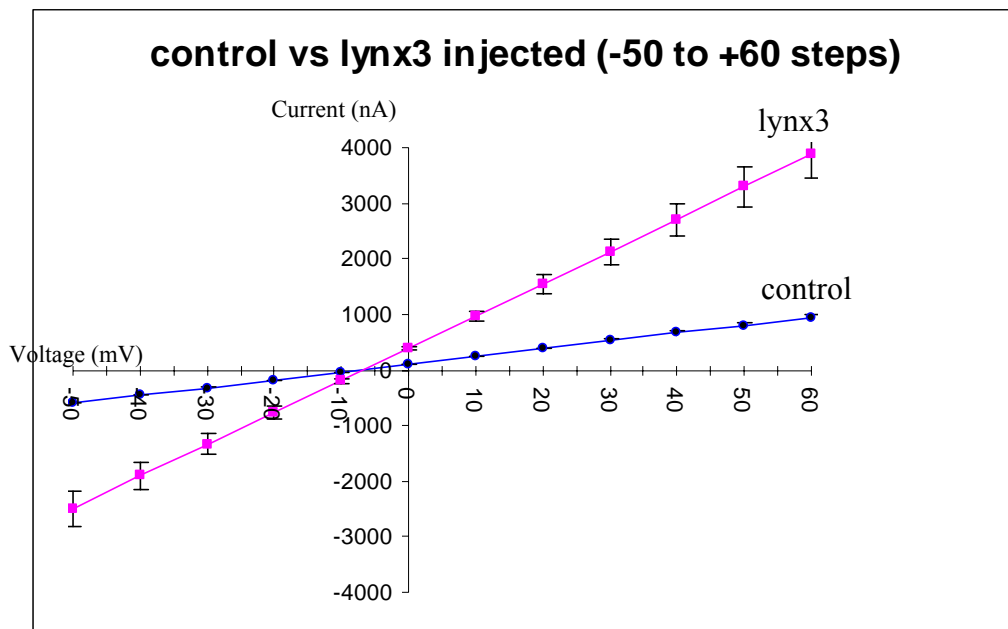


Figure 64: Current-Voltage Relationships (I-V curves) of control oocytes and lynx3 mRNA injected oocytes and a representative recording of lynx3 injected oocytes for evaluating the I-V curves. Oocytes were bathed in Ringer solution and whole cell currents were measured from a holding potential of 0 mV by sequentially stepping from -50 mV to +60 mV in 10 mV increments. Reversal potentials of both control oocytes and lynx3-injected oocytes were similar.

SITS (4-acetamido-4-isothiocyanatostilbene-2, 2-disulfonic acid), niflumic acid and bumetanide, which are potent blockers of chloride channels and also block some non-selective cation channels, do not block the lynx3-affected channel significantly. The highest blockage due to these three chemicals was caused by SITS perfusion, which was only 11%.

Another non-selective cation channel that was published was activated by bisphosphonates (BP), which are drugs commonly used to treat osteoporosis. While looking for the effect of BP to epithelial sodium channel (ENaC) in *Xenopus* oocytes, Shao et. al. identified another nonselective cation current that was induced by BP. Although this current is similar to the current elicited by lynx3, in terms of the ions passed, currents elicited by BP are completely blocked by lower pH (6.4), but lynx3 elicited current is only blocked 21% by ringer solution with a pH of 6.4. In addition, BP activated current is also blocked by 20 μ M amiloride; however, lynx3 activated current is not effected by 20 μ M amiloride, and gets blocked by 1mM amiloride by only 22%.

High levels of expression of heterologous membrane proteins have been shown to induce a hyperpolarization activated cation current in *Xenopus* oocytes previously, so I wanted to check if lynx3 elicited currents were also due to the same channels [219]. This hyperpolarization-activated cation current is blocked by DIDS (4,4'-diisothiocyanatostilbene-2, 2'-disulphonic acid) and TEA (tetraethylammonium). When lynx3-injected oocytes were perfused with ringer solution with 1mM DIDS or 100mM TEA for 20 seconds, I didn't detect any significant changes in the current, which suggests that lynx3 elicited current is different from the non-selective cation current caused by overexpression of heterologous proteins.

The last non-selective cation channel described in *Xenopus* oocytes is a current elicited by maitotoxin (MTX) [215, 220]. This current is blocked by 1mM benzamil, 1mM amiloride and 100 μ M 1-(β -(3-(4-Methoxyphenyl)-propoxy)-4-methoxyphenethyl)-1H-imidazole hydrochloride (SK&F 96365) by 81%, 62% and 65% respectively. When lynx3-injected oocytes were perfused with these solutions, lynx3-elicited current was blocked by 59% and 22.5% by benzamil and amiloride respectively, but was not affected by SK&F 96365 significantly. MTX-induced currents are also blocked by high extracellular Ca²⁺ (40mM); however, lynx3-elicited currents are not blocked by high Ca²⁺, instead they are augmented by it by 29%. These results suggest that MTX-induced currents and lynx3-induced currents are distinct.

These results show that lynx3 expression in *Xenopus* oocytes activate a novel non-selective cation current that can be blocked by 0.1mM La³⁺ by 83% and partially blocked by 4mM Ba²⁺, 1mM benzamil, 115mM NMG⁺, 1mM amiloride and ringer solution with lower pH. Since both low extracellular Ca²⁺ and high extracellular Ca²⁺ block these channels, I conclude that Ca²⁺ levels modulate these channels.

CHAPTER 6:

Discussion

Summary

The first Ly6 genes were first identified in lymphocytes [1], however, the extent of this gene family and its functions have remained largely unknown. I have analyzed 85 members of Ly6SF through phylogenetic inference and have identified new sequence similarities. I have analyzed expression patterns of four mammalian Ly6SF members, lynx2, lynx3, lynx4 and Ly6H in CNS with a particular attention to lynx2 and lynx3. I have also examined expression patterns of lynx3 outside CNS. Interactions between nAChRs and lynx1, lynx2, lynx3 and Ly6H have also been analyzed and their effects on nicotinic receptors were observed through voltage clamp recordings on oocytes. Lynx2 and lynx3 null mutant mice were made and *lynx2*^{-/-} mice have been thoroughly analyzed through behavioral phenotyping. Lynx3 was found to effect a novel non-selective cation channel in *Xenopus* oocytes and pharmacological properties of this channel has been studied.

We can draw four main conclusions from this study. First, the Ly6SF of genes is very extensive, including many members in both vertebrates and invertebrates. Although highly divergent, phylogenetic inference indicates that the Ly6SF evolved from a common ancestral gene, with recent evolutionary events that have expanded subfamilies of the Ly6SF. Second, properties of lynx1, including the ability to bind to and modulate nAChRs, are shared by other GPI-anchored Ly6SF genes expressed in neurons, allowing us to define a lynx subfamily of functional homologues within the Ly6SF. Third, despite their common functional properties *in vitro*, we can conclude the lynx family of proteins has non-redundant functions *in vivo* since the *lynx1*^{-/-} and *lynx2*^{-/-} mice exhibit different

behaviors in anxiety, motor coordination and motor learning. Fourth, Ly6H is a CNS expressed Ly6SF gene that is functionally distinct from the lynx family of nAChR modulatory proteins. Although there is not yet sufficient biochemical and genetic data to prove a general role for Ly6SF proteins as modulators of signal transduction through interactions with specific classes of cell surface proteins, the receptor modulatory activities of the lynx proteins [67, 203], the snake venom α -neurotoxins [17], the SLURP proteins [64], and the recent data on the effect of Ly6 molecules on signaling in lymphocytes [51, 221] and non-lymphoid cells [30, 222] provide strong support for this idea.

Identification and Phylogenetic Inference of Ly6 Gene

The divergence of the sequences of Ly6SF proteins suggests that they evolved from a single gene through gene duplication very early in the evolutionary process. The numbers of cysteines and the spacings between them were considered to be the only conserved traits among the superfamily. In my studies, I have not only confirmed these earlier findings in a large number of proteins, but I also have showed that some other residues are also conserved in most of the Ly6SF members. These amino acids are more likely to be involved in structural properties of the Ly6 domain since Ly6SF proteins perform a diverse array of functions.

Some sequence structures are more conserved among the lynx subfamily than they are in the rest of the Ly6 genes. The serine residues on the second and third loop of Ly6 domains, are very conserved in mouse and human lynx1, lynx2 and lynx3, however neither mouse nor human Ly6H does not have them. Sequence structures that are conserved in lynxs but not in Ly6H are especially important since Ly6H does not bind to or modulate nicotinic receptors but lynxs do. Conserved amino acids such as these serines should be investigated through targeted mutation analysis to help us learn more about the physical interaction between the nicotinic receptors and lynxs.

lynx1 and lynx2 bind to all four nAChRs that I have investigated; however, lynx3 only binds to $\alpha 4\beta 2$ and $\alpha 4\beta 4$ receptors. This is an important finding which might help us understand more about receptor binding specificity. Targeted mutations, through which different loops in the Ly6 domains of lynxs are exchanged, can be helpful to us in order to identify if any specific loop is important for target specificity. Smaller mutations inside

the loops will also be helpful to determine which amino acids are crucial for receptor modulatory function of lynxs. nAChRs are implicated in the pathobiology of many diseases, and have been drug targets [223, 224]. Specificity among different nicotinic receptors has been a significant problem for drug development and the specificity among lynxs might be important for solving this problem.

The Ly6 proteins that are expressed in lymphocytes are more closely related and they make up a single branch in the tree suggesting that they were formed by gene duplication from a single gene later in the evolutionary process. These hematopoietic cell expressed Ly6 genes are located on Ly6 locus on murine chromosome 15 and human chromosome 8, which further supports this idea.

The results presented here characterize the Ly6SF of genes from several species, and identify a large number of novel family members in both vertebrates and invertebrates. Although the 85 genes we present here encode very divergent proteins, all share the same basic genomic structure and the core cysteine residues characteristic of Ly6 domain. These properties suggest that the Ly6SF evolved from a single ancestral gene early in evolution, although more recent evolutionary events are revealed by phylogenetic inference. For example, the single branch formed by mouse and human Ly6 genes in the phylogenetic tree, and their clustering within 600CM region on murine chromosome 15 and its syntenic region on human chromosome 8, suggest that this subfamily of Ly6 genes arose recently in the mammalian lineage. Similar events may explain the phylogenetic clustering of some of the *D. melanogaster* Ly6SF genes.

Expressional and Functional Characterization of Lynx1

Homologues

Given our previous studies identifying lynx1 as a novel nAChR modulatory protein expressed in the CNS [67, 203], and recent data demonstrating that the secreted Ly6SF member SLURP1 can modulate $\alpha 7$ nAChR activity [15, 64], I sought to identify other Ly6SF members that might play a role in receptor modulation in the central or peripheral nervous systems. Here I identify lynx2 and lynx3 as functional homologues of lynx1 that are expressed in distinct populations of CNS or peripheral nervous system (PNS) neurons. Both of these molecules are GPI-anchored, bind to nAChRs and modulate their desensitization kinetics. Based on their common structure, their expression in neurons, and the abilities of lynx1, lynx2, and lynx3 to functionally modulate nAChRs, I define these genes as the lynx subfamily of receptor modulatory proteins. Although the Ly6H gene is expressed broadly and at high levels in the CNS, our assays thus far have not demonstrated functional homology with lynx family of proteins. It remains possible that further studies of Ly6H or other Ly6SF members will reveal common functional properties with lynx1, lynx2 and lynx3, and justify their inclusion into the lynx family of nAChR modulatory proteins.

While lynx1 and lynx2 are both expressed in neurons, and are able to modulate nAChR desensitization kinetics, their expression patterns and functional properties suggest non-redundant functions. Although the functional properties of lynx1 and lynx2 are quite similar based upon the co-immunoprecipitation and oocyte electrophysiology experiments, their expression in cell populations in the hippocampus and cerebral cortex differ. $\alpha 4\beta 2$, $\alpha 3\beta 4$ and $\alpha 7$ nAChRs have been reported to be expressed in hippocampus

and cortex and many neurons are affected by the actions of all three of these receptors [95, 98, 100, 105, 225, 226]. In contrast to lynx1 and lynx2, lynx3 is expressed predominantly in the periphery, including in olfactory sensory neurons, bronchial epithelial cells and in the trachea. $\alpha 4\beta 2$, $\alpha 3\beta 4$ and $\alpha 7$ nAChRs are also expressed in the bronchial epithelial cells. However, the expression of nAChRs have not been well studied in the other peripheral tissues where lynx3 is also expressed [204]. Furthermore, although lynx3 shares the ability to bind to and modulate $\alpha 4\beta 2$ and $\alpha 4\beta 4$ nAChRs with lynx1 and lynx2, it does not bind to $\alpha 7$ nAChRs. Taken together, these data demonstrate that lynx1, lynx2 and lynx3 must play distinct roles in vivo.

The expression pattern and the functional properties of Ly6H suggest that its functions in the CNS must be distinct from the lynx subfamily of proteins. I have demonstrated that it neither binds to nor modulates the activities of the major CNS expressed nAChR subtypes and the muscle nAChR. It is possible that Ly6H could modulate other nAChR subtypes not assayed in this study, however, I regard this as unlikely because none of the remaining nAChR subtypes are co-expressed in the CNS with Ly6H [100, 105, 111, 112, 227]. Ly6H expression is widespread within the CNS, but it is noticeably absent from several CNS structures, including several brainstem nuclei and the cerebellum (our unpublished data, <http://www.ncbi.nlm.nih.gov/projects/gensat/>). Given the shared structural properties of Ly6SF proteins, and common evolutionary origins of nACh, GABA, Glycine, 5-HT₃ and some glutamate receptors [69], it seems likely that Ly6H could modulate a distinct neurotransmitter receptor class.

Despite the fact that Ly6H is closely related to lynx1 subfamily members, its functional difference suggests Ly6H might be a paralog that has formed through gene duplication with loss of original function. Since lynx1, lynx2 and lynx3 all modulate nAChRs, this might be the primitive function of this subfamily of proteins, from which Ly6H diverged. This model shows how nervous system evolves new functions through gene duplication.

Lynx1 has been shown to increase agonist sensitivity for nAChRs [67]. It would be interesting to check whether lynx2 and lynx3 has a similar effect on nicotinic receptors. For this purpose, dose response curves of nicotinic receptor and lynx2/3 expressing oocytes to various concentrations of ACh could be compared with dose response curves of oocytes expressing only nicotinic receptors. Lynx1 also delays recovery of nAChRs after receptor activation [67]. In order to assess whether lynx2 and lynx3 function through the same mechanism to modulate nicotinic receptors, the abilities of lynx2 and lynx3 to delay receptor recovery can be analyzed through voltage clamp recordings in *Xenopus* oocytes.

Effects of lynx2 and lynx3 on nAChRs in mammalian cells have not been investigated. lynx1 increases the large conductance currents of nicotinic receptors in mammalian cells [67]. Analyzing modulation mechanisms of lynx2 and lynx3 in mammalian cells would help us understand the relationship between nAChRs and lynx subfamily of proteins.

Although I have established that lynx1, lynx2 and lynx3 form stable complexes with nicotinic receptors in mammalian HEK cells, I have not shown that lynx subfamily members interact with nAChRs in brain. I have unsuccessfully tried immunoprecipitating

nicotinic receptors from brain multiple times. Also, I wasn't successful in co-immunoprecipitation experiments with $\alpha 3$, $\alpha 2$, $\alpha 6$ and $\alpha 9$ subunit containing nicotinic receptors, because the available antibodies are not suitable for immunoprecipitation. Most nicotinic receptor antibodies that are commercially available have poor affinities to native receptors, which also causes problems in the immunohistochemistry studies. In order to better analyze nicotinic receptor function and effects of lynxs on them, I would need to make antibodies with higher affinities.

Gene-targeted Deletion Analysis of lynx2 and lynx3

Tobacco smoking is the leading cause of preventable death in United States and the main target of nicotine in the brain is the nAChRs. Nicotinic receptors are also involved in the pathophysiology of various neuronal and non-neuronal diseases including Alzheimer's disease, Parkinson's disease, anxiety disorders, autism and skin disorders like autoimmune pemphigus, epidermolysis bullosa as well as gastric cancer, and pancreas cancer [198, 228]. Nicotinic receptors are allosteric receptors, which go through mainly four states upon their activation: resting position, open channel, desensitized channel and closed channel. Desensitization of nicotinic receptors is an important means of modulation of their activity and lynx1 is one of the first endogenous proteins that modulates desensitization patterns of nAChRs. In my studies, I have shown that lynx2 and lynx3 can also bind to and increase desensitization speed of nAChRs. In order to analyze the *in vivo* effects of lynx2 and lynx3, I have made null mutant mice for lynx2 and lynx3. The *lynx2*^{-/-} mice show various behavioral phenotypes that were previously shown to be regulated by nicotine. These phenotypes will be described below. I am in the process of analyzing the lynx3 null mutant mice.

Effects of lynx2 null mutation on fear and anxiety

Fear and anxiety are related, but different, psychological terms. They are both arised in situations where our senses impels our brain to act, but it cannot. Fear is an intense emotion that is produced against an immediate threat. Fear produces defensive behaviors and helps survival mechanisms. Anxiety, on the other hand, is a vague discomfort reflecting distress and diffuse fears without any particular threat. In humans, anxiety can be felt in various situations including crowded places, feeling helpless due to inability to react, experiencing unpredictable events in your life, or not being able to accept certain events like losing your job or a loved one.

Nicotine alters anxiety related behaviors through its effect on nicotinic receptors. Nicotine has also been associated with panic attacks and depression. In rodents, nicotine can be anxiolytic or anxiogenic depending on the method of administration, the duration after administration and the dose of nicotine. When activation of nicotinic receptors affects serotonergic pathways, it is anxiogenic. On the other hand, anxiolytic effects of nAChRs might be due to their effects on GABAergic pathways and stress hormone levels. Anxiety related behaviors have been associated with multiple areas of the brain including amygdala, hippocampus, stria terminalis, periaqueductal gray and cortex; and nAChRs are expressed in all of these regions.

Since nicotine can stimulate release of a variety of neurotransmitters, including GABA, serotonin and dopamine in various brain areas and the desensitization kinetics of nicotinic receptors vary depending on the subunit composition, understanding specificity of the nicotinic receptor activation becomes an important issue in apprehending the relationship between nicotine and anxiety. Lynx2 is expressed in specific cell populations

in the areas associated with anxiety and it modulates nicotinic receptor desensitization, therefore, analyzing mechanisms and identifying receptor subtypes underlying the effect of *lynx2* on anxiety will be very useful for understanding the effects of nicotine on anxiety.

Among the anxiety related tests we have performed, light-dark box and social interaction tests are the potential models for generalized anxiety disorder, and elevated-plus maze is a potential model for panic disorder and generalized anxiety disorder. The *lynx2*^{-/-} mice have shown elevated anxiety related behavior in the social interaction test and light-dark box test compared to WT mice. Although acute injection of nicotine increases anxiety levels in the WT mice in light-dark box test, it had no effect on the *lynx2*^{-/-} mice. This suggests that the anxiolytic effect of nicotine might be considerably less apparent in the *lynx2*^{-/-} mice since nicotinic receptors that are normally modulated by *lynx2* are desensitizing more slowly. Also similar to *lynx1*, *lynx2* might be affecting the sensitivity of the nAChRs to nicotine, which might reduce the effect of nicotine on anxiety. Although, the *lynx2*^{-/-} mice performed comparable to the WT mice on elevated-plus maze test, this doesn't contradict with our results from the other anxiety tests since these tests measure different aspects of anxiety, and *lynx2* might be effecting one aspect while not effecting the other.

Another significant finding about anxiety in our tests was the jumping phenotype during open-field exploration test. This might indicate that the *lynx2*^{-/-} mice are more excitable than the WT mice in novel environments, however, I have not found any literature on jumping phenotype during open field exploration and I will need to perform further analysis to test the excitability phenotype.

On fear conditioning test, the *lynx2^{-/-}* mice exhibited normal contextual-associative learning behavior, however, better audio-cued-associative learning than the WT mice. Although the *lynx2^{-/-}* mice show more anxiety related behavior than the WT mice, I don't think that the audio-cued-associative learning phenotype is due to increased anxiety since the number of freezes in the 3-minute period in the novel environment, during which no tone was presented, were similar between both the *lynx2^{-/-}* and WT mice. Nicotine alters learning and memory in mice and humans, thus the increased audio-cue-associated learning in the *lynx2^{-/-}* mice might also be through disturbances in the nicotinic receptor modulation in the *lynx2^{-/-}* mice. This hypothesis can be further tested with more fear conditioning tests on nicotine or nAChR antagonist injected mice, or with patch clamp recordings on cells in basolateral amygdala, which is considered one of the primary sites associated with fear conditioning test [210]. Although both contextual associative learning and audio-cued associative learning in fear conditioning test are measures of associative learning, they are not controlled by the same brain regions. Contextual-associative learning has been shown to be controlled at least partially by hippocampus and audio-cued associative learning has been shown to be controlled mainly by basolateral amygdala. So the fact that *lynx2^{-/-}* mice have a phenotype in one of these tests but not the other doesn't contradict with each other.

However, increased learning of *lynx2^{-/-}* mice than WT animals also doesn't necessarily mean that they are smarter than WT animals, since this increased learning can be due to increased fear in these mice. Since we have already observed an increased anxiety phenotype, this hypothesis becomes stronger. In order to check whether the result

that I have gotten from the audio-cued conditioning is due to better learning capability in general, I'll have to perform more learning tests.

Cerebellum has also been shown to be involved in several anxiety related behaviors. Mice that are deficient in motor capabilities, like Lurcher mice, have shown different anxiety related behaviors; in addition, anxiolytic drugs that are widely used result in motor coordination problems and increased locomotion. Since *lynx2*^{-/-} mice have also shown motor coordination and learning abnormalities and *lynx2* is expressed in interneurons in cerebellum and very heavily expressed in inferior olive which sends cerebellum major excitatory input through climbing fibers, the motor coordination phenotype and anxiety phenotype might be interrelated and may be controlled by not only amygdala and related structures but also cerebellum. However, this hypothesis should further be tested with experiments that will be described in "Future Directions".

Effects of lynx2 null mutation on motor coordination and learning

Nicotine also effects motor coordination and motor learning. Although the *lynx2*^{-/-} mice exhibited less motor strength than the WT mice in the hanging wire test (This experiment will be repeated without a cut-off point to be analyzed with Student's-T-test), they performed significantly better than the WT mice on rotarod test which measures motor coordination. This might suggest that when desensitization of nAChRs is slower due to lack of lynx2, motor coordination improves. To test this hypothesis I analyzed the effect of nicotine and nAChR antagonist, mecamylamine on motor coordination of the *lynx2*^{-/-} mice.

When injected with nicotine, rotarod performance of the WT mice were effected, however, the *lynx2*^{-/-} mice were not effected, suggesting that the mechanism through which lynx2 effects motor coordination might be through nicotinic receptors. Intraperitoneal injections of nicotine and mecamylamine were shown to impair motor coordination in the WT mice, thus, activation and blocking of all nicotinic receptors worsens motor performance, probably due to release of various neurotransmitters from both excitatory and inhibitory synapses. Lynx2 is expressed in specific regions of the brain and the spinal cord. Since lynx2 slows desensitization, I'm hypothesizing that the cells where nicotinic receptors are affected by lynx2 modulation, are involved in one type of neurotransmitter release. So when the mice were injected with nicotine, nicotine does not affect motor performance of the *lynx2*^{-/-} mice because the normally-lynx2-expressing-cells either already have open channels, or when they are activated with nicotine, they are kept open longer. However, when nAChRs are blocked with mecamylamine, since the slowly desensitizing nicotinic receptors are also blocked, mecamylamine exerts the same

effect it does in the WT mice. Hexamethonium, which is a blocker of nicotinic receptors outside CNS, has little effect on the motor performance or learning of either the WT or the *lynx2*^{-/-} mice, which suggests that the receptors involved in rotarod performance and learning are inside the CNS.

When the mice were injected with mecamylamine, and with nicotine 10 minutes later, they acted similar to nicotine-injected mice. The reason for this might be the mechanism of action of mecamylamine. Mecamylamine has been shown to act both as a competitive antagonist and a non-competitive antagonist depending on the type of the nicotinic receptor that it blocks [130]. Therefore, the reason between the mecamylamine-nicotine injections and mecamylamine injections might be due to the type of receptors that *lynx2* is normally modulating.

Since primarily deep nuclei and cerebellum are responsible for motor coordination and learning, and *lynx2* is expressed in interneurons in cerebellum, inferior olive and scattered cells in cerebellar nuclei, I propose that the lack of modulation of nicotinic receptors by *lynx2* in these cells might be causing increased motor learning in the *lynx2*^{-/-} mice. It also might be caused by enhanced motor performance due to increased fear in *lynx2*^{-/-} mice. To test my hypothesis and to learn more about the mechanism of *lynx2* effect on motor learning and coordination, conditional *lynx2*^{-/-} mice, where only the inferior olive or interneurons in cerebellum are affected by the *lynx2*^{-/-} allele, might be generated and tested on accelerated rotarod. Double labeling with *lynx2* and different nicotinic receptor subtypes as well as patch clamp electrophysiology with different channel blockers will also improve our knowledge of which nicotinic receptor *lynx2* normally modulates in these cells. Injection of mice with nicotinic receptor subtype

specific antagonists like $\alpha 7$ receptor blocker MLA or $\alpha 4\beta 2$ receptor blocker DH β , and then testing them on rotarod also might help us understand which receptor subtype lynx2 is modulating for motor performance. In order to test whether the reason for increased motor performance of *lynx2*^{-/-} mice is due to increased fear, I can inject mice with anxiolytic drugs and test them on rotarod apparatus.

The *lynx2*^{-/-} mice have not shown any significant difference in the olfaction and pain perception tests when compared with the WT mice. However, I have not tested the effects of nicotine on the WT and *lynx2*^{-/-} mice during these tests. Since nicotine has been shown to effect both nociception and olfaction [130, 229-232], further tests, including more detailed olfaction tests and hot plate test with nicotine and mecamylamine injections are necessary to figure out if lynx2 is effecting these two pathways.

Review of Behavioral Phenotype of Lynx2 KO mice

Lynx2 KO mice have increased fear and anxiety in various tests including light-dark box, social interaction test and audio-cued fear-conditioning test. They also jump more in a novel environment, in open-field locomotion test, which might reflect increased escape tendency due to increased fear and anxiety. In rotarod test, lynx2 KO mice exhibit increased motor coordination which might reflect the effect of increased fear and anxiety on motor performance.

However, the effect of lynx2 on motor coordination and audio-cued associative learning may also be independent of its effect on anxiety and fear. lynx2 is expressed in various regions in brain and nicotinic receptors are involved in various mechanisms controlling learning and motor coordination; therefore, further tests should be performed to analyze whether the effect of lynx2 null mutation on motor coordination and fear conditioning is due to its effect on fear and anxiety.

Lynx3 is Modulating A Novel Xenopus Oocyte Channel

Although I have shown that lynx3 binds to and modulates nAChRs *in vitro*, I cannot conclude that nAChRs are the only channels affected by lynx3 in mammals. When I observed the leak currents during voltage clamp recordings in oocytes that were caused by lynx3 expression, I decided that the identity of the endogenous *Xenopus* channels opened by lynx3 will be beneficial in identifying any potential mammalian orthologs of that channel that might be modulated by lynx3. Through pharmacological analysis, I have concluded that the channel affected by lynx3 is a non-selective cation channel. In 1995, Arellano et al. [216] have identified properties of a non-selective cation current in *Xenopus* oocytes and this current was suggested to be due to hemi-gap channels by Ebihara et. al. [217]. The channel properties that were described by Arellano et. al. also match the properties of the channel that is effected by lynx3, however, lynx3 effected channel is not a hemi-gap channel since it doesn't get blocked by neither carbenoxolone nor flufenamic acid, both of which are potent blockers of hemi-gap channels.

After database searches, I have found 3 other non-selective cation channel types, however, neither one of them has a similar pharmacology to lynx3 affected channels. When I matured the lynx3 expressing oocytes with progesterone treatment, lynx3 continued to cause leak currents, suggesting that the lynx3-affected-channel continues to be expressed in mature oocytes. Thus, I conclude that lynx3 is modulating a novel non-selective cation channel in *Xenopus* oocytes.

I was not able to clone this channel yet. I am currently trying other methods, one for identifying the *Xenopus* channel, the other for finding a possible target channel in

mammals. For oocyte channel, I have collaborated with a lab in Argentina to express lynx3 in *Bufo arenarum* oocytes, and we observed that at low doses of expression lynx3 is not showing toxicity in these oocytes. We will try stronger expression of lynx3, and if that is not toxic, I will prepare mRNA from a *Xenopus* oocyte library, and screen the library for toxic effects of lynx3 and clone the channel. In order to find the mammalian channel that lynx3 might effect, I have done literature searches and have not found a channel that shares a similar pharmacology to the oocyte channel and that is expressed in lynx3 expressing tissues.

Future Directions

Mechanisms and pathways of anxiety have been studied mostly through imaging studies in humans and lesion studies in rodents. However, the lesion studies were only helpful in analyzing the effects of lesions in certain regions of the brain on various anxiety tests like light-dark box test, social interaction test and elevated-plus maze test. The lesion studies have shown that the pathways that control these tests are scattered throughout the brain and they are not controlled by the same brain regions. Therefore, more extensive imaging studies and more detailed behavior tests are required to analyze anxiety mechanisms in rodents. Anxiety trait can be influenced by strain differences, age and even the number and type of tests done on mice prior to the anxiety tests, which makes studying anxiety pathways more difficult.

Mechanisms of fear have been more extensively studied in rodents. Fear conditioning test has been used to analyze the anatomical regions, the controlling neurons and their signals for analyzing the fear pathways. These works have formed foundations of the neurobiological studies of emotion in mammals. Imaging studies in healthy human subjects and patients who suffer from psychological diseases have also helped these analysis. However, there is still much to be done to analyze neurobiology of emotions in both rodents and humans. I believe that mouse models which show an abnormality in emotional behaviors, like *lynx2*^{-/-} mice, are essential for studying these mechanisms further.

In order to analyze the function of *lynx2* in maintaining a normal level of anxiety and fear, I would like to increase the number of animals that were used in anxiety tests,

which will also make the results of the tests more statistically significant. I also would like to inject mice with different drugs including mecamylamine, to see the effect of nicotinic receptor function on the lynx2-controlled anxiety, and different anxiolytic drugs including benzodiazepines, to see whether the effect of lynx2 is through GABAergic signaling, and selective serotonin re-uptake inhibitor, SSRI, drugs, to observe whether lynx2 is working through serotonergic pathways.

More detailed anatomical analysis of the expression pattern of lynx2 will also be helpful in analyzing the pathways in which lynx2 is involved. Double labeled *in situ* hybridizations with lynx2 and markers for GABAergic neurons, and serotonergic neurons might tell us which neurons lynx2 is directly effecting. Also patch-clamp electrophysiology on the lynx2 expressing cells in WT and lynx2-null mutant mice will be helpful in understanding the electrical changes caused by lynx2 null-mutation. Immunohistochemistry with antibodies for markers for different cell types on *lynx2*^{-/-} animal brain slices will also help us analyze in more detail what effects lynx2 null mutation has in anatomical structures in these animals, if there are any anatomical effects.

Another hypothesis was the difference in the motor coordination performance of *lynx2*^{-/-} mice and WT mice might be due to increased fear in mutant animals. To test this, mice can be injected with anxiolytic drugs like benzodiazepines and SSRIs and can be tested on accelerated rotarod to see whether the increased motor performance persists.

The increase in number of freezes in fear conditioning test-part 2 should also be investigated further. To test whether the increase in *lynx2*^{-/-} mice is due to increased fear or increased learning capability, anxiety drugs might be administered prior to the test and their effects might be measured. Another curious matter about fear conditioning results

was whether the effect of lynx2 null mutation is due to differences in nicotinic receptor modulation. To test this, nicotine or nicotinic receptor antagonists, like mecamylamine, might be injected to the mice prior to the tests and their effects might be measured and compared between mutant and WT mice.

Conditional KO mice for lynx2 might be generated through breeding the mice to different cre-transgenic mice. Since lynx2 is heavily expressed in amygdala, an amygdala specific KO might tell us whether the effect of lynx2 null mutation on fear and anxiety is due to amygdala or another region. Also, cerebellum and inferior olive specific conditional lynx2 KO mice will also be useful in sorting out whether the effect of lynx2 null mutation on motor coordination is due to lack of lynx2 function in cerebellum or due to lynx2 malfunction in other brain regions.

Since lynx2 is also heavily expressed in regions associated with nociception, like anterior pretectal nucleus, I have tested lynx2 mutant mice on hot plate test but didn't see a significant difference between mutant and WT mice. Nicotinic receptors are involved in nociception mechanisms and sometimes the effect of nicotinic receptor function can only be observed when pain tests are performed after nicotine injections. That's why, I think that more pain tests including hot plate and tail-flick should be performed on lynx2 null mutant mice after nicotine, mecamylamine or saline injections and the effects of these drugs on WT and mutant mice should be compared for assessing the effect of lynx2 on nociception.

For analyzing the function of lynx3, lynx3 KO mice bred with lynx3-EGFP BAC transgenic mice can be used for anatomical analysis. EGFP expressing lynx3 KO mice and WT mice can be compared at lynx3 expression sites and if there are any anatomical

differences, the EGFP expression might make the analysis easier. Also since several ly6 family members have been implicated in nicotinic receptor mediated cell-to cell interactions, cell adhesion and cell-death, lynx3 KO mice can be subjected to different tests, like smoke inhalation, and the effects of this procedure on the epithelial cells, which express lynx3, in the nasal cavity, trachea and lungs, can be investigated.

In order to identify if there is another mammalian channel that lynx3 is modulating, a homologue of the channel that is modulated by lynx3 in *Xenopus* oocytes, I've made lynx3-BAC array mice. These mice express an EGFP-tagged-ribosomal-protein under lynx3 promoter, and when the EGFP-tagged ribosomal protein is immunoprecipitated with an anti-EGFP antibody, the total RNA in the cells that express this protein is also immunoprecipitated. When this immunoprecipitated total RNA and the not-immunoprecipitated total RNA, which is expressed in cells that do not express this protein, are compared on a microarray analysis study, the difference will give us RNA that is expressed lynx3-expressing cells. When this experiment is done in multiple tissues that have lynx3-expressing cells, like lungs and stomach, the common channels that are expressed in both these cell types might be analyzed to see which ones are the non-selective cation channel ones and the target mammalian channel might be identified. This experiment also will be helpful in identifying transcripts that are specific for these cell types. It might be the foundation of another project that analyzes epithelia specific proteins.

In order to investigate the effects of the lack of nicotinic receptors in lynx2 null mutant mice, I'll breed lynx2 mutant mice to nicotinic receptor KO animals. The double-KO mice will be then tested on the different behavior tests that I've performed on lynx2

mutant mice and the results will be compared to see whether the lack of nicotinic receptor subunits can compensate for lynx2 mutation.

There are many experiments that can be done on lynx2 and lynx3 mutant mice and the lynx3-ribosome-BAC transgenic mice, some of which are mentioned above. I believe that these tests will be extremely valuable in understanding nicotinic receptor mediated processes in both brain and epithelial cells and also in order to find epithelia specific proteins.

CHAPTER 7:

Materials and Methods

Identification and Phylogenetic Inference of Ly6 Genes

I searched NCBI and Celera genomic and est sequences to find genes that fit the following criteria:

- Their exon-intron structures were analyzed to exclude the pseudogenes
- The proteins having any other structurally important domains than Ly6 and GPI anchorage were excluded
- All the selected proteins had only one Ly6 domain

The Ly6 domains of these sequences were aligned to UPAR_LY6 protein domain HMM profile of PFAM [233]. After initial alignment using DIALIGN2 [234], we manually corrected the alignments in order to best preserve the alignments of the cysteines. The alignment sequence for all Ly6SF members analyzed were later viewed with Chroma [235]. I have collaborated with Dr. Marcelo Briones for modeling the phylogenetic tree of these proteins. Phylogenetic inference was performed using the Vanilla 1.2 frontend to PAL 1.2 (Phylogenetic Analysis Library) [207]. An unrooted tree was inferred from maximum likelihood distance matrices computed using the JTT substitution model, Gamma model for rate heterogeneity with 8 rate variations over sites and Alpha parameter equal to 1.0. The sequences of mouse and human lynx1, lynx2, lynx3 and Ly6H have been aligned using DIALIGN2 and Boxshade programs.

Cloning

For *in situ* hybridization analysis of Lynx2, the cDNA sequence encoding mouse Lynx2 flanked by its 3' and 5' untranslated sequences was subcloned into the pBluscript-

SK. For immunoprecipitation experiments, Ly6 domains and GPI anchorage sites and signals of Lynx1, Lynx2, Lynx3 and Ly6H were subcloned into mammalian expression vector pFlag-CMV-1. cDNAs encoding nAChR α_4 , β_2 , α_7 , β_4 , α_1 , β_1 , γ and δ subunits were kind gifts from Dr. Jerry A. Stitzel, Dr. Marc Ballivet and Dr. José Ramirez-LaTorre. They were flag tagged and subcloned into oocyte expression vector pCS2+ and used for immunoprecipitation and in vitro transcription experiments. cDNAs encoding Lynx1, Lynx2, Lynx3 and Ly6H were also subcloned into oocyte expression vector pCS2+ and used for in vitro transcription experiments.

For cloning the KO constructs, C57Bl6 genomic DNA containing bacterial artificial chromosomes from Research Genetics, and 10kb genomic DNA containing clones from Open BioSystems were used as template. The PCR reactions were performed with long-template PCR kit from Invitrogen. The backbones of the constructs were pBluescript vector (pSK).

RT-PCR:

The est-clones were purchased from Invitrogen, the exon-intron structures were analyzed and PCR primers were designed to span two different exons so that amplification of gDNA and cDNA would result in products with two different lengths. Single-step RT-PCR kit from Invitrogen was used for all amplifications. The sequences of the PCR primers and the lengths of the products are below.

AK008654 is located on Chr 7. PCR product length when cDNA is amplified: ~490 bp
PCR product length when gDNA is amplified: cDNA > 1500 bp

5' Primer: CAGGCTCCCAGGCCCTAC

3' Primer: GCAGGTCGATGGATGTCCA

AI747831 is located on Chr 15. PCR product length when cDNA is amplified:~350 bp

PCR product length when gDNA is amplified:>1500 bp

5' Primer: CCCAGGATGGACAATTCT

3' Primer: TGAGGGTTGTTGTTGGAAGGA

BB646386 is located on Chr 15. PCR product length when cDNA is amplified: ~840 bp

PCR product length when gDNA is amplified:~1500 bp

5' Primer: AGGCGTTGAAGTGTCATG

3' Primer: GAGGCCGAGGGCCAGCAAT

AK009303 is located on Chr 17. PCR product length when cDNA is amplified:~420 bp

PCR product length when gDNA is amplified:~1500 bp

5' Primer: GTCTTGGGCAGGTGTGTC

3' Primer: GCAAGGGGTAGCAGAGTC

AV082481 is located on Chr 15. PCR product length when cDNA is amplified:~210 bp

PCR product length when gDNA is amplified: >2500 bp

5' Primer: TGGTCTTGAGCATGGAGC

3' Primer: CAGCAGGCGATGGATACAT

AK009282 is located in Chr 2. PCR product length when cDNA is amplified: ~450 bp

PCR product length when gDNA is amplified: >3000 bp

5' Primer: CAGCCCGGAGCGGGGTGTC

3' Primer: AGAATGTGGCAGAGGAGC

For the amplification of B-actin control the following primer pair was used:

5' Primer: TGAGACCTTCAACACCCCAG

3' Primer: GAGCCAGAGCAGTAATCTCC

Northern Blot

Northern Blots were purchased from Invitrogen. Coding regions were amplified with PCR that gave 300-500bp products, which were later labeled with P32. The radioactive probed were purified with G50 columns and all hybridizations were performed in ExpressHyb hybridization buffer from Stratagene overnight at 55°C. The blots were then washed thoroughly and were exposed to films at -80°C for 24-72 hours depending on the strength of the signal.

Western Blot

For all western blots, C57Bl6 mice were sacrificed with CO2 and organs were harvested and frozen in liquid nitrogen immediately. The tissues were than sonicated in a sonication buffer in ice with 8M urea. The protein concentrations were measured with BSA measuring kit from PIERCE. Samples were mixed with sample buffer and sample reducing agent, kept in a 98C heat-block for 2 minutes, centrifuged briefly and loaded to 4-12% bis-tris gels from Novagen at equal concentrations. Gels were run at 80-90V for 2.5 hours at room temperature and were blotted to membranes with semi-dry blotting apparatus. The membranes were blocked with blocking solution of PBS with 5% milk powder and 0.5% Tween-20 for one hour at room temperature, then incubated in blocking solution with primary antibody overnight at 4°C, washed with PBS with 0.5% Tween-20 for 10 minutes at room temperature 3 times and incubated with secondary antibody in blocking solution for 45 minutes. Then they were rinsed with water once,

washed with PBS-Tween for 10 minutes, with water for 10 minutes and with PBS-Tween for another 5 minutes, treated with Immunochemiluminascence kit from Amersham for one minute and exposed to film.

In situ hybridization

Adult brain sections were prepared as described [208]. 3'UTR region of Lynx2 was used as probe for these experiments. Digoxigenin- (Dig-) labeled riboprobe was transcribed using 2 µm Dig-NTP (Boehringer-Mannheim) in the transcription reaction. Sections were incubated at 60°C overnight in hybridization buffer (50% formamide, 5X SSC, 5X Denhardt's reagent, 500 µg/ml herring sperm DNA, and 250 µg/ml yeast tRNA (Sigma R6750)) and washed extensively with 50% formamide and 2× SSC at 60°C. Riboprobe was detected with anti-Dig Fab fragments conjugated to Alkaline Phosphatase and NBT/BCIP substrate mixture.

Polyclonal Antibody Production:

Two different antibodies were made for both Lynx2 and Lynx3. All of the antibodies were made against synthesized peptides, which had the following sequences.

Lynx2 polyclonal antibody against second finger: was made against EFQLNNDCCSPEFIV, which corresponds to the peptide sequence of the first finger in lynx2 protein. Two rabbits were injected with KLH-conjugated peptides. The 4 week, 8 week, 10 week, and 20 week bleeds were IgG purified in purification columns from Pierce. The purified serums were tested on western blots at various concentrations

starting from 1:50 to 1:2000. They were also tested on lynx2 transfected HEK293 cells at different concentration to see if the antibodies bind to non-linearized lynx2.

Lynx2 polyclonal antibody against first finger: This was the first antibody made and it was made against KLH-conjugated peptide KEVTEQSAGIMYRKS, which corresponds to the sequence on the second loop of lynx2 protein. It was made the same way the first finger antibody was made. The IgG purified antibodies bound to lynx2 on western blots and lynx2-expressing HEK293 cells, however, it didn't work on brain sections so the serum was affinity purified with the peptide that it was made against.

Lynx3 polyclonal antibody against second finger: This was the first antibody made against Lynx3. The sequence of peptide that was KLH-conjugated was TTLYSLEIVFPFLGD. The 4-week, 8 week, 10 week and 14 week bleeds from the two rabbits that were injected with this peptide were tested on western blots and lynx3 transfected HEK293 cells.

Lynx3 polyclonal antibody against third finger: When the first antibody generated against lynx3 didn't work, we have generated another antibody by using the sequence from the third finger of lynx3 protein, which was: EPSDVDGIGQTRPVS.

Immunocytochemistry

For immunocytochemistry, the transfected or untransfected cells that were grown on poly-D-lysine coated cover slips were washed with PBS, fixed with 4% paraformaldehyde for 10-15 minutes, treated with blocking solution with either detergent or no detergent for one hour and were incubated overnight with primary antibodies at 4°C. The next day, the cells were washed with PBS and incubated with the secondary

antibody for 1 hour at room temperature. The cells are then washed and mounted on slides.

Histology and Immunohistochemistry

Immunohistochemistry on BAC-transgenic animals were done as described in Gong et. al [208]. For other experiments, mice were perfused with PBS, then 4% paraformaldehyde. Brains were harvested and frozen in embedding medium on dry ice, and transferred to -80°C .

For KO and WT brain sections that are prepared with Hematoxyline-Eosin staining, were cut and stained by Neuro Science Associates (NSA). The mice were perfused with PBS, followed by Na-cacodylate containing perfusion solution and Na-cacodylate wash solution. Perfusion solution contains: 1.4% Na-cacodylate, 4% paraformaldehyde, and 4% sucrose. Perfusion wash solution contains: 0.034% Na-cacodylate, 0.023% CaCl_2 , 0.8% sucrose, 0.8% NaCl, and 0.4% dextrose.

Expression and Immunoprecipitation from HEK293T Cells

HEK 293T cells were transfected by calcium phosphate precipitation with the expression vectors containing the cDNAs of Lynx1, Lynx2, Lynx3, Lynx4, Ly6H, α_7 nAChR, Flag-tagged α_4 , β_2 , β_4 , γ and δ nAChR subunits. Two days after transfection, cells were washed with PBS, harvested in lysis buffer (150 mM NaCl, 50 mM HEPES, 100 mM PMSF, 1.5 $\mu\text{g}/\text{ml}$ aprotinin, 10 $\mu\text{g}/\text{ml}$ leupeptin, and protease inhibitor cocktail) containing 1% Triton X-100 and centrifuged at 14,000 rpm for 2 min. All the other steps were same as described [67].

Injection of Xenopus Oocytes with mRNA:

The cRNAs for Lynx1, Lynx2, Lynx3, Ly6H and nAChR subunits (α_4 , β_2 , β_4 , α_1 , β_2 , γ and δ) were synthesized with T7 or SP6 RNA polymerases (mMESSAGE mMACHINE, Ambion, Austin, TX) through in vitro transcription. To quantify the yield of the synthesized transcripts, they were run on an agarose gel. *Xenopus* oocytes were prepared for injection as described [67]. Oocytes were injected with 0.5 ng of the cRNA encoding each nAChR subunit 3 ng of lynx1, lynx2, lynx3 and Ly6H. The volume injected was 20 nl per oocyte.

Electrophysiology

Functional Analysis of Lynx1 homologues in Oocytes

The voltage-clamp recordings were done on injected oocytes one to two days after injection as described [67].

Analysis of the *Xenopus* Ion Channel opened by Lynx3

In order to find the channel that was opened by lynx3 and caused the leak currents in the lynx3 injected oocytes, I've exposed the control oocytes and lynx3 injected oocytes to various solutions for 20 seconds and analyzed the recordings. The solution recipes are below:

- Composition of Ringer Solution: 115 mM NaCl, 2 mM KCl, 1.8 mM CaCl₂, 5 mM HEPES pH ~7.4Q

- To test for Na⁺ Permeability: 115 mM NMG, 2 mM KCl, 1.8 mM CaCl₂, 5mM HEPES pH ~7.4 (pH adjusted to ~7.4 with HCl (~115mM))
- To test for Ba²⁺ blockage: 115 mM NaCl, 2 mM KCl, 1.8 mM CaCl₂, 5 mM HEPES pH ~7.4, 4 mM BaCl₂
- To test permeability for Na⁺ vs K⁺: 117 mM KCl, 1.8 mM CaCl₂, 5 mM HEPES pH ~7.4
- To test for Ca²⁺-Mg²⁺: 115 mM NaCl, 2 mM KCl, 2.6 mM MgCl₂, 5 mM HEPES pH ~7.4
- To test for La³⁺ blockage: 115 mM NaCl, 2 mM KCl, 1.8 mM CaCl₂, 5 mM HEPES pH ~7.4, 0.1 mM LaCl₃
- To test permeability for Ca²⁺ vs Ba²⁺ blockage: 115 mM NaCl, 2 mM KCl, 2.6 mM MgCl₂, 5 mM HEPES pH ~7.4, 4 mM BaCl₂
- Ca-free solution with flufenamic acid-1: 115 mM NaCl, 2 mM KCl, 1.8 mM CaCl₂, 5 mM HEPES pH ~7.4, 0.5 mM EDTA, 80 μM FFA
- Ca-free solution with flufenamic acid-2: 115 mM NaCl, 2 mM KCl, 2.6 mM MgCl₂, 5 mM HEPES pH ~7.4, 80μM FFA
- High Ca Solution: 75 mM NaCl, 2 mM KCl, 40 mM CaCl₂, 5 mM HEPES pH ~7.4, 80 μM FFA
- To test permeability for NH₄⁺ vs K⁺: 117 mM NH₄Cl, 1.8 mM CaCl₂, 5 mM HEPES pH ~7.4. All K-no Na solution was used as ringer and replaced with NH₄Cl solution for 20 sec/s

To see if the following blockers of hemi-gap channels block the current caused by lynx3 expression, oocytes injected with lynx3 mRNA were perfused with the following

solutions for 20 seconds: 100 μ M Carbenoxolone + Ringer Solution, or 50 μ M FFA (flufenamic acid) + Ringer Solution

For pharmacological analysis of the target channel, I've exposed the lynx3 injected oocytes were perfused with Ringer Solution with the following chemicals for 20 seconds. At least 3 oocytes were recorded for each chemical and concentration mentioned below: 2mM SITS; 1mM DIDS; 1mM Niflumic acid; 1mM Bumetanide; ringer solution with a pH of ~6.4; 100 μ M Genistein; 20 μ M PTPI-IV; 20 μ M Amiloride; 1mM Benzamil; 20mM NH₄Cl; 100mM SKF-96365; 1mM Amiloride; 115mM NMG; 100mM TEA and 100 μ M TEA. All the chemicals were purchased from SIGMA.

Antibodies

The monoclonal antibodies anti-FlagM2, anti- α_7 mAb 306, anti- α_7 mAb 319, anti- α_4 mAb 299, anti- β_1 mAb 111 and HRP-coupled anti-Flag M2 antibodies were purchased from SIGMA.

Behavioral Phenotyping Experiments

Open-Field Exploration Test

Ethovision computer program and equipment, from NOLDUS, were used for open field exploration test. Four rectangular containers in the size of a rat cage, which were labeled as Arena 1-4, were placed under a security camera that is connected to the computer. The camera visualized the test mice as objects darker and different from background since the arenas were white and all the test mice tested were black. A

rectangular area in the middle of each arena was labeled as center of the arena. The computer recorded the movement patterns of the test mice for 20 minutes. We have recorded how many times the mice jumped manually. Four mice were tested every session. The Ethovision program did all the calculations for the behaviors that were measured. The containers were cleaned with isopropanol between each session to remove the excretions and odors of the mice from the previous session. The room that the tests were performed was darkened with black curtains and the only source of light was a light bulb in the middle of the room.

Hanging Wire Assay and Reflex Checks

For hanging wire assay, a rat cage wire lid was used. The ends of the lid were taped so that the mice could not crawl back. The mice were hang on the lid by gently shaking the lid twice when the mice are on top of the lid, then the lid was turned upside down, about one meter over a container with a lot of bedding material in it to minimize the shock of the fall on the mice. The latency of fall was measured with a stop watch. The measurement was stopped at 60 seconds whether the mice fell or not.

A clean Q-tip was used for checking eye-blink and ear-twitch reflexes. The cotton ball tip was brought close to the eye and the ability of the mice to close its eyelids was measured. For ear-twitch reflex, a clean Q-tip was used to touch mouse's ear, and the ability of the mice to twitch their ears was checked.

Rotarod Assay

Economex Rotarod equipment from Columbus Instruments was used for rotarod tests. Each mouse was tested four times a day with 5-minute intervals for four days. The

rod started to turn at a speed of 1 RPM and accelerated with a rate of 0.1RPM /sec. The latency to grab the rod and turn once or to fall was measured with a stopwatch. During experiments for testing the effect of nicotine and nicotinic antagonists, the mice were injected intraperitoneally with nicotine, saline, mecamlamine, and hexamethonium so that the injection solution would be 100-200 µl, depending on the weight of the mice. The resulting concentrations of the drugs in mice were 1mg/kg of nicotine (nicotine tartrate from SIGMA), 4mg/kg of mecamlamine (SIGMA) and 4mg/kg of hexamethonium (SIGMA). All the stock solutions and injection solutions were prepared in physiological saline. For tests with nicotine and saline, mice were injected with nicotine/saline and tested 5 minutes later. For tests with mecamlamine and hexamethonium, the mice were tested 15 minutes after injection. For mecamlamine and nicotine tests, mice were injected with mecamlamine, kept in their cages for 10 minutes, injected with nicotine and tested 5 minutes later.

Light-Dark Box Test

The test apparatus was novel to each test mouse. Test started 10 seconds after the mice were put inside the light compartment of the light-dark box for 10 minutes. A security camera that is connected to a computer with Ethovision was used for recording the movement patterns of the mice and the calculations of the entries into the light and dark compartments and the time spent in each compartment were done automatically by Ethovision program in the computer.

For testing the effect of nicotine on anxiety related behavior of *lynx2^{-/-}* mice, mice were injected with nicotine 1mg/kg and were kept in a cage for 40 minutes before the test. The same procedure was used for saline injected mice as well.

Social Interaction Test

A diagram showing the parts of social interaction test are shown in figure 49. The model for social interaction test was based on the apparatus described previously [236]. The apparatus consists of three compartments; two on each end with small wire cages in them and one middle compartment, all of which were separated with removable doors. The wires on the cages were 1 cm apart, enough to give a chance for mice to sniff each other through them. In the first part of the test, a novel mouse was placed in a cage in the first compartment, and the test mouse was placed in the middle compartment for 10 minutes for habituation. After habituation, the doors were removed and the test mouse explored freely among the compartments. The amount of time spent in each compartment and the time spent sniffing the empty cage and the cage with the novel mice were all recorded with a security camera and Ethovision program. All the calculations and measurements were made with Ethovision program on the computer.

During the second part of the test, a novel mouse was placed inside the empty cage in the third compartment and the previously associated novel mouse-1 was kept in its original cage. The test mouse roamed freely among the compartments and the analysis were done the same way. The equipment was cleaned with isopropanol between each trial.

Elevated Plus Maze Test

Each mouse was placed on the center of the apparatus facing an open-arm and its movements were recorded with Ethovision for five minutes. We also manually recorded each entry to the center, open or closed-arm. The calculations for manually recorded and computer recorded movements were all done by analysis program of Ethovision and were found to be similar. The number of entries into open arms, time spent in the center, time spent in closed arms and time spent in center area were analyzed. The equipment was cleaned with isopropanol to remove excretions and odors from the previous test mouse between each trial.

Fear Conditioning Test

A conditioning apparatus from Med Associates was used for fear conditioning tests with a program that was described earlier [237]. The mice were given 2-second 0.5mA shocks at the two last seconds of a 30-second long 80 db tone, twice on training day. The number of freezes were counted every 10 seconds before and after the shocks were given and recorded as pre-shock Day1 and post-shock Day1. 24 hours later, the mice were placed in the same environment without any tone or shock and the number of freezes every ten seconds were recorded as contextual day2. On the second part of the test, the mice were placed in a novel environment with a different ceiling, walls and a smell of orange extract and were kept in that environment for 3 minutes before subjected to an 80 db tone for another 3 minutes. The total numbers of freezes before and after tone were recorded as pre-tone day2 and during-tone day2.

Hot Plate Test

A hot plate test apparatus from Columbus Instruments was used for this pain perception test. The hot plate is kept at a constant temperature of 55°C and is covered with a clear plexiglass. The mice were placed on the plate and were kept there until they either tapped their hind feet or licked their paws. The test was performed once per animal to minimize the tissue damage. The latency to respond to pain through above means was measured with a stopwatch.

Finding Buried Food Test

The test mice were starved without food or water for 18 hours before the test. A food pellet was hidden under 1cm of bedding in a clean mouse cage and the mouse was placed in the center of the cage. The latency to the mouse to find the pellet and hold it in its front paws or eat it was measured with a stopwatch. The mice were then given food for 4 hours, and starved for another 18 hours for the next day of testing. After first day of testing, the mice were not tested for a 24-hour period and were tested the next day after 18 hour starvation. The food pellet was placed on a different location every day, for three consecutive days. Every mouse was tested only once with this test and were placed in a clean cage after each test.

Statistical Analysis

Student-T-tests were performed by using Microsoft Excel. To analyze data with repeated measurements over time, we used Mixed Effects Models, also known as Mixed ANOVA models. This approach is based on likelihood estimation rather than moment

estimation as in typical repeated-measures ANOVA analysis, and it is more robust to missing values. The mixed linear model is a generalization of the standard linear model in which errors are permitted to exhibit correlations and non-constant variability, two properties that would violate key assumptions of standard ANOVA models. The mixed model is written as:

$$\mathbf{y}=\mathbf{X}\boldsymbol{\beta}+\mathbf{Z}\boldsymbol{\gamma}+\boldsymbol{\varepsilon}$$

where to the terms $\mathbf{X}\boldsymbol{\beta}+\boldsymbol{\varepsilon}$ defining the general linear model, are added the known design matrix \mathbf{Z} , times the vector of unknown *random-effects parameters* $\boldsymbol{\gamma}$. Both $\boldsymbol{\gamma}$ and $\boldsymbol{\varepsilon}$ are assumed to follow a normal distribution with zero mean and covariance matrices \mathbf{G} and \mathbf{R} , respectively. The name *mixed model* comes from the fact that the model contains both fixed-effects parameters $\boldsymbol{\beta}$ and random-effects parameters $\boldsymbol{\gamma}$. A variety of correlation structures can be used by specifying the \mathbf{G} and \mathbf{R} matrices.

All models were fitted using the PROC MIXED procedure in SAS 9.1.3. (SAS Institute, Cary, NC). Genotype, day and its interaction were considered in all models. In the case of RR with treatment, this factor was also included and the interactions with Genotype and Day were explored. To model the within-subject covariance's structure we considered several structures available through SAS's MIXED procedure, specifically: autoregressive (ar(1)), unconstrained and compound symmetric (cs) structures. Slight variations of those models were tested and the best model, as determined through the Akaike and Bayesian Information Criteria (AIC/BIC), was selected.

Bibliography

1. McKenzie, I.F., et al., *Lymphocyte antigens: Ly-4, Ly-6, and Ly-7*. Transplant Proc, 1977. **9**(1): p. 667-9.
2. Gumley, T.P., I.F. McKenzie, and M.S. Sandrin, *Tissue expression, structure and function of the murine Ly-6 family of molecules*. Immunol Cell Biol, 1995. **73**(4): p. 277-96.
3. Pflugh, D.L., S.E. Maher, and A.L. Bothwell, *Ly-6 superfamily members Ly-6A/E, Ly-6C, and Ly-6I recognize two potential ligands expressed by B lymphocytes*. J Immunol, 2002. **169**(9): p. 5130-6.
4. Khodadoust, M.M., K.D. Khan, and A.L. Bothwell, *Complex regulation of Ly-6E gene transcription in T cells by IFNs*. J Immunol, 1999. **163**(2): p. 811-9.
5. Patterson, J.M., et al., *Characterization of Ly-6M, a novel member of the Ly-6 family of hematopoietic proteins*. Blood, 2000. **95**(10): p. 3125-32.
6. Pflugh, D.L., S.E. Maher, and A.L. Bothwell, *Ly-6I, a new member of the murine Ly-6 superfamily with a distinct pattern of expression*. J Immunol, 2000. **165**(1): p. 313-21.
7. van de Rijn, M., et al., *Mouse hematopoietic stem-cell antigen Sca-1 is a member of the Ly-6 antigen family*. Proc Natl Acad Sci U S A, 1989. **86**(12): p. 4634-8.
8. Shan, X., et al., *Characterization and mapping to human chromosome 8q24.3 of Ly-6-related gene 9804 encoding an apparent homologue of mouse TSA-1*. J Immunol, 1998. **160**(1): p. 197-208.
9. Brakenhoff, R.H., et al., *The human E48 antigen, highly homologous to the murine Ly-6 antigen ThB, is a GPI-anchored molecule apparently involved in keratinocyte cell-cell adhesion*. J Cell Biol, 1995. **129**(6): p. 1677-89.
10. Mao, M., et al., *RIG-E, a human homolog of the murine Ly-6 family, is induced by retinoic acid during the differentiation of acute promyelocytic leukemia cell*. Proc Natl Acad Sci U S A, 1996. **93**(12): p. 5910-4.
11. Gumley, T.P., et al., *Isolation and characterization of cDNA clones for the mouse thymocyte B cell antigen (ThB)*. J Immunol, 1992. **149**(8): p. 2615-8.
12. McCormack, J.M., P.J. Leenen, and W.S. Walker, *Macrophage progenitors from mouse bone marrow and spleen differ in their expression of the Ly-6C differentiation antigen*. J Immunol, 1993. **151**(11): p. 6389-98.
13. Davies, A., et al., *CD59, an LY-6-like protein expressed in human lymphoid cells, regulates the action of the complement membrane attack complex on homologous cells*. J Exp Med, 1989. **170**(3): p. 637-54.
14. Kieffer, B., et al., *Three-dimensional solution structure of the extracellular region of the complement regulatory protein CD59, a new cell-surface protein domain related to snake venom neurotoxins*. Biochemistry, 1994. **33**(15): p. 4471-82.
15. Adermann, K., et al., *Structural and phylogenetic characterization of human SLURP-1, the first secreted mammalian member of the Ly-6/uPAR protein superfamily*. Protein Sci, 1999. **8**(4): p. 810-9.
16. Miwa, T., N. Okada, and H. Okada, *Alternative exon usage in the 3' region of a single gene generates glycosylphosphatidylinositol-anchored and transmembrane forms of rat decay-accelerating factor*. Immunogenetics, 2000. **51**(2): p. 129-37.

17. Tsetlin, V., *Snake venom alpha-neurotoxins and other 'three-finger' proteins*. Eur J Biochem, 1999. **264**(2): p. 281-6.
18. Servent, D., et al., *Only snake curaremimetic toxins with a fifth disulfide bond have high affinity for the neuronal alpha7 nicotinic receptor*. J Biol Chem, 1997. **272**(39): p. 24279-86.
19. Grant, G.A., et al., *Differential roles for disulfide bonds in the structural integrity and biological activity of kappa-Bungarotoxin, a neuronal nicotinic acetylcholine receptor antagonist*. Biochemistry, 1998. **37**(35): p. 12166-71.
20. Bilwes, A., et al., *X-ray structure at 1.55 A of toxin gamma, a cardiotoxin from Naja nigricollis venom. Crystal packing reveals a model for insertion into membranes*. J Mol Biol, 1994. **239**(1): p. 122-36.
21. Sutcliffe, M.J., C.M. Dobson, and R.E. Oswald, *Solution structure of neuronal bungarotoxin determined by two-dimensional NMR spectroscopy: calculation of tertiary structure using systematic homologous model building, dynamical simulated annealing, and restrained molecular dynamics*. Biochemistry, 1992. **31**(11): p. 2962-70.
22. Dewan, J.C., G.A. Grant, and J.C. Sacchettini, *Crystal structure of kappa-bungarotoxin at 2.3-A resolution*. Biochemistry, 1994. **33**(44): p. 13147-54.
23. Shafqat, J., et al., *Extensive multiplicity of the miscellaneous type of neurotoxins from the venom of the cobra Naja naja naja and structural characterization of major components*. FEBS Lett, 1991. **284**(1): p. 70-2.
24. Tsuji, H., et al., *SLURP-2, a novel member of the human Ly-6 superfamily that is up-regulated in psoriasis vulgaris*. Genomics, 2003. **81**(1): p. 26-33.
25. Luo, C.W., H.J. Lin, and Y.H. Chen, *A novel heat-labile phospholipid-binding protein, SVS VII, in mouse seminal vesicle as a sperm motility enhancer*. J Biol Chem, 2001. **276**(10): p. 6913-21.
26. Behrendt, N., et al., *The ligand-binding domain of the cell surface receptor for urokinase-type plasminogen activator*. J Biol Chem, 1991. **266**(12): p. 7842-7.
27. Roldan, A.L., et al., *Cloning and expression of the receptor for human urokinase plasminogen activator, a central molecule in cell surface, plasmin dependent proteolysis*. Embo J, 1990. **9**(2): p. 467-74.
28. Tarui, T., et al., *Urokinase-type plasminogen activator receptor (CD87) is a ligand for integrins and mediates cell-cell interaction*. J Biol Chem, 2001. **276**(6): p. 3983-90.
29. Williams, A.F., A.G. Tse, and J. Gagnon, *Squid glycoproteins with structural similarities to Thy-1 and Ly-6 antigens*. Immunogenetics, 1988. **27**(4): p. 265-72.
30. Chou, J.H., C.I. Bargmann, and P. Sengupta, *The Caenorhabditis elegans odr-2 gene encodes a novel Ly-6-related protein required for olfaction*. Genetics, 2001. **157**(1): p. 211-24.
31. Izon, D.J., et al., *Identification and functional analysis of Ly-6A/E as a thymic and bone marrow stromal antigen*. J Immunol, 1996. **156**(7): p. 2391-9.
32. Bamezai, A. and K.L. Rock, *Overexpressed Ly-6A.2 mediates cell-cell adhesion by binding a ligand expressed on lymphoid cells*. Proc Natl Acad Sci U S A, 1995. **92**(10): p. 4294-8.

33. MacNeil, I., et al., *Isolation of a cDNA encoding thymic shared antigen-1. A new member of the Ly6 family with a possible role in T cell development.* J Immunol, 1993. **151**(12): p. 6913-23.
34. Walunas, T.L., et al., *Ly-6C is a marker of memory CD8+ T cells.* J Immunol, 1995. **155**(4): p. 1873-83.
35. Fleming, T.J., M.L. Fleming, and T.R. Malek, *Selective expression of Ly-6G on myeloid lineage cells in mouse bone marrow. RB6-8C5 mAb to granulocyte-differentiation antigen (Gr-1) detects members of the Ly-6 family.* J Immunol, 1993. **151**(5): p. 2399-408.
36. Brakenhoff, R.H., et al., *A gain of novel tissue specificity in the human Ly-6 gene E48.* J Immunol, 1997. **159**(10): p. 4879-86.
37. Reese, J.T., et al., *Downregulated expression of Ly-6-ThB on developing T cells marks CD4+CD8+ subset undergoing selection in the thymus.* Dev Immunol, 2001. **8**(2): p. 107-21.
38. Schrijvers, A.H., et al., *Evidence for a role of the monoclonal antibody E48 defined antigen in cell-cell adhesion in squamous epithelia and head and neck squamous cell carcinoma.* Exp Cell Res, 1991. **196**(2): p. 264-9.
39. de Nooij-van Dalen, A.G., et al., *Characterization of the human Ly-6 antigens, the newly annotated member Ly-6K included, as molecular markers for head-and-neck squamous cell carcinoma.* Int J Cancer, 2003. **103**(6): p. 768-74.
40. Norman, B., J. Davis, and J. Piatigorsky, *Postnatal gene expression in the normal mouse cornea by SAGE.* Invest Ophthalmol Vis Sci, 2004. **45**(2): p. 429-40.
41. Jalkut, M.W. and R.E. Reiter, *Role of prostate stem cell antigen in prostate cancer research.* Curr Opin Urol, 2002. **12**(5): p. 401-6.
42. Reiter, R.E., et al., *Prostate stem cell antigen: a cell surface marker overexpressed in prostate cancer.* Proc Natl Acad Sci U S A, 1998. **95**(4): p. 1735-40.
43. Cray, C., et al., *Regulation and selective expression of Ly-6A/E, a lymphocyte activation molecule, in the central nervous system.* Brain Res Mol Brain Res, 1990. **8**(1): p. 9-15.
44. Horie, M., et al., *Isolation and characterization of a new member of the human Ly6 gene family (LY6H).* Genomics, 1998. **53**(3): p. 365-8.
45. Apostolopoulos, J., L.J. Chisholm, and M.S. Sandrin, *Identification of mouse Ly6H and its expression in normal tissue.* Immunogenetics, 1999. **49**(11-12): p. 987-90.
46. Dessaud, E., et al., *Identification of lynx2, a novel member of the ly-6/neurotoxin superfamily, expressed in neuronal subpopulations during mouse development.* Mol Cell Neurosci, 2006. **31**(2): p. 232-42.
47. Hanninen, A., et al., *Ly-6C regulates endothelial adhesion and homing of CD8(+) T cells by activating integrin-dependent adhesion pathways.* Proc Natl Acad Sci U S A, 1997. **94**(13): p. 6898-903.
48. English, A., et al., *A monoclonal antibody against the 66-kDa protein expressed in mouse spleen and thymus inhibits Ly-6A.2-dependent cell-cell adhesion.* J Immunol, 2000. **165**(7): p. 3763-71.

49. Dumont, F.J., *Stimulation of murine T cells via the Ly-6C antigen: lack of proliferative response in aberrant T cells from lpr/lpr and gld/gld mice despite high Ly-6C antigen expression.* J Immunol, 1987. **138**(12): p. 4106-13.
50. Sagi-Assif, O., et al., *TNFalpha and anti-Fas antibodies regulate Ly-6E.1 expression by tumor cells: a possible link between angiogenesis and Ly-6E.1.* Immunol Lett, 1996. **54**(2-3): p. 207-13.
51. Stanford, W.L., et al., *Altered proliferative response by T lymphocytes of Ly-6A (Sca-1) null mice.* J Exp Med, 1997. **186**(5): p. 705-17.
52. Kosugi, A., et al., *Physical and functional association between thymic shared antigen-1/stem cell antigen-2 and the T cell receptor complex.* J Biol Chem, 1998. **273**(20): p. 12301-6.
53. Saitoh, S., et al., *Modulation of TCR-mediated signaling pathway by thymic shared antigen-1 (TSA-1)/stem cell antigen-2 (Sca-2).* J Immunol, 1995. **155**(12): p. 5574-81.
54. Noda, S., et al., *Protection from anti-TCR/CD3-induced apoptosis in immature thymocytes by a signal through thymic shared antigen-1/stem cell antigen-2.* J Exp Med, 1996. **183**(5): p. 2355-60.
55. Bamezai, A., et al., *Regulated expression of Ly-6A.2 is important for T cell development.* J Immunol, 1995. **154**(9): p. 4233-9.
56. Korty, P.E., C. Brando, and E.M. Shevach, *CD59 functions as a signal-transducing molecule for human T cell activation.* J Immunol, 1991. **146**(12): p. 4092-8.
57. Katz, B.Z., et al., *An association between high Ly-6A/E expression on tumor cells and a highly malignant phenotype.* Int J Cancer, 1994. **59**(5): p. 684-91.
58. Kimura, Y., et al., *Genomic structure and chromosomal localization of GML (GPI-anchored molecule-like protein), a gene induced by p53.* Genomics, 1997. **41**(3): p. 477-80.
59. Apostolopoulos, J., I.F. McKenzie, and M.S. Sandrin, *Ly6d-L, a cell surface ligand for mouse Ly6d.* Immunity, 2000. **12**(2): p. 223-32.
60. Jerusalinsky, D. and A.L. Harvey, *Toxins from mamba venoms: small proteins with selectivities for different subtypes of muscarinic acetylcholine receptors.* Trends Pharmacol Sci, 1994. **15**(11): p. 424-30.
61. de Weille, J.R. and M. Lazdunski, *ATP-sensitive K⁺ channels reveal the effects of intracellular chloride variations on cytoplasmic ATP concentrations and mitochondrial function.* Biochem Biophys Res Commun, 1990. **168**(3): p. 1137-42.
62. Albrand, J.P., et al., *NMR and restrained molecular dynamics study of the three-dimensional solution structure of toxin FS2, a specific blocker of the L-type calcium channel, isolated from black mamba venom.* Biochemistry, 1995. **34**(17): p. 5923-37.
63. Fischer, J., et al., *Mutations in the gene encoding SLURP-1 in Mal de Meleda.* Hum Mol Genet, 2001. **10**(8): p. 875-80.
64. Chimienti, F., et al., *Identification of SLURP-1 as an epidermal neuromodulator explains the clinical phenotype of Mal de Meleda.* Hum Mol Genet, 2003. **12**(22): p. 3017-24.

65. Arredondo, J., et al., *Biological effects of SLURP-1 on human keratinocytes*. J Invest Dermatol, 2005. **125**(6): p. 1236-41.
66. Arredondo, J., et al., *SLURP-2: A novel cholinergic signaling peptide in human mucocutaneous epithelium*. J Cell Physiol, 2006. **208**(1): p. 238-45.
67. Ibanez-Tallon, I., et al., *Novel modulation of neuronal nicotinic acetylcholine receptors by association with the endogenous prototoxin lynx1*. Neuron, 2002. **33**(6): p. 893-903.
68. Devillers-Thiery, A., et al., *Functional architecture of the nicotinic acetylcholine receptor: a prototype of ligand-gated ion channels*. J Membr Biol, 1993. **136**(2): p. 97-112.
69. Le Novere, N., P.J. Corringer, and J.P. Changeux, *The diversity of subunit composition in nAChRs: evolutionary origins, physiologic and pharmacologic consequences*. J Neurobiol, 2002. **53**(4): p. 447-56.
70. Millar, N.S., *Assembly and subunit diversity of nicotinic acetylcholine receptors*. Biochem Soc Trans, 2003. **31**(Pt 4): p. 869-74.
71. McGehee, D.S., *Molecular diversity of neuronal nicotinic acetylcholine receptors*. Ann N Y Acad Sci, 1999. **868**: p. 565-77.
72. Racke, K., U.R. Juergens, and S. Matthiesen, *Control by cholinergic mechanisms*. Eur J Pharmacol, 2006. **533**(1-3): p. 57-68.
73. Spindel, E.R., *Neuronal nicotinic acetylcholine receptors: not just in brain*. Am J Physiol Lung Cell Mol Physiol, 2003. **285**(6): p. L1201-2.
74. Le Novere, N. and J.P. Changeux, *Molecular evolution of the nicotinic acetylcholine receptor: an example of multigene family in excitable cells*. J Mol Evol, 1995. **40**(2): p. 155-72.
75. Tsunoyama, K. and T. Gojobori, *Evolution of nicotinic acetylcholine receptor subunits*. Mol Biol Evol, 1998. **15**(5): p. 518-27.
76. Bertrand, D., et al., *Unconventional pharmacology of a neuronal nicotinic receptor mutated in the channel domain*. Proc Natl Acad Sci U S A, 1992. **89**(4): p. 1261-5.
77. Dani, J.A., *Open channel structure and ion binding sites of the nicotinic acetylcholine receptor channel*. J Neurosci, 1989. **9**(3): p. 884-92.
78. Xu, W., et al., *Multiorgan autonomic dysfunction in mice lacking the beta2 and the beta4 subunits of neuronal nicotinic acetylcholine receptors*. J Neurosci, 1999. **19**(21): p. 9298-305.
79. Witzemann, V., et al., *Acetylcholine receptor epsilon-subunit deletion causes muscle weakness and atrophy in juvenile and adult mice*. Proc Natl Acad Sci U S A, 1996. **93**(23): p. 13286-91.
80. Duclert, A. and J.P. Changeux, *Acetylcholine receptor gene expression at the developing neuromuscular junction*. Physiol Rev, 1995. **75**(2): p. 339-68.
81. Samson, A., et al., *The mechanism for acetylcholine receptor inhibition by alpha-neurotoxins and species-specific resistance to alpha-bungarotoxin revealed by NMR*. Neuron, 2002. **35**(2): p. 319-32.
82. Karlin, A., *Structure of nicotinic acetylcholine receptors*. Curr Opin Neurobiol, 1993. **3**(3): p. 299-309.
83. Brejc, K., et al., *Crystal structure of an ACh-binding protein reveals the ligand-binding domain of nicotinic receptors*. Nature, 2001. **411**(6835): p. 269-76.

84. Le Novere, N., T. Grutter, and J.P. Changeux, *Models of the extracellular domain of the nicotinic receptors and of agonist- and Ca²⁺-binding sites*. Proc Natl Acad Sci U S A, 2002. **99**(5): p. 3210-5.
85. Fruchart-Gaillard, C., et al., *Experimentally based model of a complex between a snake toxin and the alpha 7 nicotinic receptor*. Proc Natl Acad Sci U S A, 2002. **99**(5): p. 3216-21.
86. Miyazawa, A., Y. Fujiyoshi, and N. Unwin, *Structure and gating mechanism of the acetylcholine receptor pore*. Nature, 2003. **423**(6943): p. 949-55.
87. Unwin, N., *Refined structure of the nicotinic acetylcholine receptor at 4A resolution*. J Mol Biol, 2005. **346**(4): p. 967-89.
88. Kukhtina, V., et al., *Intracellular domain of nicotinic acetylcholine receptor: the importance of being unfolded*. J Neurochem, 2005.
89. Karlin, A., *Emerging structure of the nicotinic acetylcholine receptors*. Nat Rev Neurosci, 2002. **3**(2): p. 102-14.
90. Karlin, A. and M.H. Akabas, *Toward a structural basis for the function of nicotinic acetylcholine receptors and their cousins*. Neuron, 1995. **15**(6): p. 1231-44.
91. Moise, L., et al., *NMR structural analysis of alpha-bungarotoxin and its complex with the principal alpha-neurotoxin-binding sequence on the alpha 7 subunit of a neuronal nicotinic acetylcholine receptor*. J Biol Chem, 2002. **277**(14): p. 12406-17.
92. Marks, M.J., et al., *Variation of nicotinic binding sites among inbred strains*. Pharmacol Biochem Behav, 1989. **33**(3): p. 679-89.
93. Quik, M., et al., *Localization of nicotinic receptor subunit mRNAs in monkey brain by in situ hybridization*. J Comp Neurol, 2000. **425**(1): p. 58-69.
94. Dominguez del Toro, E., et al., *Immunocytochemical localization of the alpha 7 subunit of the nicotinic acetylcholine receptor in the rat central nervous system*. J Comp Neurol, 1994. **349**(3): p. 325-42.
95. Broide, R.S., et al., *Developmental expression of alpha 7 neuronal nicotinic receptor messenger RNA in rat sensory cortex and thalamus*. Neuroscience, 1995. **67**(1): p. 83-94.
96. Happe, H.K. and B.J. Morley, *Nicotinic acetylcholine receptors in rat cochlear nucleus: [125I]-alpha-bungarotoxin receptor autoradiography and in situ hybridization of alpha 7 nAChR subunit mRNA*. J Comp Neurol, 1998. **397**(2): p. 163-80.
97. Caruncho, H.J., et al., *Subcellular localization of the alpha 7 nicotinic receptor in rat cerebellar granule cell layer*. Neuroreport, 1997. **8**(6): p. 1431-3.
98. Fabian-Fine, R., et al., *Ultrastructural distribution of the alpha7 nicotinic acetylcholine receptor subunit in rat hippocampus*. J Neurosci, 2001. **21**(20): p. 7993-8003.
99. Adams, C.E., et al., *Alpha7-nicotinic receptor expression and the anatomical organization of hippocampal interneurons*. Brain Res, 2001. **922**(2): p. 180-90.
100. Wada, E., et al., *Distribution of alpha 2, alpha 3, alpha 4, and beta 2 neuronal nicotinic receptor subunit mRNAs in the central nervous system: a hybridization histochemical study in the rat*. J Comp Neurol, 1989. **284**(2): p. 314-35.

101. Nakayama, H., et al., *Expression of the nicotinic acetylcholine receptor alpha4 subunit mRNA in the rat cerebellar cortex*. Neurosci Lett, 1998. **256**(3): p. 177-9.
102. Moser, N., et al., *Alpha4-1 subunit mRNA of the nicotinic acetylcholine receptor in the rat olfactory bulb: cellular expression in adult, pre- and postnatal stages*. Cell Tissue Res, 1996. **285**(1): p. 17-25.
103. Perry, D.C., et al., *Measuring nicotinic receptors with characteristics of alpha4beta2, alpha3beta2 and alpha3beta4 subtypes in rat tissues by autoradiography*. J Neurochem, 2002. **82**(3): p. 468-81.
104. Boulter, J., et al., *Isolation of a cDNA clone coding for a possible neural nicotinic acetylcholine receptor alpha-subunit*. Nature, 1986. **319**(6052): p. 368-74.
105. Yeh, J.J., et al., *Neuronal nicotinic acetylcholine receptor alpha3 subunit protein in rat brain and sympathetic ganglion measured using a subunit-specific antibody: regional and ontogenic expression*. J Neurochem, 2001. **77**(1): p. 336-46.
106. Winzer-Serhan, U.H. and F.M. Leslie, *Codistribution of nicotinic acetylcholine receptor subunit alpha3 and beta4 mRNAs during rat brain development*. J Comp Neurol, 1997. **386**(4): p. 540-54.
107. Gahring, L.C., K. Persiyanov, and S.W. Rogers, *Neuronal and astrocyte expression of nicotinic receptor subunit beta4 in the adult mouse brain*. J Comp Neurol, 2004. **468**(3): p. 322-33.
108. Dineley-Miller, K. and J. Patrick, *Gene transcripts for the nicotinic acetylcholine receptor subunit, beta4, are distributed in multiple areas of the rat central nervous system*. Brain Res Mol Brain Res, 1992. **16**(3-4): p. 339-44.
109. Turner, J.R. and K.J. Kellar, *Nicotinic cholinergic receptors in the rat cerebellum: multiple heteromeric subtypes*. J Neurosci, 2005. **25**(40): p. 9258-65.
110. Ishii, K., J.K. Wong, and K. Sumikawa, *Comparison of alpha2 nicotinic acetylcholine receptor subunit mRNA expression in the central nervous system of rats and mice*. J Comp Neurol, 2005. **493**(2): p. 241-60.
111. Wada, E., et al., *The distribution of mRNA encoded by a new member of the neuronal nicotinic acetylcholine receptor gene family (alpha 5) in the rat central nervous system*. Brain Res, 1990. **526**(1): p. 45-53.
112. Le Novere, N., M. Zoli, and J.P. Changeux, *Neuronal nicotinic receptor alpha 6 subunit mRNA is selectively concentrated in catecholaminergic nuclei of the rat brain*. Eur J Neurosci, 1996. **8**(11): p. 2428-39.
113. Elgoyhen, A.B., et al., *alpha10: a determinant of nicotinic cholinergic receptor function in mammalian vestibular and cochlear mechanosensory hair cells*. Proc Natl Acad Sci U S A, 2001. **98**(6): p. 3501-6.
114. Khan, I., et al., *Nicotinic acetylcholine receptor distribution in relation to spinal neurotransmission pathways*. J Comp Neurol, 2003. **467**(1): p. 44-59.
115. Zoli, M., et al., *Developmental regulation of nicotinic ACh receptor subunit mRNAs in the rat central and peripheral nervous systems*. J Neurosci, 1995. **15**(3 Pt 1): p. 1912-39.
116. Zia, S., et al., *Nicotine enhances expression of the alpha 3, alpha 4, alpha 5, and alpha 7 nicotinic receptors modulating calcium metabolism and regulating adhesion and motility of respiratory epithelial cells*. Res Commun Mol Pathol Pharmacol, 1997. **97**(3): p. 243-62.

117. Maus, A.D., et al., *Human and rodent bronchial epithelial cells express functional nicotinic acetylcholine receptors*. *Mol Pharmacol*, 1998. **54**(5): p. 779-88.
118. Sekhon, H.S., et al., *Prenatal nicotine increases pulmonary alpha7 nicotinic receptor expression and alters fetal lung development in monkeys*. *J Clin Invest*, 1999. **103**(5): p. 637-47.
119. Wang, Y., et al., *Human bronchial epithelial and endothelial cells express alpha7 nicotinic acetylcholine receptors*. *Mol Pharmacol*, 2001. **60**(6): p. 1201-9.
120. Grando, S.A., et al., *A nicotinic acetylcholine receptor regulating cell adhesion and motility is expressed in human keratinocytes*. *J Invest Dermatol*, 1995. **105**(6): p. 774-81.
121. Grando, S.A., *Receptor-mediated action of nicotine in human skin*. *Int J Dermatol*, 2001. **40**(11): p. 691-3.
122. Nguyen, V.T., et al., *Synergistic control of keratinocyte adhesion through muscarinic and nicotinic acetylcholine receptor subtypes*. *Exp Cell Res*, 2004. **294**(2): p. 534-49.
123. Beckel, J.M., et al., *Expression of functional nicotinic acetylcholine receptors in rat urinary bladder epithelial cells*. *Am J Physiol Renal Physiol*, 2006. **290**(1): p. F103-10.
124. Stewart, T.A. and I.T. Forrester, *Identification of a cholinergic receptor in ram spermatozoa*. *Biol Reprod*, 1978. **19**(5): p. 965-70.
125. Young, R.J. and J.C. Laing, *The binding characteristics of cholinergic sites in rabbit spermatozoa*. *Mol Reprod Dev*, 1991. **28**(1): p. 55-61.
126. Nguyen, V.T., et al., *Choline acetyltransferase, acetylcholinesterase, and nicotinic acetylcholine receptors of human gingival and esophageal epithelia*. *J Dent Res*, 2000. **79**(4): p. 939-49.
127. Kawashima, K. and T. Fujii, *Extraneuronal cholinergic system in lymphocytes*. *Pharmacol Ther*, 2000. **86**(1): p. 29-48.
128. Sato, K.Z., et al., *Diversity of mRNA expression for muscarinic acetylcholine receptor subtypes and neuronal nicotinic acetylcholine receptor subunits in human mononuclear leukocytes and leukemic cell lines*. *Neurosci Lett*, 1999. **266**(1): p. 17-20.
129. Kimura, R., et al., *Nicotine-induced Ca²⁺ signaling and down-regulation of nicotinic acetylcholine receptor subunit expression in the CEM human leukemic T-cell line*. *Life Sci*, 2003. **72**(18-19): p. 2155-8.
130. Giniatullin, R.A., et al., *Rapid relief of block by mecamylamine of neuronal nicotinic acetylcholine receptors of rat chromaffin cells in vitro: an electrophysiological and modeling study*. *Mol Pharmacol*, 2000. **58**(4): p. 778-87.
131. Ascher, P., W.A. Large, and H.P. Rang, *Studies on the mechanism of action of acetylcholine antagonists on rat parasympathetic ganglion cells*. *J Physiol*, 1979. **295**: p. 139-70.
132. Fieber, L.A. and D.J. Adams, *Acetylcholine-evoked currents in cultured neurones dissociated from rat parasympathetic cardiac ganglia*. *J Physiol*, 1991. **434**: p. 215-37.
133. Gurney, A.M. and H.P. Rang, *The channel-blocking action of methonium compounds on rat submandibular ganglion cells*. *Br J Pharmacol*, 1984. **82**(3): p. 623-42.

134. Paton, W.D. and E.J. Zaimis, *Paralysis of autonomic ganglia by methonium salts*. Br J Pharmacol Chemother, 1951. **6**(1): p. 155-68.
135. Gerzanich, V., R. Anand, and J. Lindstrom, *Homomers of alpha 8 and alpha 7 subunits of nicotinic receptors exhibit similar channel but contrasting binding site properties*. Mol Pharmacol, 1994. **45**(2): p. 212-20.
136. Seguela, P., et al., *Molecular cloning, functional properties, and distribution of rat brain alpha 7: a nicotinic cation channel highly permeable to calcium*. J Neurosci, 1993. **13**(2): p. 596-604.
137. Charnet, P., et al., *Pharmacological and kinetic properties of alpha 4 beta 2 neuronal nicotinic acetylcholine receptors expressed in Xenopus oocytes*. J Physiol, 1992. **450**: p. 375-94.
138. Orr-Urtreger, A., et al., *Mice deficient in the alpha7 neuronal nicotinic acetylcholine receptor lack alpha-bungarotoxin binding sites and hippocampal fast nicotinic currents*. J Neurosci, 1997. **17**(23): p. 9165-71.
139. Buisson, B., et al., *Human alpha4beta2 neuronal nicotinic acetylcholine receptor in HEK 293 cells: A patch-clamp study*. J Neurosci, 1996. **16**(24): p. 7880-91.
140. Nashmi, R., et al., *Assembly of alpha4beta2 nicotinic acetylcholine receptors assessed with functional fluorescently labeled subunits: effects of localization, trafficking, and nicotine-induced upregulation in clonal mammalian cells and in cultured midbrain neurons*. J Neurosci, 2003. **23**(37): p. 11554-67.
141. Cachelin, A.B. and R. Jaggi, *Beta subunits determine the time course of desensitization in rat alpha 3 neuronal nicotinic acetylcholine receptors*. Pflugers Arch, 1991. **419**(6): p. 579-82.
142. Colquhoun, L.M. and J.W. Patrick, *Alpha3, beta2, and beta4 form heterotrimeric neuronal nicotinic acetylcholine receptors in Xenopus oocytes*. J Neurochem, 1997. **69**(6): p. 2355-62.
143. Colquhoun, L.M. and J.W. Patrick, *Pharmacology of neuronal nicotinic acetylcholine receptor subtypes*. Adv Pharmacol, 1997. **39**: p. 191-220.
144. Levin, E.D., *Nicotinic systems and cognitive function*. Psychopharmacology (Berl), 1992. **108**(4): p. 417-31.
145. Grutzendler, J. and J.C. Morris, *Cholinesterase inhibitors for Alzheimer's disease*. Drugs, 2001. **61**(1): p. 41-52.
146. McGehee, D.S., et al., *Nicotine enhancement of fast excitatory synaptic transmission in CNS by presynaptic receptors*. Science, 1995. **269**(5231): p. 1692-6.
147. Gray, R., et al., *Hippocampal synaptic transmission enhanced by low concentrations of nicotine*. Nature, 1996. **383**(6602): p. 713-6.
148. Xu, W., et al., *Megacystis, mydriasis, and ion channel defect in mice lacking the alpha3 neuronal nicotinic acetylcholine receptor*. Proc Natl Acad Sci U S A, 1999. **96**(10): p. 5746-51.
149. Zoli, M., et al., *Increased neurodegeneration during ageing in mice lacking high-affinity nicotine receptors*. Embo J, 1999. **18**(5): p. 1235-44.
150. Picciotto, M.R., et al., *Abnormal avoidance learning in mice lacking functional high-affinity nicotine receptor in the brain*. Nature, 1995. **374**(6517): p. 65-7.

151. Picciotto, M.R., et al., *Acetylcholine receptors containing the beta2 subunit are involved in the reinforcing properties of nicotine*. Nature, 1998. **391**(6663): p. 173-7.
152. Salas, R., et al., *Altered anxiety-related responses in mutant mice lacking the beta4 subunit of the nicotinic receptor*. J Neurosci, 2003. **23**(15): p. 6255-63.
153. Cordero-Erausquin, M., et al., *Nicotinic receptor function: new perspectives from knockout mice*. Trends Pharmacol Sci, 2000. **21**(6): p. 211-7.
154. Labarca, C., et al., *Point mutant mice with hypersensitive alpha 4 nicotinic receptors show dopaminergic deficits and increased anxiety*. Proc Natl Acad Sci U S A, 2001. **98**(5): p. 2786-91.
155. Ross, S.A., et al., *Phenotypic characterization of an alpha 4 neuronal nicotinic acetylcholine receptor subunit knock-out mouse*. J Neurosci, 2000. **20**(17): p. 6431-41.
156. Marubio, L.M., et al., *Reduced antinociception in mice lacking neuronal nicotinic receptor subunits*. Nature, 1999. **398**(6730): p. 805-10.
157. Broide, R.S. and F.M. Leslie, *The alpha7 nicotinic acetylcholine receptor in neuronal plasticity*. Mol Neurobiol, 1999. **20**(1): p. 1-16.
158. Broide, R.S., et al., *Increased sensitivity to nicotine-induced seizures in mice expressing the L250T alpha 7 nicotinic acetylcholine receptor mutation*. Mol Pharmacol, 2002. **61**(3): p. 695-705.
159. Champtiaux, N., et al., *Distribution and pharmacology of alpha 6-containing nicotinic acetylcholine receptors analyzed with mutant mice*. J Neurosci, 2002. **22**(4): p. 1208-17.
160. Vetter, D.E., et al., *Role of alpha9 nicotinic ACh receptor subunits in the development and function of cochlear efferent innervation*. Neuron, 1999. **23**(1): p. 93-103.
161. Sacco, K.A., K.L. Bannon, and T.P. George, *Nicotinic receptor mechanisms and cognition in normal states and neuropsychiatric disorders*. J Psychopharmacol, 2004. **18**(4): p. 457-74.
162. Wevers, A. and H. Schroder, *Nicotinic acetylcholine receptors in Alzheimer's disease*. J Alzheimers Dis, 1999. **1**(4-5): p. 207-19.
163. Guan, Z.Z., et al., *Decreased protein levels of nicotinic receptor subunits in the hippocampus and temporal cortex of patients with Alzheimer's disease*. J Neurochem, 2000. **74**(1): p. 237-43.
164. Court, J., et al., *Nicotinic receptor abnormalities in Alzheimer's disease*. Biol Psychiatry, 2001. **49**(3): p. 175-84.
165. Wang, H.Y., et al., *Amyloid peptide Abeta(1-42) binds selectively and with picomolar affinity to alpha7 nicotinic acetylcholine receptors*. J Neurochem, 2000. **75**(3): p. 1155-61.
166. Wang, H.Y., et al., *beta-Amyloid(1-42) binds to alpha7 nicotinic acetylcholine receptor with high affinity. Implications for Alzheimer's disease pathology*. J Biol Chem, 2000. **275**(8): p. 5626-32.
167. Dineley, K.T., et al., *Accelerated plaque accumulation, associative learning deficits, and up-regulation of alpha 7 nicotinic receptor protein in transgenic mice co-expressing mutant human presenilin 1 and amyloid precursor proteins*. J Biol Chem, 2002. **277**(25): p. 22768-80.

168. DeLaGarza, V.W., *Pharmacologic treatment of Alzheimer's disease: an update*. Am Fam Physician, 2003. **68**(7): p. 1365-72.
169. de Rijk, M.C., et al., *Prevalence of Parkinson's disease in Europe: A collaborative study of population-based cohorts*. Neurologic Diseases in the Elderly Research Group. Neurology, 2000. **54**(11 Suppl 5): p. S21-3.
170. Bosboom, J.L., D. Stoffers, and E. Wolters, *The role of acetylcholine and dopamine in dementia and psychosis in Parkinson's disease*. J Neural Transm Suppl, 2003(65): p. 185-95.
171. Rajput, A.H., et al., *A case-control study of smoking habits, dementia, and other illnesses in idiopathic Parkinson's disease*. Neurology, 1987. **37**(2): p. 226-32.
172. Grandinetti, A., et al., *Prospective study of cigarette smoking and the risk of developing idiopathic Parkinson's disease*. Am J Epidemiol, 1994. **139**(12): p. 1129-38.
173. Kelton, M.C., et al., *The effects of nicotine on Parkinson's disease*. Brain Cogn, 2000. **43**(1-3): p. 274-82.
174. Fagerstrom, K.O., et al., *Nicotine may relieve symptoms of Parkinson's disease*. Psychopharmacology (Berl), 1994. **116**(1): p. 117-9.
175. Clemens, P., et al., *The short-term effect of nicotine chewing gum in patients with Parkinson's disease*. Psychopharmacology (Berl), 1995. **117**(2): p. 253-6.
176. Vieregge, A., et al., *Transdermal nicotine in PD: a randomized, double-blind, placebo-controlled study*. Neurology, 2001. **57**(6): p. 1032-5.
177. DiCicco-Bloom, E., et al., *The developmental neurobiology of autism spectrum disorder*. J Neurosci, 2006. **26**(26): p. 6897-906.
178. Fombonne, E., *Epidemiological surveys of autism and other pervasive developmental disorders: an update*. J Autism Dev Disord, 2003. **33**(4): p. 365-82.
179. Steffenburg, S., et al., *A twin study of autism in Denmark, Finland, Iceland, Norway and Sweden*. J Child Psychol Psychiatry, 1989. **30**(3): p. 405-16.
180. Croonenberghs, J., et al., *Peripheral markers of serotonergic and noradrenergic function in post-pubertal, caucasian males with autistic disorder*. Neuropsychopharmacology, 2000. **22**(3): p. 275-83.
181. Jamain, S., et al., *Linkage and association of the glutamate receptor 6 gene with autism*. Mol Psychiatry, 2002. **7**(3): p. 302-10.
182. Lee, M., et al., *Nicotinic receptor abnormalities in the cerebellar cortex in autism*. Brain, 2002. **125**(Pt 7): p. 1483-95.
183. Perry, E.K., et al., *Cholinergic activity in autism: abnormalities in the cerebral cortex and basal forebrain*. Am J Psychiatry, 2001. **158**(7): p. 1058-66.
184. Martin-Ruiz, C.M., et al., *Molecular analysis of nicotinic receptor expression in autism*. Brain Res Mol Brain Res, 2004. **123**(1-2): p. 81-90.
185. Pomerleau, O.F., *Nicotine as a psychoactive drug: anxiety and pain reduction*. Psychopharmacol Bull, 1986. **22**(3): p. 865-9.
186. Gilbert, D.G., et al., *Effects of smoking/nicotine on anxiety, heart rate, and lateralization of EEG during a stressful movie*. Psychophysiology, 1989. **26**(3): p. 311-20.
187. Breslau, N., M. Kilbey, and P. Andreski, *Nicotine dependence, major depression, and anxiety in young adults*. Arch Gen Psychiatry, 1991. **48**(12): p. 1069-74.

188. Breslau, N. and D.F. Klein, *Smoking and panic attacks: an epidemiologic investigation*. Arch Gen Psychiatry, 1999. **56**(12): p. 1141-7.
189. Picciotto, M.R., D.H. Brunzell, and B.J. Caldarone, *Effect of nicotine and nicotinic receptors on anxiety and depression*. Neuroreport, 2002. **13**(9): p. 1097-106.
190. Tournier, J.M., et al., *alpha3alpha5beta2-Nicotinic acetylcholine receptor contributes to the wound repair of the respiratory epithelium by modulating intracellular calcium in migrating cells*. Am J Pathol, 2006. **168**(1): p. 55-68.
191. Chernyavsky, A.I., et al., *Differential regulation of keratinocyte chemokinesis and chemotaxis through distinct nicotinic receptor subtypes*. J Cell Sci, 2004. **117**(Pt 23): p. 5665-79.
192. Grando, S.A., *Biological functions of keratinocyte cholinergic receptors*. J Invest Dermatol Symp Proc, 1997. **2**(1): p. 41-8.
193. Arredondo, J., et al., *Central role of fibroblast alpha3 nicotinic acetylcholine receptor in mediating cutaneous effects of nicotine*. Lab Invest, 2003. **83**(2): p. 207-25.
194. Arredondo, J., et al., *A receptor-mediated mechanism of nicotine toxicity in oral keratinocytes*. Lab Invest, 2001. **81**(12): p. 1653-68.
195. Arredondo, J., et al., *Receptor-mediated tobacco toxicity: regulation of gene expression through alpha3beta2 nicotinic receptor in oral epithelial cells*. Am J Pathol, 2005. **166**(2): p. 597-613.
196. Son, J.H. and S. Meizel, *Evidence suggesting that the mouse sperm acrosome reaction initiated by the zona pellucida involves an alpha7 nicotinic acetylcholine receptor*. Biol Reprod, 2003. **68**(4): p. 1348-53.
197. Shin, V.Y., et al., *Nicotine induces cyclooxygenase-2 and vascular endothelial growth factor receptor-2 in association with tumor-associated invasion and angiogenesis in gastric cancer*. Mol Cancer Res, 2005. **3**(11): p. 607-15.
198. Shin, V.Y. and C.H. Cho, *Nicotine and gastric cancer*. Alcohol, 2005. **35**(3): p. 259-64.
199. Orr-Urtreger, A., et al., *Increased severity of experimental colitis in alpha 5 nicotinic acetylcholine receptor subunit-deficient mice*. Neuroreport, 2005. **16**(10): p. 1123-7.
200. Kawashima, K. and T. Fujii, *The lymphocytic cholinergic system and its contribution to the regulation of immune activity*. Life Sci, 2003. **74**(6): p. 675-96.
201. Wang, H., et al., *Nicotinic acetylcholine receptor alpha7 subunit is an essential regulator of inflammation*. Nature, 2003. **421**(6921): p. 384-8.
202. Lindstrom, J., *Autoimmune diseases involving nicotinic receptors*. J Neurobiol, 2002. **53**(4): p. 656-65.
203. Miwa, J.M., et al., *lynx1, an endogenous toxin-like modulator of nicotinic acetylcholine receptors in the mammalian CNS*. Neuron, 1999. **23**(1): p. 105-14.
204. Proskocil, B.J., et al., *Acetylcholine is an autocrine or paracrine hormone synthesized and secreted by airway bronchial epithelial cells*. Endocrinology, 2004. **145**(5): p. 2498-506.
205. Sekhon, H.S., et al., *Expression of lynx1 in developing lung and its modulation by prenatal nicotine exposure*. Cell Tissue Res, 2005. **320**(2): p. 287-97.

206. Ibanez-Tallon, I., et al., *Tethering naturally occurring peptide toxins for cell-autonomous modulation of ion channels and receptors in vivo*. *Neuron*, 2004. **43**(3): p. 305-11.
207. Drummond, A. and K. Strimmer, *PAL: an object-oriented programming library for molecular evolution and phylogenetics*. *Bioinformatics*, 2001. **17**(7): p. 662-3.
208. Gong, S., et al., *A gene expression atlas of the central nervous system based on bacterial artificial chromosomes*. *Nature*, 2003. **425**(6961): p. 917-25.
209. Boyce, S., et al., *Analgesic and toxic effects of ABT-594 resemble epibatidine and nicotine in rats*. *Pain*, 2000. **85**(3): p. 443-50.
210. Fanselow, M.S. and J.E. LeDoux, *Why we think plasticity underlying Pavlovian fear conditioning occurs in the basolateral amygdala*. *Neuron*, 1999. **23**(2): p. 229-32.
211. Rauch, S.L., L.M. Shin, and C.I. Wright, *Neuroimaging studies of amygdala function in anxiety disorders*. *Ann N Y Acad Sci*, 2003. **985**: p. 389-410.
212. Davis, M. and P.J. Whalen, *The amygdala: vigilance and emotion*. *Mol Psychiatry*, 2001. **6**(1): p. 13-34.
213. Costall, B., et al., *The actions of nicotine and cocaine in a mouse model of anxiety*. *Pharmacol Biochem Behav*, 1989. **33**(1): p. 197-203.
214. Rees, H. and M.H. Roberts, *The anterior pretectal nucleus: a proposed role in sensory processing*. *Pain*, 1993. **53**(2): p. 121-35.
215. Weber, W.M., et al., *Maitotoxin induces insertion of different ion channels into the *Xenopus* oocyte plasma membrane via Ca(2+)-stimulated exocytosis*. *Pflugers Arch*, 2000. **439**(3): p. 363-9.
216. Arellano, R.O., R.M. Woodward, and R. Miledi, *A monovalent cationic conductance that is blocked by extracellular divalent cations in *Xenopus* oocytes*. *J Physiol*, 1995. **484** (Pt 3): p. 593-604.
217. Ebihara, L., **Xenopus* connexin38 forms hemi-gap-junctional channels in the nonjunctional plasma membrane of *Xenopus* oocytes*. *Biophys J*, 1996. **71**(2): p. 742-8.
218. Bahima, L., et al., *Endogenous hemichannels play a role in the release of ATP from *Xenopus* oocytes*. *J Cell Physiol*, 2006. **206**(1): p. 95-102.
219. Tzounopoulos, T., J. Maylie, and J.P. Adelman, *Induction of endogenous channels by high levels of heterologous membrane proteins in *Xenopus* oocytes*. *Biophys J*, 1995. **69**(3): p. 904-8.
220. Bielfeld-Ackermann, A., C. Range, and C. Korbmayer, *Maitotoxin (MTX) activates a nonselective cation channel in *Xenopus laevis* oocytes*. *Pflugers Arch*, 1998. **436**(3): p. 329-37.
221. Henderson, S.C., M.M. Kamdar, and A. Bamezai, *Ly-6A.2 expression regulates antigen-specific CD4+ T cell proliferation and cytokine production*. *J Immunol*, 2002. **168**(1): p. 118-26.
222. Choi, S.J., et al., *Cloning and identification of human Sca as a novel inhibitor of osteoclast formation and bone resorption*. *J Clin Invest*, 1998. **102**(7): p. 1360-8.
223. Gotti, C., et al., *Brain neuronal nicotinic receptors as new targets for drug discovery*. *Curr Pharm Des*, 2006. **12**(4): p. 407-28.
224. Bencherif, M. and J.D. Schmitt, *Targeting neuronal nicotinic receptors: a path to new therapies*. *Curr Drug Targets CNS Neurol Disord*, 2002. **1**(4): p. 349-57.

225. Alkondon, M. and E.X. Albuquerque, *The nicotinic acetylcholine receptor subtypes and their function in the hippocampus and cerebral cortex*. Prog Brain Res, 2004. **145**: p. 109-20.
226. Del Toro, D.R., T.A. Park, and J.J. Wertsch, *Development of a model of the premotor potential*. Arch Phys Med Rehabil, 1994. **75**(5): p. 493-7.
227. Morley, B.J., *The embryonic and post-natal expression of the nicotinic receptor alpha 3-subunit in rat lower brainstem*. Brain Res Mol Brain Res, 1997. **48**(2): p. 407-12.
228. Chowdhury, P., et al., *Pathophysiological effects of nicotine on the pancreas: an update*. Exp Biol Med (Maywood), 2002. **227**(7): p. 445-54.
229. Thuerauf, N., et al., *The influence of mecamylamine on trigeminal and olfactory chemoreception of nicotine*. Neuropsychopharmacology, 2006. **31**(2): p. 450-61.
230. Hozumi, S., et al., *Characteristics of changes in cholinergic function and impairment of learning and memory-related behavior induced by olfactory bulbectomy*. Behav Brain Res, 2003. **138**(1): p. 9-15.
231. Vincler, M., *Neuronal nicotinic receptors as targets for novel analgesics*. Expert Opin Investig Drugs, 2005. **14**(10): p. 1191-8.
232. Han, K.J., et al., *Antinociceptive effect of nicotine in various pain models in the mouse*. Arch Pharm Res, 2005. **28**(2): p. 209-15.
233. Bateman, A., et al., *The Pfam protein families database*. Nucleic Acids Res, 2004. **32**(Database issue): p. D138-41.
234. Morgenstern, B., *DIALIGN 2: improvement of the segment-to-segment approach to multiple sequence alignment*. Bioinformatics, 1999. **15**(3): p. 211-8.
235. Goodstadt, L. and C.P. Ponting, *CHROMA: consensus-based colouring of multiple alignments for publication*. Bioinformatics, 2001. **17**(9): p. 845-6.
236. Nadler, J.J., et al., *Automated apparatus for quantitation of social approach behaviors in mice*. Genes Brain Behav, 2004. **3**(5): p. 303-14.
237. Caldarone, B.J., C.H. Duman, and M.R. Picciotto, *Fear conditioning and latent inhibition in mice lacking the high affinity subclass of nicotinic acetylcholine receptors in the brain*. Neuropharmacology, 2000. **39**(13): p. 2779-84.